The PHILOSOPHICAL MAGAZINE

FIRST PUBLISHED IN 1798

L. 44 SEVENTH SERIES No. 351 April 1953

A Journal of Theoretical Experimental and Applied Physics

PRICE 15s. 0d.
Annual Subscription £8 0s. 0d. payable in advance

D AND PUBLISHED BY TAYLOR & FRANCIS LTD., RED LION COURT, FLEET ST., LONDON, E.C.4.

Early Scientific Publications

DIARY OF ROBERT HOOKE, M.A., M.D., F.R.S.
1672-1680

Edited by **H. W. ROBINSON** and **W. ADAMS**
Recommended for publication by the Royal Society, London

25/-
net

"This vivid record of the scientific, artistic and social activities of a remarkable man during remarkable years has too long remained in obscurity."—Extract from foreword by Sir Frederick Gowland Hopkins, O.M., President of the Royal Society.

MATHEMATICAL WORK OF JOHN WALLIS, D.D., F.R.S.

By **J. F. SCOTT, Ph.D., B.A.**

12/6
net

"His work will be indispensable to those interested in the early history of The Royal Society. I commend to all students of the Seventeenth Century, whether scientific or humane, this learned and lucid book."—Extract from foreword by Prof. E. N. da C. Andrade, D.Sc., Ph.D., F.R.S.
Recommended for publication by University of London

CORRESPONDENCE AND PAPERS OF EDMOND HALLEY

Arranged and Edited by **EUGENE FAIRFIELD MACPIKE**

21/-
net

First published on behalf of The History of Science Society by Oxford University Press. Now re-issued by Taylor & Francis, Ltd.

MEMOIRS OF SIR ISAAC NEWTON'S LIFE

5/-
net

By **WILLIAM STUKELEY, M.D., F.R.S., 1752**
From an Original Manuscript
Now in the possession of the Royal Society, London

HEVELIUS, FLAMSTEED AND HALLEY

12/6
net

Three Contemporary Astronomers and their Mutual Relations
By **EUGENE FAIRFIELD MACPIKE**
Published by arrangement with The History of Science Society

Established
over 150 years

TAYLOR & FRANCIS, LTD.
RED LION COURT, FLEET ST., LONDON E.C.
PRINTERS & PUBLISHERS OF SCIENTIFIC BOOKS

XLI. *Some Experiments on Photographic Sensitivity*

By J. M. Hedges and J. W. Mitchell
H. H. Wills Physical Laboratory, University of Bristol*

[Received December 20, 1952]

Abstract

A technique is described for the preparation of optically clear silver bromide in the form of thin plane parallel sheets with flat surfaces. These sheets have been used to investigate the formation of the latent image under illumination.

It has been found that the distribution of the latent image between the surface and the interior of the crystals depends on their physical properties, on the nature of the sensitizing layers present on their surfaces, and on the exposure. A surface latent image is formed, together with a weak internal latent image, when well annealed crystals are exposed to light. A surface latent image, on the other hand, is not formed with strained sheets of pure silver bromide, if they have not been annealed at all or only at low temperatures. With such material, an internal latent image is formed by the separation of silver along dislocation lines, which may form the boundaries of an irregular polyhedral structure. The crystals may then be developed after the dissolution of the surface with a solvent for silver bromide.

Crystals which give a strong internal image and no surface latent image may be sensitized for the formation of a surface latent image by the condensation on their surfaces of thin films of silver, gold and of certain metallic sulphides from atomic or molecular beams. After a brief exposure to light, a surface latent image is formed on the sensitized crystals which can be developed to a normal negative image (black in the exposed regions). Longer exposures cause the disappearance of the surface latent image in the exposed areas and the formation of a surface latent image in the unexposed areas. The reversed or positive image (white in exposed regions) can also be developed. This behaviour corresponds to solarization in the photographic process. The internal latent image did not show any trace of reversal or solarization even after very prolonged exposures.

The thin films of the sensitizer are shown to provide traps for positive holes but not for electrons. This seems to be the role of the chemical sensitizers. The recognition of this fact necessitates a revision of the ideas on sensitivity specks which have previously been accepted. It is now suggested that sensitivity centres rather than specks are involved and that these are regions of localized structural imperfection. The

* Communicated by the Authors.

traps for the electrons are provided by the silver ions associated with them.

All the experimental evidence is consistent with the hypothesis that the latent image consists of a group of silver atoms exceeding a critical size and situated either on the external surface or on an internal surface associated with a mechanical imperfection of the crystal (e.g. a dislocation).

The experimental results lead to a new working hypothesis on the formation of the latent image in silver bromide crystals which appears to account satisfactorily for: (1) the distribution of the latent image between the surface and the interior of the crystal under different circumstances; (2) the formation of the latent sub-image and its transformation to a stable latent image; (3) low and high intensity reciprocity failure and the influence of chemical sensitization upon them; and finally, (4) solarization.

§ 1. Introduction

The microcrystals of silver halide which, suspended in gelatine, form the sensitive layer of any photographic material possess the remarkable property of forming a latent image during a brief exposure to light, the presence of which causes them to be reduced to metallic silver in a photographic developer. Since the absorption of an extremely small amount of energy suffices for the formation of a latent image which is not directly observable, there has been much speculation as regards its precise nature, mode of formation and function in initiating the development of the microcrystal.

It has been established that the latent image can be located both at the external surface and within the microcrystals and it has become customary to refer to these as the surface and the internal latent images (Berg, Marriage and Stevens 1941, Stevens 1942, see also Berg 1947). The present investigation is concerned mainly with the surface latent image and with the sensitization of single crystals of silver bromide for its formation. Observations have also been made on the internal latent image and some of these, which have a direct bearing on the formation of the surface latent image, are included in this paper. The bulk of the work on the internal latent image will, however, be the subject of another communication.

Although many alternative possibilities have been suggested, it is now generally accepted (see, for example, Mees 1942) that the surface latent image consists of a speck of silver at the interface between the silver halide and the surrounding medium and that this silver speck provides a nucleus for the reduction of the microcrystal to metallic silver in the photographic developer. The precise mechanism whereby the speck is formed and the part played by chemical sensitization in facilitating its formation are, however, much more obscure.

We shall now consider two theories of the formation of the surface latent image in chemically sensitized grains. In the first theory, which was advanced by Gurney and Mott (1938) (see also Mott 1941), chemical

sensitization was introduced only insofar as it provided surface particles to act as traps for electrons. In the development of this theory, Gurney and Mott applied to the formation of the surface latent image the two-stage mechanism for photochemical changes in the silver halides with which they had explained the observed separation of silver in the form of discrete particles during the later stages of photolysis. They based this mechanism upon the experimental facts that the silver halides are both electronic photoconductors and ionic conductors at room temperature. In applying it to the formation of the surface latent image, they assumed that the electrons, which are liberated when photons are absorbed by the silver halide, are trapped by sensitivity specks of silver or of silver sulphide on the surfaces and then neutralized by the motion of interstitial silver ions to the trapping sites. The theory thus provides a transport mechanism to explain the localized separation of silver atoms at the sensitivity specks which was postulated in the concentration speck theory of photographic sensitivity (Sheppard, Trivelli, and Loveland 1925). The behaviour of the positive holes or bromine atoms which must be liberated at the same time as the electrons or silver atoms, according to the postulates underlying these theories, was not considered in detail in either of them ; it was not unreasonably assumed that they escaped at the surface of the crystal and reacted with molecules in the surrounding medium. There is now, however, good reason for believing that, if an electron were trapped at the surface of the grain by a sensitivity centre of the type envisaged by Sheppard and his co-workers, it would attract a positive hole which would recombine with it before an interstitial silver ion could move up to form a silver atom (see, for example, Mitchell 1952 a). Although attempts were made to avoid this difficulty by the introduction of further hypotheses (see, for example, Mott 1948), it remained as a fundamental weakness of the Gurney–Mott theory of the formation of the surface latent image.

The theory of the formation of the surface latent image advanced by Mitchell (1948, 1949 a, b, 1951 a, b ; see also Pick 1951) is, on the other hand, a theory of the interaction of both holes and electrons with the groups of atoms and molecules introduced by chemical sensitization. According to Mitchell (1948), the silver which separates to form the latent image during exposure to light is already present in the silver halide microcrystals, the equivalent amount of bromine having been removed during chemical sensitization. As an example, in grains which have been simultaneously or successively sensitized with a sulphur compound and by reduction (Lowe, Jones and Roberts 1951), the theory provides a mechanism for the tranference of the finely dispersed silver introduced by reduction sensitization to the sensitivity centres assumed, as in the earlier theories, to be associated with sulphur sensitization. It is thus a theory of the redistribution during exposure of an excess of silver in chemically sensitized grains rather than a theory of the primary photolysis of the silver halide as was envisaged by Sheppard and his co-workers and by Gurney and Mott.

Now there are three states in which the sensitizing atoms or molecules may be present in the surface layers of the silver halide crystals of an emulsion. Groups of atoms or molecules may be : (1) present on external surfaces ; (2) situated in regions of structural imperfection in the immediate neighbourhood of the surface ; (3) built substitutionally into the surface layers in association with vacant halide ion lattice sites.

In his first paper on the subject, in which he introduced vacant halide ion lattice sites into the discussion of chemical sensitization for the first time, Mitchell (1948) dealt with the third alternative. He assumed that the sensitizing atoms and molecules are incorporated substitutionally in the surface layers of the silver halide grains and that their primary function is to trap positive holes and electrons at spatially separated sites and thus to lessen their probability of recombination. To begin with, he postulated that the space charges created by the trapping of the electronic charges are neutralized by the motion of vacant halide ion lattice sites ; he later modified this mechanism, substituting neutralization through the displacement of silver ions by way of interstitial positions, vacant silver ion lattice sites or surface sites (Mitchell 1951 a, b).

The evidence at present available points to the absence of vacant halide ion lattice sites in any significant concentration in crystals of pure silver halides in equilibrium at room temperature (Mitchell 1952 a). This does not, however, exclude the possibility that such sites may be incorporated in the lattice by one of the following two mechanisms : (*a*) the reduction to a silver atom of a silver ion occupying a kink site (Kossel 1927, Stranski 1928) while crystal growth is proceeding so that fresh ions are being continuously deposited on the surface ; (*b*) the attachment of a silver sulphide or a silver oxide molecule to a kink site during crystal growth. In these cases, the electrical neutrality of the lattice may be preserved by the omission of a bromide ion from an adjacent site, and vacant bromide ion sites may thus be built into the crystal in association with foreign atoms and molecules, even though such sites are present in negligible concentrations in thermal equilibrium.

The second alternative might also be realized under the conditions of chemical sensitization of an emulsion ; this involves the building of the sensitizing atoms and molecules into the surface layers of the crystal in cracks and other imperfections, so that they preserve their chemical identity, which is not the case when they are incorporated substitutionally. The sensitizing atoms and molecules are indeed most likely to be formed at regions of surface imperfection where the most reactive sites are to be found and further crystal growth may result in their being built into such regions. This would increase the local imperfection and consequently the probability of trapping electrons there. The foreign atoms and molecules might themselves, of course, combine with the positive holes.

The two alternatives for the incorporation of sensitizing atoms and molecules so far discussed lead to an attractive working hypothesis

for further research on chemical sensitization; both may, indeed, be realized in practice. It became increasingly evident, however, that such theoretical speculation on the detailed nature of chemical sensitization, although stimulating, was not leading to sound progress, owing to the lack of experimental evidence on the properties of the surfaces of silver halide crystals covered with layers of sensitizing substances. It was not, for instance, known whether the presence of such layers on the external surface would cause spontaneous fogging, or whether their primary purpose was to provide traps for electrons or for holes. A new approach to the subject of chemical sensitization was clearly necessary.

A method for investigating chemical sensitization based upon the use of sections of single crystals of silver bromide as the experimental material was therefore developed. These were produced in the form of thin sheets with flat plane parallel surfaces by crystallizing a film of molten silver bromide between two optically polished flats of Pyrex glass. The main object of the work was to obtain evidence which would permit the assessment of the relevance of the alternative theories of chemical sensitization and the formation of the latent image to actual photochemical processes. For this reason surface layers of various sensitizers were evaporated onto the surface of some of the crystals.

The distribution of the latent image between the surface and the interior of the crystals was found to depend upon whether the crystals were exposed in a strained condition, or after annealing at low temperatures which caused the development of a polyhedral sub-structure, or after annealing at high temperatures. When non-sensitized crystals of pure silver bromide were used, a surface latent image was formed only in fully annealed crystals. Here the internal latent image was relatively unimportant. With strained specimens, whether or not lightly annealed, a surface latent image was not formed. Silver then separated in dislocations, and revealed, for instance, the boundaries of the polyhedral sub-structure referred to above. This silver formed an internal latent image. These experimental observations are in good agreement with the theoretical deductions made by Mitchell (1952 b) in a recent paper on the application of the Gurney–Mott mechanism to the formation of the latent image in chemically non-sensitized crystals of silver halides.

It was next demonstrated that the condensation of thin films of silver, gold and of metallic sulphides on silver halide crystals from atomic and molecular beams of these substances confers upon them the properties usually associated with the corresponding types of chemical sensitization.

Taken as a whole, the experimental results lead to the following conclusions:

(1) A surface latent image can only be produced in non-sensitized crystals when relatively perfect; very little internal image is then formed.

(2) An internal image is formed in non-sensitized, strained or polygonized, silver bromide crystals by the separation of silver at dislocations and at systems of dislocations. Under these conditions,

any silver atoms which might separate at the surface provide traps for positive holes, so no surface latent image is formed.

(3) The surfaces of all crystals, strained or unstrained, can be sensitized for the formation of a surface latent image by the deposition of thin layers of silver, gold and of the sulphides of trivalent arsenic and antimony and monovalent thallium.

(4) One function of these sensitizing layers is to provide traps for positive holes. They do not provide traps for electrons at room temperature.

(5) The experimental results indicate that the density of traps for electrons in silver bromide crystals is greatest at regions of structural imperfection. Such regions are sensitivity centres.

(6) In sensitized crystals, positive holes are trapped by particles of the sensitizing substance and, less effectively, by bromide ions occupying kink sites. Electrons are trapped by silver ions at imperfections on external surfaces or within the crystals. The space charges thus created are then neutralized by the motion of silver ions from the neighbourhood of the trapped holes to the neighbourhood of the trapped electrons.

(7) A succession of these events, each transferring a silver atom to the sensitivity centre, builds up a group of silver atoms which represents the latent sub-image.

(8) The second function of the groups of atoms and molecules of the sensitizing layer now comes into play. The groups near the sensitivity centres provide condensation nuclei for the silver atoms of the sub-image and increase their size to form a stable latent image.

(9) When such particles exceed a critical size they can act as development centres and initiate the reduction of the silver bromide.

The experimental results provide strong supporting evidence for the Gurney–Mott two-stage mechanism for photochemical changes but not for the Gurney–Mott theory of the formation of the surface latent image. It has been demonstrated that the electrons are not trapped by sensitivity specks of silver or of a metallic sulphide and that the sensitizing substance plays an essential role in trapping positive holes. In this respect, the evidence supports the postulate of Mitchell on the necessity for trapping holes and electrons at separated sites. The mechanism for the formation of the latent image which emerges from the experimental work and which is presented in the final section was, however, not fully covered by any previous theory.

In concluding this introduction, it may perhaps be well to emphasize that the possibility that the atoms or molecules of the sensitizing substance are incorporated in the surface layers of silver bromide crystals is not relevant to the interpretation of the results of this experimental work. Such a building in of the sensitizing substance, either mechanically or substitutionally, was deliberately excluded in the design of the experiments, which did not aim at reproducing the conditions prevailing during the chemical sensitization of the silver halide microcrystals of an emulsion. Such work has, however, now been in progress at Bristol for some time and the results (Evans and Mitchell,

to be published) establish that the large single crystals of silver bromide can be sensitized in the same environment, by the same reagents, under precisely the same physico-chemical conditions as the microcrystals of a silver bromide emulsion. The properties of the sensitizing layers produced in this way appear to correspond very closely indeed with those of the thin films deposited in the present experimental work.

§ 2. Experimental Methods

Preparation of Fused Silver Bromide

The raw materials used were very pure silver nitrate provided by Kodak Ltd., Harrow, and hydrobromic acid of ' Analar ' quality supplied by British Drug Houses. Silver bromide was precipitated by running equivalent quantities of N/10 solutions of silver nitrate and hydrobromic acid, preheated to 60°C, at slow equal rates through concentric jets into a large beaker in which the mixed solutions were vigorously stirred. The use of the concentric jets ensures that the precipitated silver bromide is not subsequently brought into contact with solutions containing an excess of silver ions or of bromide ions. After thirty minutes at 60°C, the precipitate was washed a number of times by decantation and then filtered with a sintered glass Buchner funnel. It was rapidly dried to a free flowing powder in a vacuum freeze-dryer, the temperature of the powder being finally raised to 200°C. Doubly distilled water from all glass stills was used throughout and every precaution taken to minimize contamination.

The silver bromide was now transferred to a Hysil glass tube to which a side arm containing a phial of bromine, frozen in liquid air, was sealed. The tube was evacuated with a mercury diffusion pump and sealed off from the pumping system. The silver bromide was melted by placing the tube in an electric furnace at a temperature of 450°C, the side arm containing the bromine being meanwhile warmed up to 60–70°C. After half an hour, the bromine was re-frozen, the tube was opened, and the clear molten silver bromide filtered through a series of fine glass capillary tubes into a Hysil tube mounted vertically in another electric furnace which was also at 450°C. A slow stream of pure dry nitrogen was passed to displace oxygen which reacts with silver bromide at this temperature. As an intermediate step in the preparation of thin sheets, the silver bromide was converted into pellets of suitable size by transferring it, a globule at a time, with a thin walled glass tube to a cold Hysil plate which immediately chilled the pellets and thus prevented any reaction with the oxygen of the atmosphere.

Preparation of Thin Sheets of Silver Bromide

Sheets of silver bromide were prepared by crystallizing thin films of the molten material between circular polished plates of Pyrex glass, 2 in. in diameter. For this purpose, a stainless steel slab 24 in. long by 6 in. wide by $\frac{1}{2}$ in. thick was heated to a temperature of 550°C at a distance of 6 to 9 in. from one end. When steady conditions were

established, the other end reached a temperature of about 100°c. Two Pyrex plates were carefully cleaned and gradually heated by slowly displacing them up the temperature gradient. During this time, they were protected from contamination with Hysil glass covers. Three short sections of Hysil glass rod of either 0·010 in. or 0·015 in. in diameter were now placed radially and symmetrically round the edge of one of the plates which was then covered with the other plate. The pellet of silver bromide was melted in a Hysil tube which was drawn out to a fine capillary at one end ; a slow stream of pure nitrogen was passed through it to displace the air. The molten globule was then rapidly transferred through the capillary to the thin gap between the Pyrex plates and drawn into it by capillary attraction. By following this procedure, the silver bromide was exposed to air for the minimum time while in the molten state. The sandwich was now displaced down the temperature gradient until the temperature at the forward edge of the molten film fell to the melting point when a small seed crystal formed there. Further slow displacement, which was effected mechanically, converted the bulk of the film into a single crystal or a few large crystals ; a [100] direction was usually within 15° of the normal to the surface. The contraction of the silver bromide which accompanies solidification causes the formation of a pipe at the rearward edge of the sheet. The less pure material of this region was sometimes polycrystalline and was never used for experimental work.

Single crystal sheets with other orientations appeared by chance from time to time for no apparent reason. In particular, at one period a series of sheets with perfect (111) orientation was produced. Sheets with special orientations were, however, usually grown by a modification of the above method. With a diamond saw, a segment was cut from the forward edge of the upper plate so that a seed crystal could be mounted on a glass wedge in contact with the thin film. As before, the sandwich was displaced down the temperature gradient until solidification began at the forward edge of the film. The seed crystal, which was to determine the orientation, was then placed in position and the sandwich displaced in the direction of increasing temperature until the edge remelted and the lower portion of the seed melted into contact with it. Reversal of the direction of displacement then resulted in the crystallization of the layer with an orientation determined by the planes of the seed crystal which were parallel to the surfaces of the glass discs. Crystals of silver bromide with (111) surfaces have been produced by this method using as seeds appropriately oriented sections cut from (100) sheets. Attempts to use sections of (111) orientation placed in contact with the lower plate as seeds and cooling them with a small jet of nitrogen to prevent their melting have not been particularly successful.

After the complete solidification of the silver bromide, the sandwich was slowly displaced down the remainder of the temperature gradient and allowed to cool to room temperature. To prevent contamination

and scratching of the soft surfaces, the sheets were kept between the glass discs until required for use. They could then be readily separated by placing the sandwich in a crystallizing dish and covering it with distilled water but thereafter the greatest care had to be taken to avoid marking the surfaces.

Pyrex glass and silver bromide have widely differing coefficients of thermal expansion and yet adhere strongly to each other when not immersed in water. The silver bromide sheets which are produced by the method described here are consequently always strained and, when examined in the polarizing microscope, they have the appearance of the crystals in a thin section of a coarsely crystalline granite. This provides a very direct method for selecting areas suitable for different experiments. Unannealed strained material or polygonized material was used for the bulk of the experiments because it provided a better model for the microcrystals of silver bromide emulsions than fully annealed material, in which very little internal latent image was usually formed.

The sheets were, however, often annealed after their separation from the glass plates. For this, they were placed on discs of Pyrex glass of 2 in. diameter and packed into a vertical tube with suitable separators. A sidearm containing a phial of bromine was sealed on and the apparatus was then sealed to a vacuum manifold and exhausted with the bromine cooled in liquid air. It was sealed off and placed in a vertical tube furnace at a temperature of 150° to 400° for four hours, the tube containing the bromine being maintained at a temperature which corresponded to a vapour pressure of 2 atmospheres of bromine. After four hours, the bromine was cooled to a low temperature and equilibrium with the crystals re-established at the lower vapour pressure. The apparatus was then slowly cooled to room temperature. This appears to be the only method of producing single crystals of silver bromide of stoichiometric composition. The crystals produced in this way were optically clear and showed a negligible fog level.

The annealing of strained crystals in the temperature range between 150°c and 350°c developed a polyhedral sub-structure (Cahn 1950) and caused the disappearance of the bulk of the strain birefringence. The polygonized structure was clearly revealed when particles of silver separated in the walls and networks of dislocations constituting the boundaries between adjacent polyhedral elements on exposure to light (Hedges and Mitchell 1953). It slowly disappeared when the crystals were annealed above 350°c and very little internal separation of silver then occurred even on prolonged exposure.

Preparation of Specimens

The sheets were cut into square sections, with a side of 5 to 7 mm, with a clean razor blade on a piece of plate glass. They were then mounted on 3 in. by 1 in. microscope slides with the minimum quantity of Styrax mounting medium or of hard cooked Canada Balsam.

To allow the surface to come to equilibrium after cutting and mounting and to remove any silver produced by the reaction of the silver bromide with the iron of the blade, all the specimens were treated for 30 minutes with a 10% solution of potassium bromide in distilled water which had been saturated with bromine. After this, the surface was brought to a standard state for most of the experimental work by treatment with a 5% solution of semi-carbazide nitrate in a 10% solution of potassium bromide and then thoroughly washed and dried. It should be emphasized that careful comparative tests demonstrated that these treatments were without effect on the experimental results.

Surfaces prepared in this way on strained or polygonized crystals of very pure silver bromide showed a low surface density of fog specks which were of physical origin. They could be eliminated by treating the surface with effective antifoggants, but this was not done in any of the experimental work described in this paper. They could also be eliminated by crystallizing silver bromide from a super-saturated solution in hydrobromic acid upon the surface and thus forming an oriented overgrowth of small crystals, with a side of approximately 10 microns. Although such specimens are being used for experiments on sensitization by digestion with solutions of inert gelatine and added sensitizers (Evans and Mitchell, to be published), they have not been used in the present work; consequently the photomicrographs of the areas used as controls always show a certain surface density of fog specks.

Sensitization of the Surfaces of Specimens

The primary purpose of these experiments was to establish whether the surface of a single crystal of silver bromide, with one of the crystallographic orientations usually found in the microcrystals of photographic emulsions, could be sensitized for the formation of a surface latent image with a thin film of silver, gold or of a metallic sulphide. The most direct method of solving the problem was found to be the condensation of thin films of these substances on the surfaces of the crystals by exposing them to well collimated atomic or molecular beams under high vacuum conditions.

The apparatus used for this purpose had a lower flanged glass bowl with four tungsten electrodes sealed through its base. It was sealed to the manifold of a high vacuum system comprising a trap cooled in liquid air, a mercury vapour diffusion pump and a two stage rotary backing pump. Parallel tungsten strips for evaporating silver and gold from beads of these metals were mounted on two pairs of leads close to the centre of the bowl and shielded from each other with a sheet of molybdenum. Metallic sulphides were evaporated from a narrow, vertical flanged silica tube which rested in a closely wound coil of nichrome. The apparatus has been used for the individual, successive or simultaneous evaporation of sensitizing substances but only the

results of experiments with surfaces sensitized with single substances are reported in this paper. When the evaporators had been prepared and charged, a doubly flanged glass tube was cemented into position with Apiezon W wax which was protected from radiation from the evaporating filaments with a cylindrical metal shield. This glass tube carried a pair of anodized aluminium discs connected by three threaded steel rods. On the frame thus formed were mounted two beam defining apertures, the magnetically controlled shutter for determining the condensation time, and three studs for accurately locating the specimen holder.

After the surface conditioning treatment described above, the specimen was mounted in the holder, and, if required, one or more straight edges were positioned in front of it to define the area of the sensitizing deposit. The flanged cover was cemented in position and the pressure was reduced to 10^{-6} mm Hg for the evaporation. The amount of radiation from the filaments falling on the surface during sensitization with gold and silver was reduced to a minimum by the beam defining apertures and the results showed that this did not cause fogging of the specimen. The radiation emitted during the evaporation of the metallic sulphides selected for the work was completely negligible. The apparatus was always allowed to cool to room temperature in vacuum and the sensitized sheets were exposed immediately after their removal from it and developed soon afterwards.

Exposure of the Specimens to Light

Specimens were exposed to both steady and intermittent light sources. For steady exposures, a tungsten ribbon filament lamp and both a medium and a high pressure mercury vapour lamp were used. The filament or arc was imaged into the centre of a good quality anastigmat, mounted in a Compur shutter, with a second anastigmat. A slit mounted in contact with this latter lens, was imaged at the conjugate point of the first lens as a sharply defined uniformly illuminated patch of light which was used for exposing the specimens. Scattered light was eliminated as far as possible by mounting a slit or straight edge immediately in front of the specimen. Exposures of less than five seconds were timed with the Compur shutter and longer exposures were timed using the shutter in conjunction with a stop watch. Filters were used where required, to isolate relatively broad bands from the radiations of the mercury vapour lamps.

For one important series of experiments, a sharply focussed reduced image of a uniformly illuminated slit was formed on the surface of the specimen with a $\times 20$ achromatic objective using the vertical illuminator of the microscope. The specimen could be traversed with the mechanical stage of the microscope and a series of exposures of different durations thus made. The separation of photolytic silver during illumination through the vertical illuminator both near and well below the surface

could be followed by observing the field with the cardioid ultra-microscope using intense orange red illumination. With this arrangement, experiments could also be made in which the surface was covered with a thin film of a solution confined between the underside of a cover glass and the specimen.

For intermittent illumination, the arc channel of a 250 watt high pressure mercury vapour lamp was focussed with an achromatic lens at the centre of a lens mounted as close as possible to the plane of a slotted disc. The second lens formed an image of the aperture of the first lens and was combined with a cylindrical lens to produce a horizontal rectangular patch of light. The specimen was exposed behind a slit or straight edge in the focal plane of the combination. The slotted disc was driven by a 3000 r.p.m. synchronous motor and the width and spacing of the slots determined an exposure of 50 micro-seconds at a repetition rate of 800 per second. The high pressure mercury vapour lamp produced a periodic output with 100 light pulses per second. The exposures given by successive pulses were consequently not uniform but this does not affect any of the qualitative conclusions drawn from the work.

For a number of experiments with monochromatic light, the principal lines of the mercury vapour arc were isolated with a single monochromator of Littrow type combined with broad band filters. This was constructed from an achromatic lens, a 60° angle dense flint prism, and a surface silvered optical flat. The horizontal exit slit of the illuminating system was used as the source. This apparatus provided both steady and intermittent monochromatic illumination. The specimen was mounted above the optical axis of the system and the image of the slit in the required monochromatic radiation was selected and focussed on to it.

Exposure of Specimens to Light with the Application of Synchronized Voltage Pulses

In many experiments it was desirable to attempt to separate the electrons and holes created by the absorption of photons in the silver bromide so that their individual interactions with the sensitizing layers could be studied. This was done by mounting a condenser in contact with the surface of the specimen and applying voltage pulses synchronized with the light pulses. The use of the condenser arrangement obviated difficulties which would otherwise arise from the separation of silver and bromine due to electrolysis of the silver bromide.

The condenser was constructed as follows. The surface of the specimen was covered with a very thin uniform cleavage plate of mica and two pieces of silver foil were placed in position. They were used as electrodes for applying the voltage pulses and their edges defined the slit through which the specimen was illuminated. They were covered with a further thin sheet of mica and the condenser thus formed was pressed into gentle contact with the surface of the specimen with a section of a 3 in. by 1 in. slide and two clips.

The voltage pulses, which were of square topped form, were produced by deflecting a fraction of the focussed beam emerging from the rotating slotted disc on to a photelectric cell and then amplifying the output with a pulse shaping circuit to give voltage pulses, synchronized with the light pulses, with a constant maximum amplitude of 500 to 1 000 volts and a width of 50 microseconds.

Development of the Specimens

Many different developers were used during the early stages of the investigation and the results of experiments on development will be reported in another paper (Keith and Mitchell, to be published).

The specimens from which the photomicrographs reproduced in this paper were prepared were all developed in the following solution for times between 30 seconds and four minutes :

Metol	0·67 g
Sodium sulphite (anhydr)	26 g
Hydroquinone	2·5 g
Sodium carbonate (anhydr)	26 g
Potassium bromide	0·67 g
Gelatine	1·67 g
Water to make	1 000 cc.

The gelatine was swelled in cold distilled water and then dispersed in hot water before being added to the solution of the remaining chemicals. The addition of gelatine to the developer caused a slight reduction in the surface density of fog specks. A further slight reduction could be effected by the addition of pinacryptol yellow and of certain antifoggants but these were seldom used.

Mounting of Specimens

After development, the specimens were thoroughly washed in a slow stream of distilled water, dried and mounted either in Styrax mounting medium, or in Canada Balsam dissolved in xylene, and protected with a cover glass.

§ 3. Experimental Results

Experiments with Non-sensitized Crystals of Pure Silver Bromide

The aim of the first series of experiments was to establish whether a latent image was formed in a crystal of pure silver bromide when it was exposed to light with a wave-length in the absorption band. The results proved that a latent image was always formed and that its distribution between the surface and the interior depended upon the physical properties of the crystal.

Single crystals which had been annealed within 20° of the melting point until no further changes occurred gave only a weak internal image ; a developable surface latent image was formed over a considerable range

of exposures. The internal image could be revealed by treating the surface with a dilute solution of potassium cyanide, and developed after thorough washing of the surface with distilled water; it was formed only in the immediate neighbourhood of the surface. Prolonged exposures caused the appearance, at the surface, of thread-like or filamentary growths of silver and of etch pits. The exposed region of a well annealed crystal could always be developed with a normal surface developer.

A latent image was never formed at the surface when unsensitized, strained or polygonized crystals were exposed to light. The experiments covered a wide range of exposures with varying intensities and exposure times and included exposures to very low intensities and to high intensity intermittent illumination. After development, the surface density of fog in the exposed region was always indistinguishable from that in the unexposed region.

The exposures, both to steady and to intermittent illumination, were therefore increased until a visible greenish-grey image of print-out silver was formed and the specimen was developed as before. In the exposed region, discrete specks of silver, which could be observed with the ultramicroscope, were formed both apparently at the surface and beneath it. They were, however, unable to initiate the reduction of the silver bromide in their neighbourhood and thus did not constitute a surface latent image. This is illustrated in fig. 1 (Plate 17) which shows the boundary between the exposed and the unexposed region after development. It was observed that the density of fog was the same in the exposed and the unexposed regions (three fog specks only are reproduced in the figures), and that the particles of photolytic silver were ineffective as development centres. Only when the exposures were prolonged to the point where massive filamentary threads and particles of photolytic silver had separated, with partial disintegration of the surface due to extensive pitting, was there any enhancement in the surface developability of the exposed region; the effects then observed were quite different from those in other experiments in which a surface latent image was formed by a short exposure to light.

In a further series of experiments, the specimens were positioned on the stage of the microscope and the surface was illuminated with an intense orange red beam using the dark field illuminator of the ultramicroscope. It was first confirmed that the specimen was optically clear. The exposure was made through the vertical illuminator of the microscope and interrupted as soon as the first scattering centres were observed at the surface of the crystal. The surface was then developed but no trace of an image was ever found.

It was therefore assumed that all the particles of silver which were observed in these experiments were actually located beneath the surface. This was confirmed by treating the surface with warm nitric acid, which

instantly removed a thin film of silver, but, under the same conditions, left the particles of photolytic silver completely unchanged. The density of these particles decreased as the depth below the surface increased. They separated preferentially in the walls and networks of dislocations which form the boundaries of the polyhedral sub-structure and divide the crystal up into elements of almost identical crystallographic orientation (Hedges and Mitchell 1953). The revelation of this structure in a single crystal of silver bromide, annealed at a low temperature, through the separation of silver in the boundaries during the progress of a photolytic exposure is particularly striking when visual observations are made with the ultra-microscope and the illumination takes place through the vertical illuminator. It was observed that the pattern extended to ever increasing depth with increasing duration of exposure and that the particles in any particular region apparently ceased to grow after reaching a certain critical size. For a strained but partially polygonized specimen, the sub-structure is illustrated in fig. 2 (Plate 17) which is a photo-micrograph of the same region as fig. 1 with the microscope focussed 10 microns below the surface. The distribution of the internal silver in a polygonized specimen is shown in fig. 3 (Plate 18).

Continuing work on the hypothesis that the particles of silver of the print-out image were actually all below the surface, strained or polygonized specimens were exposed through a slit until a print-out image was produced and then treated for a minute with a very weak solution of potassium cyanide to dissolve the surface layer of silver bromide. They were then thoroughly washed and developed in the metol hydroquinone developer. A sharply defined dense black negative image (black in the exposed regions) of the slit was formed demonstrating clearly that the internal photolytic silver could initiate development when it was laid bare by treating the surface with a solvent for silver bromide. The exposed region could also be developed with the internal latent image developer used by Stevens (1942), and with the metol hydroquinone developer used throughout the present work after the addition of ammonium thiocyanate or sodium or ammonium thiosulphate.

Experiments were then made in which the exposure was steadily reduced until only the first traces of photolytic silver were observable in the ultra-microscope. An internal latent image could then be developed as before when the surface was first treated with a weak solution of potassium cyanide. Still shorter exposures which produced no visible change (the same as those which caused the formation of a negative surface latent image on surfaces of specimens sensitized with silver) gave a developable internal latent image, and there was no trace of a surface image. An exposed area of a polygonized specimen, developed after the dissolution of the surface layers of silver bromide with a dilute solution of potassium cyanide, is illustrated in fig. 4

(Plate 19). There were very few fog specks in the unexposed control area. It will be noted that the distribution of the internal development centres corresponds with the boundaries of the polygonized structure.

It was found that the internal image formed in strained and polygonized crystals was attacked by the same reagents and under the same conditions as the internal latent image in a photographic emulsion. It was, moreover, not attacked by dilute solutions of potassium ferricyanide. These are good reasons for believing that the large strained or polygonized single crystals of silver bromide provide a useful model for the microcrystals of the emulsion.

Summarizing, a surface latent image was only formed during the exposure of relatively perfect crystals of pure silver bromide which form a weak internal image. Taken in conjunction with the experiments on the surfaces of similar crystals covered with thin films of silver, which are described in the next section, the results with strained and polygonized specimens lead to the working hypothesis that a surface latent image is not formed because any silver which actually separated at the surface would trap a fraction of the positive holes corresponding to the electrons trapped to form the internal silver. In the annealed crystals, on the other hand, silver is formed as follows. A bromide ion occupying a kink site traps a positive hole; a bromine atom, or, in the case of a double event, a bromine molecule may then escape from the surface. This will leave one or two silver atoms to contribute to the latent image. It appears that the greatest density of reactive sites on the surface is associated with the structural imperfections which form the fog specks on development. The etch pits, already mentioned, which appear after prolonged photolytic exposures, are formed by the escape of bromine from these imperfections and the migration away of silver ions.

As a test of the above hypothesis, the surface was covered with a thin film of a 5% solution of semi-carbazide nitrate (an efficient halogen acceptor) and exposed through the vertical illuminator of the microscope. The specimens were then thoroughly washed and developed. An intense negative image was formed on the surface after an exposure of the same order as that required for a surface sensitized with a thin film of silver or of gold. Control experiments showed that the presence of a film of water in contact with the surface during exposure did not in any way facilitate the formation of a surface latent image. Further experiments with aqueous solutions of other halogen acceptors gave similar results; hydrazine hydrobromide, sodium nitrite, sodium sulphite and a number of strongly adsorbed organic halogen acceptors were used. This work establishes that a developable latent image can be formed on the surface by exposing the crystal while it is in contact with a solution with strong halogen accepting properties. An example is given in fig. 5 (Plate 19) which shows a surface developed after exposure under a 5% solution of semi-carbazide nitrate.

The negative results of all the experiments with crystals of pure silver bromide suggested that in strained or polygonized crystals any silver atoms which separated at the surface recombined with bromine atoms to form molecules of silver bromide. An attempt was therefore made to separate the electrons and the positive holes by exposing to intermittent light while synchronized voltage pulses were applied to the electrodes defining the slit (see the experimental section for details). Although it was anticipated that a developable surface latent image would be formed by the separation of silver under the anode and the escape of bromine under the cathode, the results of a long series of experiments were entirely negative. An internal latent image was, however, formed under the anode. This appears to indicate that, even under these conditions, any silver atoms which separate at the surface recombine with bromine atoms to form molecules of silver bromide.

Experiments with Silver Bromide Surfaces covered with Thin Films of Silver

The object of a second series of experiments was to determine the properties of silver bromide crystals covered with thin films of silver, which were condensed by allowing a beam of silver atoms to fall on the surface for a definite time. The evidence in the literature and recent experimental work at Bristol indicate that such films are built up from discrete particles consisting of groups of silver atoms (Holloway 1952). This will certainly be so in the present series of experiments where the surface density of silver atoms was usually less than that corresponding to a monolayer ; here the considerations of Reinders and Hamburger (1932, 1933) are relevant.

According to these ideas, a thin film of silver deposited from a beam of silver atoms upon the surface of a crystal of silver bromide should provide an accurate model of the surface latent image. The aim of the first experiment was therefore to find out whether the surface of a silver bromide crystal which was covered with a thin film of silver was reduced to metallic silver in the metol hydroquinone developer without previous exposure to light. A layer with 10^{15} atoms of silver/cm^2 was deposited while half of the surface of the crystal was protected from the beam with a straight edge. The presence of this layer caused immediate and rapid reduction of the surface of the silver bromide crystal in the developer. The boundary between the two parts of the surface is shown in fig. 6 (Plate 20). The silver produced by development could be dissolved away in nitric acid to reveal a heavily corroded silver bromide surface. A silver film with this mean surface density of silver atoms showed the same behaviour towards solutions of oxidizing agents such as chromic acid as does the surface latent image of a photographic emulsion. Although not providing conclusive proof, this evidence strongly suggests that the model which supposes that the surface latent image consists of a speck of silver on the surface of the grain is well founded.

The properties of surfaces covered with these fogging layers of silver were now studied in greater detail with particular regard to their interaction with electrons and holes in the first stage of a Gurney–Mott mechanism. A strip of silver with 10^{15} silver atoms/cm^2 was deposited across the centre of the specimen which was then exposed through a slit at right angles to the edge of the deposit and developed. With a very short and critically determined exposure, a negative image (black in exposed areas) was formed in the non-fogged illuminated part of the surface without any apparent change elsewhere. This image disappeared when the exposure was lengthened and an internal image was then formed and built up in the illuminated area. It was clear that the destruction of the surface image was due to the release of bromine associated with the formation of the internal image. At the same time, the width of the strip of silver decreased in the exposed part and increased in the unexposed part of the specimen. This is illustrated in fig. 7 (Plate 20) which shows the surface after development. The spreading of the developed area away from the edge of the silver deposit, which increases with the duration of the exposure, is particularly significant. An area near the edge of the image after development is shown at a higher magnification in fig. 8 (Plate 21). It will be noted that development centres have appeared on the surface which are clustered in groups. The fact that this surface latent image spreads steadily away from the strip of deposited silver with increasing exposure seems to demonstrate conclusively that even particles of silver on the surface which can act as development centres do not provide traps for electrons. If they did, there is no reason for supposing that a surface latent image would be formed anywhere except in the immediate neighbourhood of the strip of silver. It is clear from these experiments that the electrons are being captured by silver ions in the non-sensitized surface of the silver bromide rather than by the groups of silver atoms of the thin film of silver. When these experiments were repeated using polygonized material instead of strained material, it was found that the most effective trapping sites for the electrons were situated along the intersections of the boundaries of the internal polyhedral network with the surface of the crystal.

These observations agree well with a recent discussion of the role of structural imperfections in the formation of the latent image (Mitchell 1952 b). There are two causes for the narrowing of the original silver deposit in the exposed region ; first, trapping of positive holes or reaction with part of the bromine liberated during the formation of the internal latent image in the exposed area, and, secondly, reaction with a fraction of the bromine atoms, equivalent in number to the silver atoms which separate to form the latent image of the un-exposed area. A longer exposure causes the complete disappearance of the silver deposit in the exposed area and the sharp boundary which then divides the exposed area from the un-exposed area after development is shown in fig. 9

(Plate 21). It may be said that the silver deposit from this area is re-distributed as a result of the exposure, part of it forming the surface and internal latent images in the un-exposed region and part a fraction of the internal latent image in the exposed area. Many further experiments were designed to test these conclusions and of these only one which is particularly significant will be described.

In this experiment, a square array of circular spots of silver was produced on the surface of the crystal of silver bromide by allowing silver atoms from the atomic beam to pass through fine holes drilled in a mask of sheet nickel. As before, the mean surface density of silver atoms was $10^{15}/cm^2$. This density of silver atoms just ensures the developability of the surface of the crystal of silver bromide under the deposit. Two thirds of the specimen was covered with a straight edge and the remaining third exposed to light from a mercury vapour lamp for a few seconds and the specimen was then developed. This experiment was repeated many times with different exposures. It illustrates all the features which have been established for surfaces of crystals of silver bromide covered with thin films of silver. With a very short and critically determined exposure a negative surface latent image was formed in the exposed area without any perceptible change in the dimensions of the patches (which developed to a higher density) compared with an unexposed specimen. With longer exposures, the negative image disappeared, and there was a steady contraction in the size of the patches in the illuminated area accompanied by an increase in the diameters of the spots in the shadow area. From now on, an internal latent image was built up in the exposed area. This was followed by a steady decrease in the size of the spots nearer the straight edge and a corresponding increase in the size of those further away. The expansion of the spots illustrates clearly that electrons are being trapped by surface sites near their edges rather than by their constituent groups of silver atoms. The contraction of those near the illuminated area shows that holes are trapped by the silver atoms. The nett result of exposure to light is a redistribution of the silver of the deposited spots to form both a surface and an internal latent image. The fact that the expanded discs have sharply defined boundaries shows that any electrons trapped by surface sites away from the silver deposit recombine with positive holes diffusing into the shadow region so that there is no resultant photochemical effect. The development area associated with a patch of silver film can expand under the combined influence of diffusing electrons and positive holes because the original surface density of groups of silver atoms in the patch is greater than is necessary for the complete blackening of its area during development. Consequently, if electrons are trapped by sites on the surface near its edge and holes are trapped by groups of silver atoms associated with it, a subsequent motion of silver ions will result in the redistribution of the silver of the deposit with the expansion of the area of development. When strained or

polygonized single crystals are used for these experiments, a weak internal image is formed throughout the region in the shadow by the trapping of electrons by silver ions associated with dislocations. A dense negative internal image is then always formed in the illuminated area.

The next question which naturally presents itself is : can the surface of a crystal of silver bromide be sensitized for the formation of a surface latent image by a uniform layer of silver atoms with a lower surface density than that used in the previous experiments ? From the earliest days of the development of photographic science, it has been suggested that the sensitization of a silver halide emulsion depended, at least to a certain extent, upon a partial reduction of the surfaces of the microcrystals to metallic silver. The experiments of Lowe, Jones, and Roberts (1951) on reduction sensitization with stannous chloride establish that this type of sensitization is indeed likely to be found. In the present series of experiments, it was observed that when a uniform thin film of silver with a surface density of silver atoms of $10^{14}/cm^2$ was deposited on half of the surface of a silver bromide crystal, which was then developed without exposure to light, the surface density of fog was the same in the control region as in the sensitized region. This important result establishes that groups of silver atoms below a certain critical size do not act as development centres for normal surface development, a conclusion of considerable importance in discussions of the nature of the latent sub-image and of the formation of the latent image (see, for example, Burton 1946, Berg and Burton 1948). When a surface covered with a uniform deposit of silver was given a short exposure behind a slit, a negative latent image was formed. Figure 10 (Plate 22) shows the unexposed control area of a sensitized specimen after development and fig. 11 (Plate 22) shows the centre of the exposed area on the same specimen. Longer exposures caused the formation of a positive image of the slit. There was now a somewhat smaller density of fog specks in the exposed than in the unexposed control region and the edges of the shadow near the slit were outlined by a heavy deposit of developed silver. An internal latent image was formed in the exposed area. These experiments establish that the surface of the crystal of silver bromide can be sensitized for the formation of a surface latent image by the presence of a thin film of silver with a mean surface density of 10^{14} atoms/cm^2. This sensitizing film of silver was unaffected by water, but was destroyed by treatment with a dilute solution of potassium ferricyanide.

The experiments in which intermittent light pulses were used for illuminating the specimen while synchronized voltage pulses were applied to the silver electrodes defining the slit were now repeated with silver sensitized crystals. In all the experiments, a heavy deposit of silver was formed under the anode as shown in fig. 12 (Plate 23). This proves that the first stage in the formation of the latent image in a silver sensitized crystal depends upon a displacement of electrons. The holes, in experiments on sensitized surfaces, will combine with silver atoms

to form silver ions which can drift towards the trapped electrons during the dark interval. It will be recalled that negative results were obtained when this experiment was attempted with a non-sensitized surface. In these and other experiments, it was observed that a grain boundary hinders the diffusion of electrons in polycrystalline material.

The whole of the evidence presented in this section is consistent with the conclusion that one function of the sensitizing layer of silver is to trap positive holes, or in other words, to combine with bromine atoms. Traps for electrons are always provided by silver ions associated with structural imperfections of the crystals, but, in the absence of chemical sensitization, the surface traps are ineffective because the trapping of electrons by them is followed by their recombination with positive holes. The evidence suggests that, with silver sensitized crystals, the formation of the latent image depends upon the redistribution of the finely dispersed silver of the sensitizing layer, silver atoms being effectively transferred to localized regions of structural imperfection on the surface and in the interior where silver ions provide traps for electrons. At the surface, the silver atoms will then condense upon nuclei provided by the groups of silver atoms of the sensitizing layer and transform these groups into development centres. The extended regions where there is a high local density of traps for electrons are thus to be regarded as the sensitivity centres in the sense in which both Sheppard and Gurney and Mott used the term.

Throughout the experiments in this section, exposures have been made to the total radiation from a tungsten strip filament lamp, to the total radiation from the mercury vapour lamps, and to the green line and the violet group of lines in the mercury vapour lamps. The slight differences which have been observed with these sources will require further and more detailed investigation to justify the space which would be required for their description. Here it is sufficient to state that all the effects described can be attributed to the liberation of mobile holes and electrons through the absorption of photons by the silver bromide.

Experiments with Silver Bromide Surfaces covered with Thin Films of Gold

The whole series of experiments, described in the previous section, with thin films of silver deposited on the surfaces of single crystals of silver bromide was now repeated with thin films of gold. Precisely the same observations were made and it appeared that the properties of the gold films were not significantly different from those of the silver films and that they had the same function in the formation of the surface latent image. A detailed description of the experimental observations is therefore unnecessary but a number of photo-micrographs will be included.

Figure 13 (Plate 23) shows a phenomenon which was observed in all the experiments with surfaces sensitized with thin films of gold but never in those with silver. After the development of a gold sensitized surface without previous exposure, a pattern of unresolved particles could be

observed on the surface with the microscope. This provides evidence to support the assumption that the thin film of gold used for sensitization consists of discrete particles. This subject is being further investigated, using physical developers for thin films of both gold and silver. Figure 14 (Plate 24) shows another area of the same gold sensitized specimen as fig. 13 after it had received a brief exposure; a negative image was formed. With gold as with silver sensitized surfaces, longer exposures caused the disappearance of the surface latent image, an internal image being formed in the exposed part, and the appearance of a positive surface latent image near the edges of the slit defining the illuminated area. Figure 15 (Plate 24) is a photo-micrograph of the central region of a fogging gold strip after part of it had been completely bleached by exposure through a slit. This should be compared with fig. 9. Figure 16 (Plate 25) shows a region near the edge of the positive surface image produced in an experiment of the type illustrated in figs. 7 and 8. The clustering of the development centres about particular sites on the surface is noteworthy. These sites lie approximately along the lines of intersection with the surface of the polyhedral sub-structure of the partially polygonized crystal of which the internal surfaces were active in the formation of the internal latent image. This is further evidence that silver ions associated with localized structural imperfections of the surface provide the most effective trapping sites for electrons.* A thorough study was made of the distribution of these trapping sites on the surfaces of crystals which had received different thermal treatments before strips of gold film were deposited upon them. A clear correlation emerged between the strain birefringence patterns, the distribution of fog specks, the centres of crystallization for microcrystals of silver bromide separating conformably on the surface from a supersaturated solution of silver bromide in hydrobromic acid, the regions of localized trapping of electrons on the surface and the polyhedral sub-structure revealed by photolytic exposures. This is an aspect of considerable importance in the application of the results of the present researches to corresponding phenomena in photographic emulsions.

Experiments with Surfaces covered with Thin Films of Metallic Sulphides

The technique which was used to deposit thin films of silver and of gold on the surfaces of crystals of silver bromide could not be directly applied to silver sulphide because of the low temperature at which this compound decomposes. Although the resultant sulphur and silver might be condensed in turn upon the surfaces, there was no likelihood that they would recombine at a reasonable rate, if at all, at low temperatures and an undesirable ambiguity would in any case be introduced by the presence of the silver. The whole range of metallic sulphides was therefore considered and thallous sulphide was selected as the sulphide with the properties most like those of silver sulphide

* This experiment furnishes a valuable method for determining the distribution of traps for electrons on the surface of a crystal of silver bromide.

which might be expected to sublime without decomposition at low temperatures. Antimony sulphide (Sb_2S_3) and the two arsenious sulphides, realgar (As_4S_4) and orpiment (As_4S_6) were also used. All these sulphides volatilize at low temperatures and the structures of the two arsenious sulphides have been determined in the vapour phase by the electron diffraction method (Lu and Donohue 1944 a, b). This is a considerable advantage in experimental work of this kind. The experiments with thin films of thallous sulphide are of particular interest. Particles of thallous sulphide may themselves be able to sensitize the surface. But even if thallous sulphide should react with silver bromide in the dry system before development, which seems unlikely, the product could only be an equivalent number of molecules of silver sulphide and thallous bromide. Thus, in either case, the existence of a type of sulphur sensitization in which the metallic sulphide is present on the surface of the crystal of silver bromide appears to be demonstrated. The four sulphides were prepared by placing the required amounts of spectroscopically pure metal and very pure coarsely crystalline sulphur in the two limbs of an inverted 'Y' tube made from transparent fused silica. The tube was then evacuated and sealed off from the pumping system. The metal was melted and heated until it was condensing freely at the top of its limb of the 'Y'. The sulphur was then heated and the two elements brought to reaction in this zone. At the end of the violent reaction, the fused sulphide was heated to a temperature of 800°C for a considerable time to complete the reaction. The tube was then tilted until an elongated globule was formed in one of the limbs. After crystallization, the thin rod was very readily broken up into a mass of fine cleavage fragments for the experiments. These will be described in turn, beginning with those on thallous sulphide.

A film of this substance could be deposited which did not cause any significant change in the surface density of fog specks on development. A short exposure of the sensitized surface to light resulted in the formation of a negative latent image and the centre of an exposed area after development is shown in fig. 17 (Plate 25). With strained or polygonized material, reversal, accompanied by the formation of an internal latent image, was caused by only slightly longer exposures. After normal surface development, the exposed part of the surface was then completely clear apart from a certain residual density of fog specks while a dense image was formed in the shadow regions near the edges of the slit. The surface was heavily fogged by thicker films of thallous sulphide and it was estimated on the basis of quantitative experiments that the transition occurred at a nominal thickness between one tenth and one monolayer.

The experiments, which have already been described for silver and gold, in which a strip of a thin film of the sensitizer of sufficient thickness to cause fog was deposited down the centre of the specimen which was then exposed with the illuminating slit at right angles to the edge of the deposit were now repeated with thallous sulphide. Precisely the

same observations were made as have already been detailed in the discussion of the corresponding experiments with thin films of silver. These experiments demonstrate that the particles of thallous sulphide of the thin films, just like the silver and gold particles do not trap electrons. There is equally clear evidence that the thallous sulphide provides traps for positive holes. If silver sulphide were present at the same surface molecular density, it could not be expected to have very different properties. The possibility that the sensitizing substance might react with bromine or with positive holes was not considered by either Sheppard and his co-workers or by Gurney and Mott.

The surface of a silver bromide crystal was also sensitized by a thin film of antimony sulphide. Figure 18 (Plate 26) shows an unexposed area of the surface after development and fig. 19 (Plate 26) another area of the same specimen developed after a very short exposure. As with thallous sulphide, a negative surface latent image was formed over a very short range of exposures, before reversal with the formation of a positive surface image and a negative internal image set in. The same observations were made with thicker fogging strips of antimony sulphide as were made with thallous sulphide, but still thicker layers of antimony sulphide completely protected the surface from the developer. Exactly the same observations were made with films of realgar (arsenious sulphide, As_4S_4). With increasing thickness, they sensitized, fogged and finally protected the surface from the developer. The molecules in the thinnest films of realgar did not act as effective traps for electrons but trapped positive holes or reacted with bromine atoms.

The outstanding substance of this group of metallic sulphides was orpiment (arsenious sulphide, As_4S_6). Thin films of orpiment sensitized the surface over a wide range of exposures for the formation of a negative latent image. Figure 20 (Plate 27) shows a sensitized surface developed without exposure. The presence of the sensitizing substance is evidenced by the distribution of unresolved diffraction discs. Figure 21 (Plate 27) is a photo-micrograph of the boundary between the exposed and the unexposed area on the same specimen, and fig. 22 (Plate 28) shows the central part of the exposed area. Orpiment was unique among the metallic sulphides investigated in that it did not cause the fogging of the surface at any film thickness, although as with antimony sulphide and realgar, thicker films protected the surface from the developer.

Its remarkable efficiency as a sensitizer for the surface latent image is probably accounted for partly by this fact, which permitted much thicker deposits to be used, partly by the relatively large potential combining power for bromine per molecule of orpiment and, lastly, partly by the possibility that orpiment acts as an optical sensitizer for the formation of the surface latent image. It is noteworthy that, with orpiment, atoms of sulphur will be in contact with the surface of the silver bromide when the molecule lies on the surface, whereas with the other sulphides used contact will be made by atoms of the metal. With surfaces sensitized with orpiment, very long exposures, sufficient to

produce a visible image of internal print out silver, were required for the reversed or solarization of the surface latent image.

Experiments with strips of deposits, thicker than were needed for chemical sensitization, gave the same results as had been obtained with silver, gold and the other metallic sulphides. They confirm the conclusion that the particles of the sulphide in the thin film do not provide effective traps for electrons although they trap positive holes or react with bromine atoms. As in the experiments with thin films of silver and gold, the electrons are trapped by silver ions associated with imperfect regions of the surface. It is worth remarking that in all the experiments with surfaces sensitized with thin films the exposure at which reversal of the surface latent image became evident depended upon the nature of the sensitizing layer and upon the extent to which an internal latent image was formed. Gold and arsenious sulphide proved to be the most effective sensitizing substances and fully annealed single crystals which formed very little internal image provided the best material for the formation of a surface latent image.

In all the experiments with strained or polygonized crystals it was evident that the chemical sensitizer was not fully effective because it was partly destroyed by bromine equivalent in amount to the silver which separated to form the internal latent image. The formation of an internal latent image which is not active in a normal developer is thus clearly undesirable. On the other hand, the traps for electrons which concentrate the separated silver atoms in localized regions of the surface in this series of experiments appear to be associated with the intersections with the surface of the cellular network of the polyhedral sub-structure upon which the internal latent image is formed.

§ 4. Conclusions

During the early stages of the formation of the latent image in chemically sensitized crystals, there is no photolysis of the silver bromide and bromine does not escape to the surroundings. The experimental results lead to the conclusion that the latent image is formed by the separation of an amount of silver, determined by the exposure, at the sensitivity centres and the reaction of a chemically equivalent amount of the sensitizer with bromine. In the case of reduction sensitization, exemplified in the present work by the deposition of a thin layer of silver on the surface of the crystal, this involves a redistribution of the silver of the sensitizing layer with its concentration at the sensitivity centres under the influence of light. The electrons are trapped by silver ions associated with localized regions of structural imperfection. Positive holes are trapped mainly by groups of atoms or molecules of the sensitizer, and when this is exhausted, a surface latent image is no longer formed with the high quantum efficiency characteristic of chemically sensitized crystals.

These experimental results clearly demand a revision of the theory of the formation of the surface latent image in silver bromide crystals in which the sensitizing substance is present on the external surface. The

observation that electrons are not trapped by particles of metallic sulphides is, at first sight, difficult to reconcile with the conclusions drawn by Lowe, Jones and Roberts (1951) on the effect of sulphur sensitization in altering the distribution of the latent image between the surface and the interior of the grain. This observation seemed adequately explained by the assumption, that the sensitivity specks, produced by sulphur sensitization, provided deeper surface traps for electrons than any present in the non-sensitized grains. It is clear, therefore, that an alternative explanation must be found for this effect of chemical sensitization and also for the other photographic effects which appeared to be satisfactorily accounted for by the Gurney–Mott theory.

Taken as a whole, the results provide clear evidence for the operation of the Gurney–Mott two stage mechanism in the formation of the latent image in large single crystals of silver halides. In the first—the electronic stage of the mechanism—electrons and positive holes are liberated by the absorption of photons in the silver bromide. Both then diffuse freely through the crystal until they either recombine or are trapped at separated sites. The trapping of the holes and electrons completes the electronic stage of the mechanism. It results in the creation of space charges which are then, in the second—the ionic stage of the mechanism—neutralized by the motion of silver ions from sites near where positive holes were trapped to sites where electrons were trapped.

The discussion of the formation of the latent image is complicated by the fact that its distribution between the surface and the interior of the silver bromide crystals depends upon the physical state of the crystals, on the nature of the sensitizing layers present upon their surfaces, and on the exposure.

The first topic which must be considered is the nature of the sensitivity centres. According to the experimental results, the sensitivity centres in both chemically non-sensitized and chemically sensitized crystals are provided by the same structural imperfections. In the crystals used in the experiments described in this paper, these imperfections are the boundaries of the internal three dimensional network of polyhedral elements and the two dimensional polygonal network formed by the intersection of this structure with the external surface of the crystal. Such a detailed model may not be possible in other cases. Internal concentrations of dislocations would, however, always provide internal sensitivity centres, and a number of structural imperfections of the surface with equivalent properties have already been described (Mitchell 1951 a, 1952 b). The sensitivity centres, thus envisaged, are extended structures, for instance dislocations (lines) or arrays of dislocations (surfaces). These provide regions of localized imperfections at the surface of the silver bromide crystal itself and also surfaces, within the crystal, where there are relatively high concentrations of silver ions occupying sites of low negative electrostatic potential. The sensitivity centres are not localized particles of foreign sensitizing substance which, as the

experimental evidence clearly demonstrates, do not provide traps for electrons and can therefore not play a primary role in the concentration of silver atoms.

Silver bromide is a surface ionic conductor at room temperature; mobile silver ions will therefore be present on both external and internal surfaces. There is no corresponding evidence for a motion of bromide ions, and this suggests that the free negative charge, equivalent to that of the mobile silver ions, will be fixed as excess bromide ions occupying kink sites on external surfaces or jogs along edge dislocations of internal surfaces.

A number of remarks will now be made on the trapping of holes and electrons in the first stage of the formation of the latent image. In chemically non-sensitized crystals, the positive holes will be trapped by bromide ions occupying kink sites on both the external surfaces and internal surfaces of the crystals. It is clear that the trapping of a positive hole to form a bromine atom on an internal surface can lead to no resultant photochemical effect because of ultimate recombination with an electron or with a separated silver atom. The trapping of positive holes by bromide ions occupying kink sites on the external surface, can, on the other hand, be followed by the escape of bromine as atoms or molecules from the surface, leaving a localized positive charge. The trapping of electrons by mobile silver ions or by silver ions occupying kink sites on the external surface will produce silver atoms which then provide effective traps for positive holes, as the experimental evidence clearly indicates. Thus the trapping of electrons by silver ions on the external surface will lead to their recombination with positive holes, while the trapping of positive holes by bromide ions of internal surfaces will be followed by their recombination with electrons. For a resultant photochemical effect bromine must escape from the surface of the crystal and this means that more positive holes than electrons must be trapped at the external surface with the result that the surface will acquire a positive charge. In the interior of the crystal more electrons must be trapped by silver ions on internal surfaces than positive holes by bromide ions occupying kink sites. Indeed, this excess number of electrons must be equivalent to the number of bromine atoms which escape from the surface. This means that there will be a positive charge at the surface of the crystal with an equivalent negative charge on the interior.

These space charges will now be neutralized by the drift of holes and electrons and of silver ions in the resulting field. The motion of the electronic carriers can lead only to recombination; but silver ions drifting to an internal surface will neutralize the space charge and leave silver atoms in the boundary. The efficiency of the formation of the internal latent image will therefore be determined by the rate of absorption of photons compared with the rate at which the space charges created by the trapping of the holes and electrons can be

neutralized by the motion of the defects of the lattice of silver ions. There can only be a very low efficiency for the formation of latent image at surface sensitivity centres in chemically non-sensitized crystals which form an internal latent image.

When there is no internal structural imperfection permitting the formation of an internal latent image, the escape of bromine from the surface of the crystal during exposure to light must lead to the formation of a surface latent image through the separation of silver atoms ; here, however, owing to recombination between positive holes and electrons, only a low quantum efficiency would be expected. This behaviour has been observed with well annealed crystals of very pure silver bromide.

These observations on the formation and distribution of the latent image in chemically non-sensitized grains are in agreement with the experimental results.

We have now to try to understand how chemical sensitization leads to a great increase in the overall efficiency with which a latent image is formed and to the formation of a surface latent image, even though, as already emphasized, the same numbers of both surface and internal traps for electrons are active as in the non-sensitized crystals. We believe that the solution of this problem is to be found in the following considerations.

In non-sensitized crystals, the electron is trapped at a sensitivity centre by a mobile silver ion or by a silver ion on a kink site. This normally occurs in the interior of the crystal because there are many more traps there. The positive hole will recombine unless it is trapped by a bromide ion occupying a kink site at the surface and bromine then escapes. Since illumination will set up a negative space charge in the interior with a positive charge at the surface by the processes just discussed, the trapping of holes at the surface will be a rare occurrence. The rate at which the internal latent image can be formed will be determined by the rate at which silver ions drift from the surface to the interior of the crystals to neutralize the negative space charge there.

In chemically sensitized crystals, on the other hand, as well as a limited number of traps for electrons, there will be a high surface density of traps for positive holes. During the initial stages of the exposure, some electrons are trapped in the interior, and a space charge is then set up which prevents further trapping there until it is neutralized by the motion of silver ions.

Electrons and holes can continue being trapped at the surface because this does not set up any field between the surface and the interior but only intense fields in the surface. The formation of silver at the surface rather than in the interior is favoured for the following reason. Before further electrons can be trapped at internal sensitivity centres, to form more silver atoms there, silver ions must drift to the sensitivity centres essentially from the surface ; the distance is relatively large and the effective field is small. At the surface, on the other hand, we are concerned

with the motion of silver ions in much more localized and therefore more intense fields between sites where electrons were trapped and sites where holes were trapped. It is clear that the neutralization of the space charges by the drift of ions will proceed much more rapidly on the surface so that in illuminated chemically sensitized crystals silver atoms will be able to separate at a higher rate at surface sensitivity centres than in the interior.

These arguments will no longer apply when a fraction of the silver atoms chemically equivalent to the amount of sensitizer on the surface has been concentrated at the sensitivity specks. The further trapping of electrons at the surface will then only result in their recombination with positive holes. The effective surface traps for positive holes will be provided by the concentration of silver atoms and the effective traps for the electrons by the silver ions of the internal surfaces. The resultant electrostatic field is now such that further exposure will result in the transference of the silver which initially formed the surface latent image at the sensitivity centres to the internal surfaces, where it will build up the internal latent image ; the quantum efficiency will however be low because of the recombination of many pairs of electrons and positive holes. This process appears to account satisfactorily for the observed disappearance of the surface latent image and the building up of the internal latent image with prolonged exposures, during the experiments. We believe that it leads to an explanation of the phenomenon of solarization and that the solarization of the surface latent image should be accompanied by an increase in the internal latent image.

If the rate of absorption of quanta greatly exceeds the rate at which the space charges of the surface layer can be neutralized by the motion of silver ions, more electrons will be trapped by silver ions on internal surfaces. Holes will still be trapped by atoms or molecules of the sensitizing substance on the external surface. The overall quantum efficiency for the separation of silver will fall ; a distributed surface latent image will be formed instead of a localized one, and the internal image will be increased.

The completion of the two stages of the formation of the latent image so far considered will result in the transference of silver atoms from the neighbourhood of groups of atoms or molecules of the sensitizing substance to the sensitivity centres to form a localized latent sub-image of silver atoms. These silver atoms will now slowly condense to larger aggregates by diffusion processes.

Although the experimental evidence demonstrates that, at room temperature, the silver ions associated with structural imperfections provide traps for electrons, which the groups of atoms or molecules of the sensitizing substance apparently do not, this must not be taken to imply that such groups, when associated with sensitivity centres (where, in the case of chemical sensitization in photographic emulsions, they

are indeed likely to be formed), have no role in the formation of the surface latent image other than that of trapping positive holes and directly or indirectly furnishing silver ions. It has been shown experimentally, in a very direct way, that there is a continuous change from a sensitizing layer to a fogging layer with increasing surface density of gold or silver atoms. With layers of which the thickness is less than that of a monatomic layer, this is almost certainly to be attributed to a steady increase in the size of the largest groups of atoms, because new nuclei are unlikely to be formed. Now we may reasonably assume that the sensitizing layers of silver and of gold consist of discrete groups of atoms just below the critical size required for a development centre. The diffusion of a silver ion to a kink site on the surface, where an electron had previously been trapped to form a silver atom, simply restores the kink site, leaving a silver atom in the neighbourhood. In the presence of mobile silver ions, a silver atom will also be mobile, and able to attach itself to one of the groups of sensitizing atoms or molecules. The initial grouping of silver atoms, which represents the first stage in the concentration of the silver at the sensitivity centre, has the properties usually associated with the surface latent sub-image. The attachment of these silver atoms to the groups of gold and silver atoms, which may occur for a considerable period after exposure, will transform the sensitizing centres into development centres with the formation of a stable surface latent image. As concentration centres, groups of atoms of silver and gold might be expected to be more effective than groups of molecules of metallic sulphides, but this is pure speculation. Groups of silver atoms may also be present on internal surfaces having been introduced in the case of the crystals used in the present work, by pre-exposure to light with a wavelength at the long wave edge of the absorption band. These may have the same role of collecting photochemically produced silver atoms to form the internal latent image as have the surface specks in the formation of the surface latent image. Such groups may also be introduced in the microcrystals of emulsions by precipitation and physical ripening under definite physico-chemical conditions.

The presence of nuclei provided by groups of atoms of silver or of gold, and possibly also of molecules of metallic sulphides, to which silver atoms can be added to transform them into development centres, will reduce the possibility of thermal dispersion which might occur if nuclei had to be formed from the beginning by the grouping of separated silver atoms in chemically-non-sensitized or inefficiently sensitized grains. Moreover, the presence of the sensitizing substance on the external surface will diminish the probability of recombination between the separated silver atoms of the surface latent image and positive holes or bromine atoms.

The groups of atoms and molecules of the sensitizing substance thus appear to have two main functions : (1) to provide nuclei for the condensation of silver atoms formed when electrons are trapped by silver ions

associated with the sensitivity centres even though the particles of sensitizing substance do not directly trap electrons; (2) to combine with positive holes and thus to prevent their recombination with electrons.

These mechanisms for the formation of the surface and the internal latent images in both chemically non-sensitized and chemically sensitized grains appear to be in good agreement with the experimental results. They can be applied to account for the observed distribution of the latent image between the surface and the interior of the crystals after different exposures. High and low intensity reciprocity failure, solarization, the Clayden effect, and the Herschel, Debot and Weigert effects will be discussed in another paper in which more experiments on the distribution and re-distribution of the latent image will be described.

It will be clear from this account of the conclusions drawn from the experimental work that although the details of the concentration speck theory of Sheppard and of the theory of the formation of the surface latent image of Gurney and Mott are not established, the final result of the exposure of the grain as far as the formation of the surface latent image is concerned is the same as would have been deduced by them. Their sensitivity speck, assumed to be a particle of silver or of silver sulphide whose primary function was to trap electrons has been replaced by a new concept, that of a localized yet extended region of surface structural imperfection or a growth structure in the case of the grains of an emulsion. The silver ions of this extended sensitivity centre trap the electrons. Yet, in the case of the microcrystals of the emulsion, these imperfect regions of the surface will provide the most reactive sites for attack by chemical reagents or for the adsorption of large molecules. Consequently the largest groups of atoms or molecules of the sensitizing substance are most likely to be formed there. These, as has been pointed out, can add to themselves the photochemically produced silver atoms to form the latent image which consists of a group of silver atoms exceeding a certain critical size. Here we see aspects of both the earlier theories. The essentially new idea, established by the present work, which was not included in these theories is that, before a surface latent image can be formed with any useful efficiency, traps must be provided for positive holes as well as for electrons and this is an important function of the chemical sensitizer. It is not sufficient to assume that bromine atoms will combine with molecules of gelatine adsorbed at the surface (compare, Mott 1948). Recent experiments have demonstrated that sensitivity for the formation of a surface latent image on large single crystals of the type used for the present work first appears after a period of digestion of the crystal with an 'inert' gelatine and the most probable result of this digestion is the formation of groups of silver atoms on the surface of the crystal. The experimental results thus do not fully support any previous theories. Most of these theories, if they survived for any length of time, contained certain elements of validity, and it is now possible to discern more clearly the contributions made by the different investigators. The

essential soundness of all the previous lines of theoretical development is fully established by the fact that they led to the working hypothesis which formed the basis of the present investigation. Working hypothesis are meant to be tested experimentally and their formulation is not to be regarded as an end in itself. The working hypothesis which has been outlined in this paper must in the same way be tested experimentally from as many aspects as possible and amended where necessary until it is generally acceptable or rejected when it has outlived its usefulness.

Acknowledgments

Professor N. F. Mott and Dr. W. F. Berg have made many critical comments during the progress of this work which have been of value in determining the design of experiments. We wish to thank J. Burrow and D. A. Jones for the assistance which they have rendered throughout the investigation. Their keen interest was particularly appreciated during the early stages when many difficulties were being encountered and little progress made. The work has been supported by a grant from the Kodak Research Laboratories, Harrow, which is gratefully acknowledged. The investigation has been carried out during the tenure of a University of Bristol Graduate Scholarship by J. M. Hedges.

References

Berg, W. F., 1947, *Reports on Progress in Physics*, **11,** 248.
Berg, W. F., and Burton, P. C., 1948, *Photo. J.*, **88B,** 84.
Berg, W. F., Marriage, A., and Stevens, G. W. W., *Photo. J.*, **81,** 413.
Burton, P. C., 1946, *Photo. J.*, **86B,** 62.
Cahn, R. W., 1950, *J. Inst. Metals*, **76,** 121.
Gurney, R. W., and Mott, N. F., 1938, *Proc. Roy. Soc.* A, **164,** 151.
Hedges, J. M., and Mitchell, J. W., 1953, *Phil. Mag.* [7], **44,** 223.
Holloway, D. G., 1952, *Ph.D. Thesis*, University of Bristol.
Kossel, W., 1927, *Gött. Nachr.* (Math. Phys. Kl.), 135.
Lowe, W. G., Jones, J. E., and Roberts, H. E., 1951, *Fundamentals of Photographic Sensitivity* (London : Butterworths), p. 112.
Lu, Chi-Sia, and Donohue, J., 1944 a, *J.A.C.S.*, **66,** 824 ; 1944 b, *Ibid.*, **66,** 818.
Mees, C. E. K., 1942, *The Theory of the Photographic Process* (New York : Macmillan), p. 138.
Mitchell, J. W., 1948, *Sciences et Industries photographiques* [2], **19,** 361 ; 1949 a, *Phil. Mag.* [7], **40,** 249 ; 1949 b, *Ibid.* [7], **40,** 667 ; 1951 a, *Bull. Soc. Roy. Sci. Liege*, **4,** 300 ; 1951 b, *Fundamentals of Photographic Sensitivity* (London : Butterworths), p. 242 ; 1952 a, *Photo. J.*, **92B,** 38 ; 1952 b, *Sciences et Industries photographiques* [2], **23,** 457.
Mott, N. F., 1941, *Photo. J.*, **81,** 62 ; 1948, *Ibid.*, **88B,** 119.
Pick, H., 1951, *Naturwiss.*, **38,** 323.
Reinders, W., and Hamburger, L., 1932, *Z. wiss. Phot.*, **31,** 32 ; 1933, *Ibid.*, **31,** 265.
Sheppard, S. E., Trivelli, A. P. H., and Loveland, R. P., 1925, *J. Franklin Inst.*, **200,** 51.
Stevens, G. W. W., 1942, *Photo. J.*, **82,** 42.
Stranski, J. N., 1928, *Z. phys. Chem.*, **136,** 259.

Fig. 1

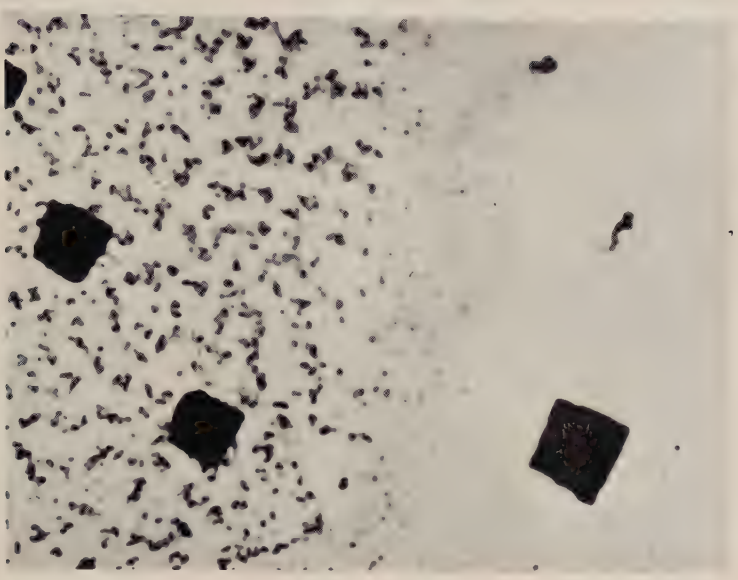

Exposed. Unexposed.

The surface of a strained and partly polygonized single crystal of silver bromide developed after prolonged exposure to the total radiation from a high pressure mercury vapour lamp. The photograph shows the boundary between the exposed region and the unexposed region. The photolytic silver did not initiate the development of the surface of the crystal. ×1120

Fig. 2

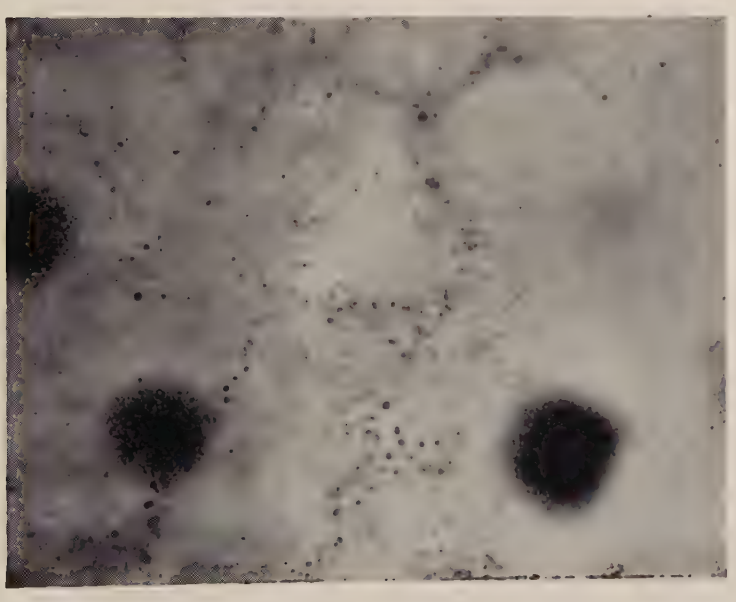

Exposed. Unexposed.

The same area as fig. 1 with the microscope focussed 10 microns below the surface. Note the concentration of the particles of photolytic silver upon the boundaries of the cellular sub-structure of the crystal referred to in the text. ×1120

Fig. 3

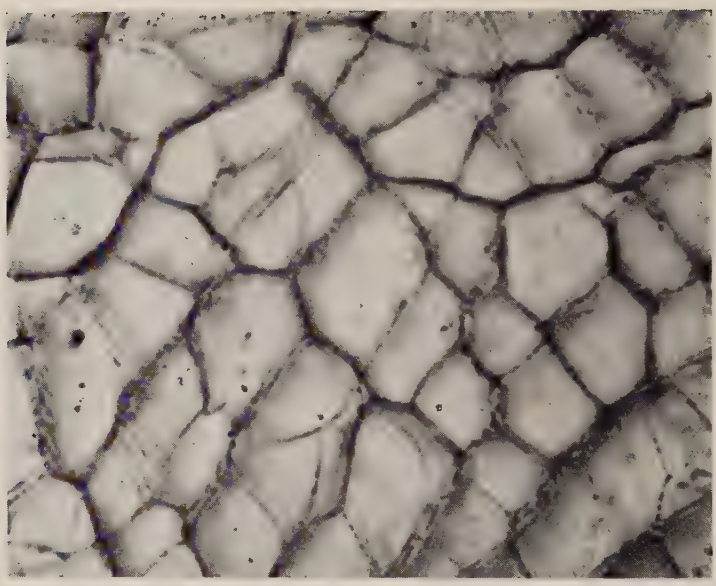

An area 10 microns below the surface of a single crystal of silver bromide photographed after a polyhedral sub-structure produced by low temperature annealing had been revealed by exposure to filtered radiation in the long wave tail of the absorption band of silver bromide. ×1120

Fig. 4

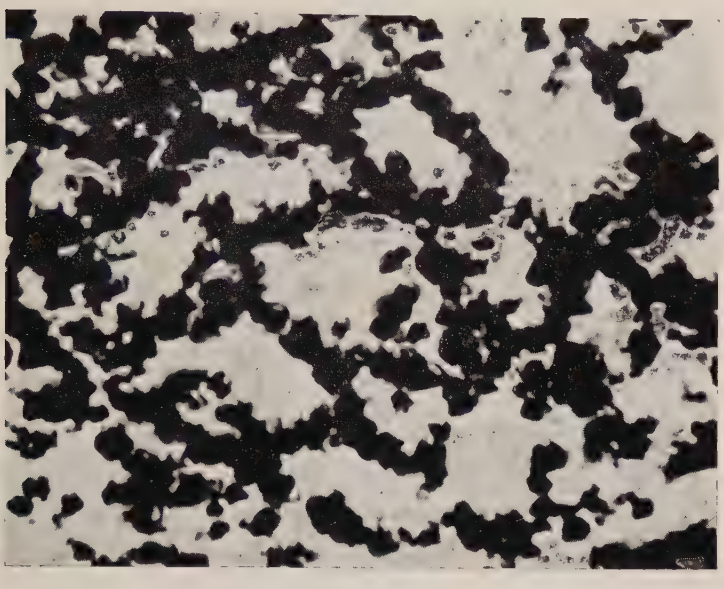

An area of a crystal of silver bromide from the same specimen as that of fig. 3 exposed and then developed after the dissolution of the surface layer of silver bromide in a very dilute solution of potassium cyanide. This demonstrates the existence of an internal latent image. It is to be noted that the development centres are associated with the boundaries of the polyhedral sub-structure. ×1120

Fig. 5

Exposed. Unexposed.

The boundary between the exposed area and the unexposed area of a crystal of silver bromide developed after exposure under a thin film of an aqueous 5% solution of semi-carbazide nitrate. A surface latent image was formed in the exposed area under these conditions. ×1000

Fig. 6

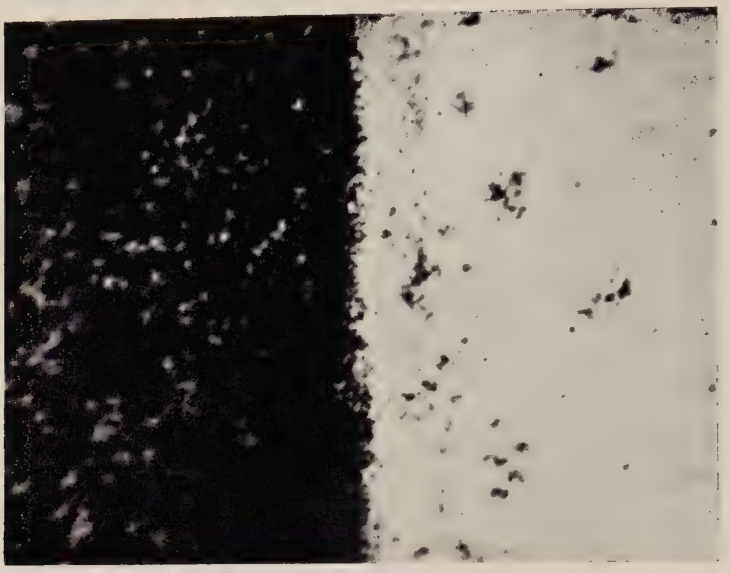

Silver film. No silver film.

The boundary between an area upon which a thin film of silver with an average surface atomic density of 10^{15} atoms/cm^2 had been deposited and an area which was protected from the atomic beam by a straight edge after development. This demonstrates that groups of silver atoms on the surface of a crystal of silver bromide can act as development centres. ×500

Fig. 7

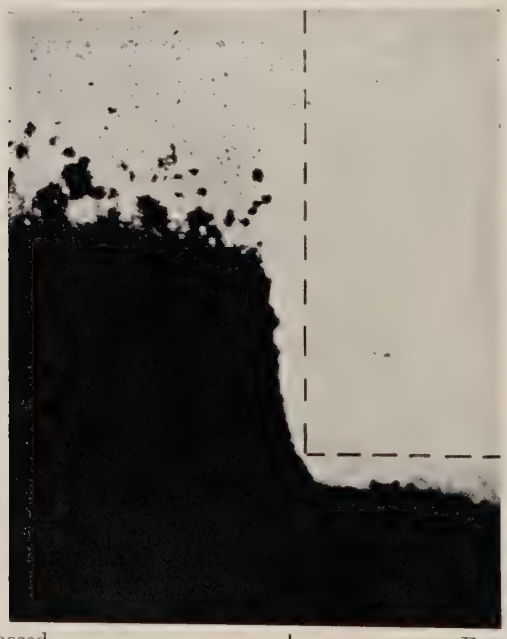

Unexposed. Exposed.

Edge of straight edge.

A thin film of silver in the form of a narrow strip was first deposited on the surface of the specimen and the original boundary of the strip is indicated by the horizontal dotted line. The specimen was now exposed to the total radiation from a mercury vapour lamp through a vertical slit, the position of one edge of which is indicated by the vertical dotted line. After development, it was observed that the silver strip had been partially bleached in the exposed area on the right while a positive surface latent image had formed in the shadow region on the left. The surprising observation was that this latent image spread steadily away from the edge of the strip as the exposure was prolonged. This seems to force the conclusion that silver ions, probably associated with structural imperfections on the surface provide more effective traps for electrons than particles of silver. ×112

Fig. 8

Wholly unexposed area.

An area near the edge of the positive surface latent image of fig. 7 photographed at a higher magnification. The clustering of the development centres about certain zones is to be noted. ×300

Fig. 9

Unexposed. Exposed.

A photomicrograph taken near the centre of a thin film of silver deposited in the form of a narrow strip and developed after prolonged exposure to the total radiation from a mercury vapour lamp through a slit at right angles to the strip. This demonstrates that the silver in the exposed area was bleached completely away. It should be remarked that an internal latent image was formed in the exposed region which could be developed after the partial dissolution of the surface of the crystal with a dilute solution of potassium cyanide. The thin films of silver used in the experiments illustrated in figs. 7, 8 and 9 had initially the minimum surface density of atoms (10^{15}/cm^2) required for the fogging of the surface. ×750

Fig. 10

Unexposed area.

The surface of a single crystal of silver bromide developed without previous exposure to light after the deposition of a thin film of silver with a surface density of 10^{14} silver atoms/cm^2 upon it. The density of fog was precisely the same as in a control area upon which no silver was deposited. This demonstrates that a thin film of silver can be present on the surface probably in the form of discrete groups of silver atoms without fogging the surface. This is an extremely important conclusion. ×1120

Fig. 11

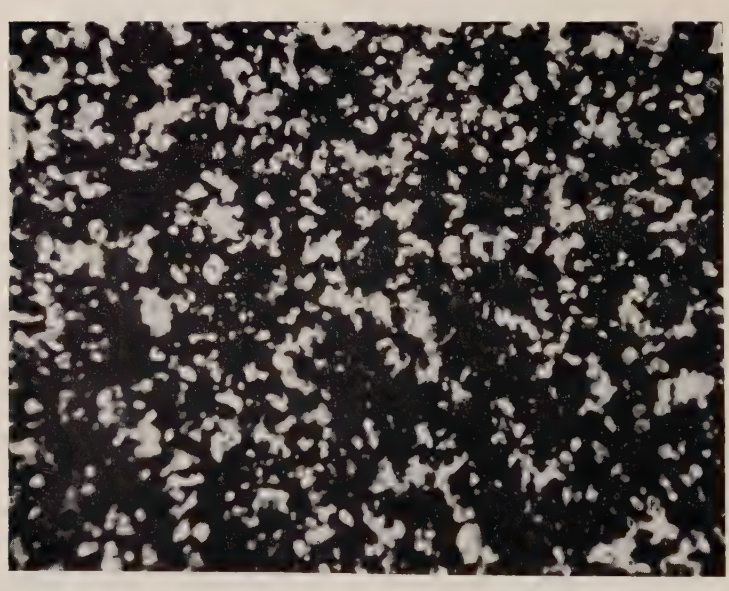

Exposed area.

Another area of the same sensitized single crystal of silver bromide as fig. 10 developed after a short exposure to the total radiation from a mercury vapour lamp. A negative surface latent image was formed. It is difficult to imagine that any process could have occurred other than the photochemical aggregation of the silver atoms to form particles of the same dimensions as those in the films with an average surface density of 10^{15} silver atoms/cm^2 which cause the surface to be developed without exposure to light. ×1120

Fig. 12

Unexposed area under anode. | Edge of slit and anode. Exposed.

A photomicrograph of the area of a silver sensitized surface under the anode in the experiment in which the surface was illuminated with pulses of light which fell on to a slit formed by two silver electrodes to which synchronized voltage pulses were applied. Development revealed that a surface latent image had been formed under the anode. This experiment provides definite evidence for the concept that the first stage in the formation of the surface latent image depends on a motion of electrons. ×450

Fig. 13

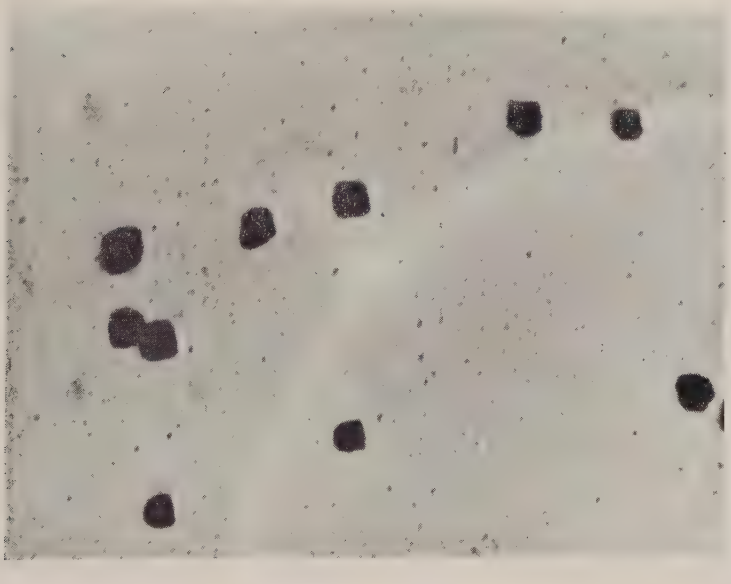

Unexposed area.

A section of the surface of a single crystal of silver bromide upon which a thin film of gold had been deposited developed without previous exposure to light. The distribution of discrete specks on the surface which was never observed in experiments on non-sensitized surfaces or on surfaces sensitized with thin films of silver is evidence of the presence of the sensitizing film of gold. ×1120

Fig. 14

Exposed area.

Another area of the same specimen as fig. 13 developed after a very short exposure to the total radiation from a mercury vapour lamp. A negative surface latent image was formed. ×1120

Fig. 15

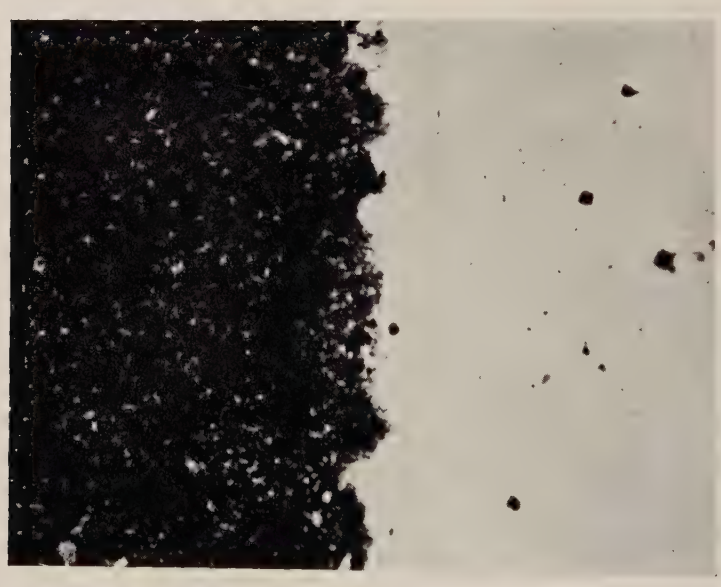

Unexposed. Exposed.

A photomicrograph of the central area of a strip of a thin film of gold developed after it had been exposed through a slit positioned at right angles to the strip. The gold was bleached in the exposed area and an internal latent image was formed there. The result of the same experiment with a thin film of silver of comparable thickness is illustrated in fig. 9. ×1120

Fig. 16

Wholly unexposed area.

Clusters of development centres near the edge of the positive surface latent image which formed in the shadow region during the experiment illustrated in fig. 15. The grouping of these centres about what are probably structural imperfections of the surface is well illustrated. ×1120

Fig. 17

Exposed area.

The surface of a specimen sensitized with thallous sulphide developed after a very short exposure to the total radiation of a mercury vapour lamp. The surface latent image shows reversal after comparatively short exposures on such sensitized surfaces. ×1120

Fig. 18

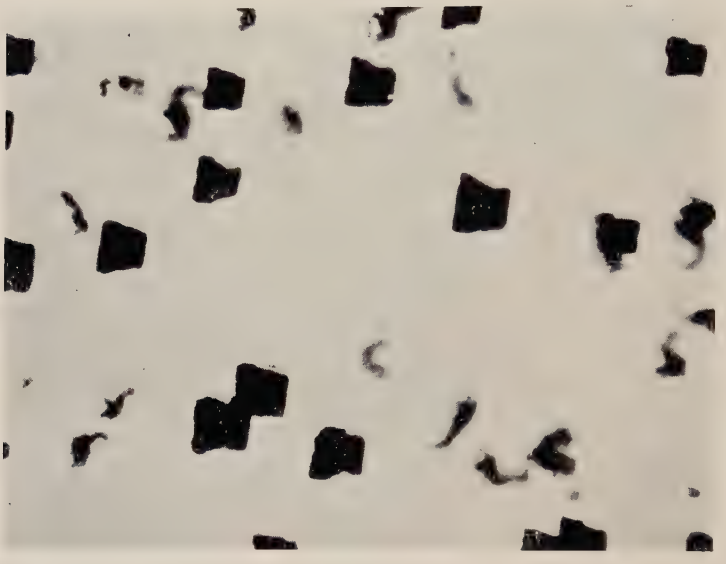

Unexposed.

The surface of a single crystal of silver bromide sensitized with a thin film of antimony sulphide (Sb_2S_3) developed without previous exposure to light. ×1120

Fig. 19

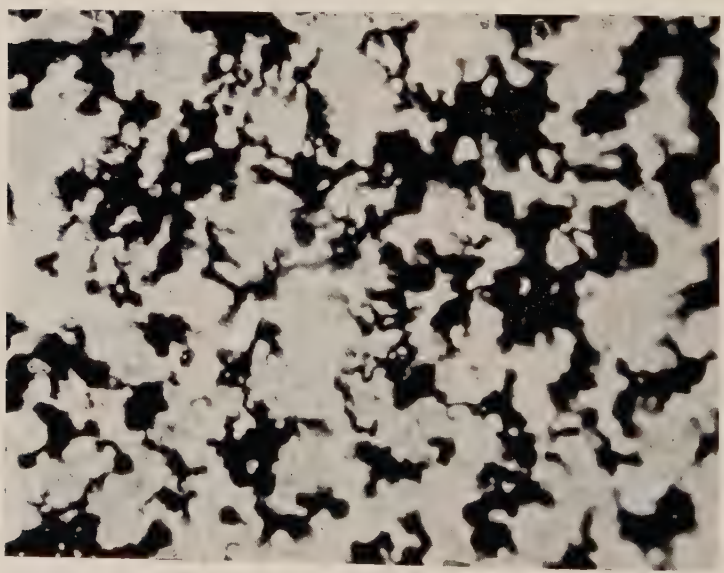

Exposed.

Another part of the surface of the same specimen as fig. 18 developed after a very short exposure to the total radiation from a mercury vapour lamp. ×1120

Fig. 20

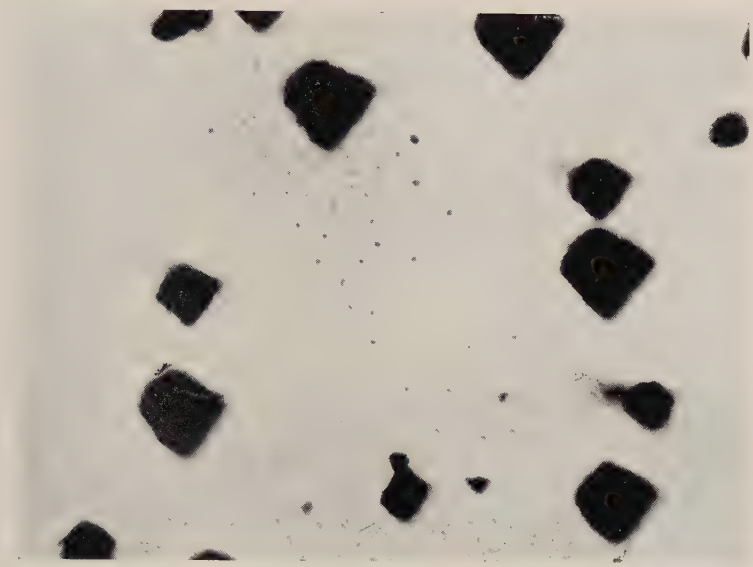

Unexposed.

The surface of a specimen sensitized with a thin film of orpiment (arsenious sulphide, As_4S_6) developed without previous exposure to light. Discrete specks appeared as with the gold sensitizing films illustrated in fig. 13. ×1120

Fig. 21

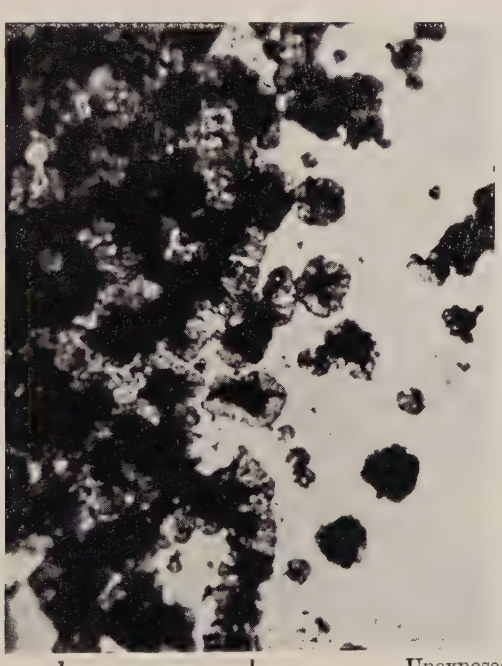

Exposed. | Unexposed.

Edge of slit.

The boundary between the exposed region and the unexposed region of a surface sensitized with orpiment. Even the shortest exposures produced a strong negative surface latent image. ×1000

Fig. 22

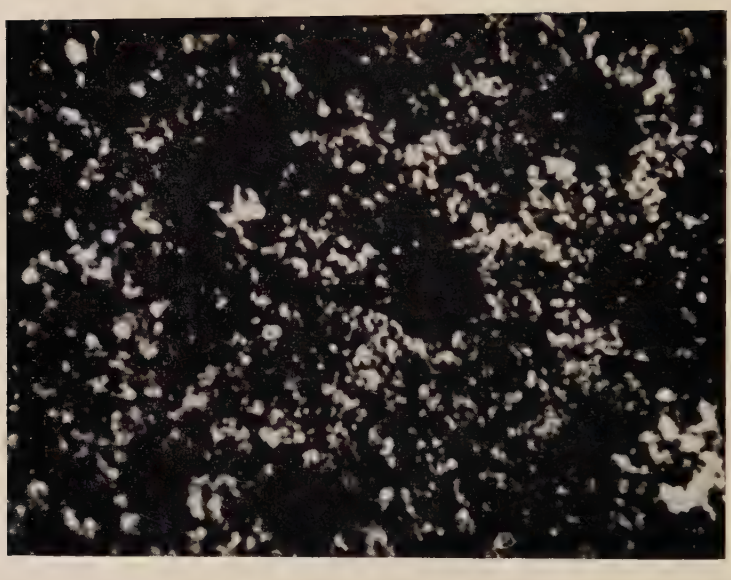

Exposed area.

A photomicrograph of the middle of the exposed area of the specimen of fig. 21. It was not possible to obtain a comparable density after the development of exposed surfaces sensitized with the other metallic sulphides of this series of experiments because of the early onset of the reversal of the surface latent image which was noted. ×1120

XLII. *The Laminar Boundary Layer of a Rotating Body of Revolution*

By C. R. Illingworth
Department of Mathematics, The University, Manchester, 13*

[Received January 8, 1953]

Abstract

By combining the von Mises and the Mangler transformations for laminar boundary layers, it is found that, in some cases, compressible boundary-layer flow round a rotating body of revolution can be correlated to an incompressible flow somewhat similar to plane boundary-layer flow. The boundary layer in conefield flow past a rotating circular cone is thereby considered in detail.

§ 1. Introduction

Although the theories of plane boundary layers and of axially symmetric boundary layers round non-rotating bodies of revolution are now well-developed, problems on rotating bodies of revolution such as spinning projectiles do not appear to have so far received much attention. This paper attempts to investigate the modifications to the aforesaid theories that are necessitated by introducing transverse flow due to the spin of the body of revolution.

The paper starts, in § 2, by assembling the equations of motion for the compressible boundary layer of a spinning body. Thereafter, it seems natural to introduce two transformations which have proved useful in previous work on non-rotating bodies and plane flow. The first of these is the Mangler transformation (Mangler 1948), which changes a given problem of compressible (or incompressible) flow round a non-rotating body into a corresponding problem in compressible (or incompressible) plane flow, and the second is the von Mises transformation, a transformation, which, among others, has been successful in changing certain cases of plane compressible flow into corresponding incompressible flow problems (Illingworth 1949). These two transformations are used simultaneously in § 3 to correlate the compressible flow with uniform main stream round a spinning body to an incompressible ' plane ' flow.† In § 4, by solving the ' plane ' flow, information is obtained about the boundary layer on a spinning circular cone in a supersonic stream (with conefield flow). It is found that in ballistic applications the effect of the spin on the boundary layer is small, so that the primary (longitudinal) flow can be found just as if the body were not rotating, and afterwards the secondary (transverse) flow due to the spin can be determined. The actual procedure to be used

* Communicated by Professor M. J. Lighthill.

† By this is meant a velocity field and a temperature field described by artificial equations having the characteristics of the boundary-layer equations in incompressible plane flow.

in such cases of relatively slow rotation is discussed in § 5. Finally, in the Appendix, the relationship between the compressible axially-symmetric flow and incompressible 'plane' flow for non-uniform main streams is investigated. Correlations are found to exist for certain main-stream velocity distributions.

§ 2. Equations of Flow

We choose non-rotating coordinates x, y, with x representing distance measured along a meridian curve from the nose of the body and y representing distance along the normal; $r(x)$ is the radius of the body at the station x. With u, v representing the x and y components of velocity, and w the transverse component due to spin, the equations of steady flow in the boundary layer are

$$\frac{\partial}{\partial x}(r\rho u)+\frac{\partial}{\partial y}(r\rho v)=0, \quad . \quad . \quad . \quad . \quad . \quad . \quad . \quad (1)$$

$$\rho\left(u\frac{\partial u}{\partial x}+v\frac{\partial u}{\partial y}-\frac{w^2}{r}\frac{dr}{dx}\right)=\rho_1 u_1\frac{du_1}{dx}+\frac{\partial}{\partial y}\left(\mu\frac{\partial u}{\partial y}\right), \quad . \quad . \quad (2)$$

$$\rho\left[u\frac{\partial(rw)}{\partial x}+v\frac{\partial(rw)}{\partial y}\right]=\frac{\partial}{\partial y}\left[\mu\frac{\partial(rw)}{\partial y}\right], \quad . \quad . \quad . \quad . \quad (3)$$

$$\rho\left(u\frac{\partial i}{\partial x}+v\frac{\partial i}{\partial y}\right)+u\rho_1 u_1\frac{du_1}{dx}=\frac{1}{\sigma}\frac{\partial}{\partial y}\left(\mu\frac{\partial i}{\partial y}\right)+\mu\left[\left(\frac{\partial u}{\partial y}\right)^2+\left(\frac{\partial w}{\partial y}\right)^2\right], \quad . \quad (4)$$

and

$$\frac{\gamma-1}{\gamma}\rho i=p=p_1=\frac{\gamma-1}{\gamma}\rho_1 i_1. \quad . \quad . \quad . \quad . \quad . \quad . \quad (5)$$

Here, p, ρ and i denote pressure, density and specific enthalpy; σ is the Prandtl number, and μ is the viscosity. The suffix 1 refers to the main stream, where conditions depend only on x. In the main stream, Bernoulli's equation

$$i_1+\tfrac{1}{2}u_1^2=\text{const.}=h_1, \quad . \quad . \quad . \quad . \quad . \quad . \quad . \quad (6)$$

is satisfied.

As in the theory of plane flow, it is possible to some extent to correlate compressible and incompressible flows, by reducing the equations in certain circumstances to forms in which the density does not appear explicitly. One way of doing this is to use the von Mises transformation, which expresses the flow in terms of the independent variables x, ψ, the latter being the stream function defined by

$$r\rho u=\frac{\partial\psi}{\partial y}, \qquad r\rho v=-\frac{\partial\psi}{\partial x}. \quad . \quad . \quad . \quad . \quad . \quad . \quad (7)$$

These two relations replace (1). Since $\partial/\partial x$ becomes $\partial/\partial x-r\rho v\partial/\partial\psi$ and $\partial/\partial y$ becomes $r\rho u\partial/\partial\psi$, eqns. (2), (3) and (4) are transformed into

$$\rho\left(u\frac{\partial u}{\partial x}-\frac{w^2}{r}\frac{dr}{dx}\right)=\rho_1 u_1\frac{du_1}{dx}+r^2\rho u\frac{\partial}{\partial\psi}\left(\mu\rho u\frac{\partial u}{\partial\psi}\right), \quad . \quad . \quad (8)$$

$$\frac{\partial(rw)}{\partial x}=r^2\frac{\partial}{\partial\psi}\left[\mu\rho u\frac{\partial(rw)}{\partial\psi}\right], \quad . \quad . \quad . \quad . \quad . \quad . \quad (9)$$

$$\rho\frac{\partial i}{\partial x}+\rho_1 u_1\frac{du_1}{dx}=\frac{1}{\sigma}r^2\rho\frac{\partial}{\partial\psi}\left(\mu\rho u\frac{\partial i}{\partial\psi}\right)+r^2\mu\rho^2 u\left[\left(\frac{\partial u}{\partial\psi}\right)^2+\left(\frac{\partial w}{\partial\psi}\right)^2\right] \quad . \quad (10)$$

Just as for plane flow, in the special case $\sigma=1$, we can find a simpler alternative to the energy eqn. (10). This is obtained by adding (8), and (9) multiplied by w, to (10), whence

$$\frac{\partial h}{\partial x}=r^2\frac{\partial}{\partial\psi}\left(\mu\rho u\frac{\partial h}{\partial\psi}\right), \quad \ldots\ldots\ldots \quad (10\,a)$$

where $h=i+\frac{1}{2}(u^2+w^2)$ is the total specific energy in the boundary layer.

We now introduce non-dimensional dependent variables (indicated by bars) by means of

$$u=u_1\bar{u}, \qquad w=\omega r\bar{w}, \qquad i=i_1\bar{i}, \qquad h=h_1\bar{h}, \quad \ldots \quad (11)$$

where ω is the angular velocity of the rotating body. Then

$$\rho_1=\rho\bar{\imath}, \quad \ldots\ldots\ldots\ldots \quad (12)$$

because $\rho i=\rho_1 i_1$, from (5).

We also adopt the law that the viscosity varies as the absolute temperature, which implies that

$$\mu\rho=\mu_1\rho_1, \quad \ldots\ldots\ldots\ldots \quad (13)$$

yielding obvious simplifications in (8), (9) and (10). When the independent variable x is replaced by

$$s=\int_0^x r^2\mu_1\rho_1 u_1\,dx, \quad \ldots\ldots\ldots \quad (14)$$

our equations take their final forms

$$\frac{1}{u_1}\frac{du_1}{ds}(\bar{u}^2-\bar{\imath})+\bar{u}\frac{\partial\bar{u}}{\partial s}-\frac{\omega^2}{{u_1}^2}r\frac{dr}{ds}\bar{w}^2=\bar{u}\frac{\partial}{\partial\psi}\left(\bar{u}\frac{\partial\bar{u}}{\partial\psi}\right), \quad \ldots \quad (15)$$

$$\frac{\partial(r^2\bar{w})}{\partial s}=\frac{\partial}{\partial\psi}\left[\bar{u}\frac{\partial(r^2\bar{w})}{\partial\psi}\right], \quad \ldots\ldots\ldots \quad (16)$$

$$\frac{\partial\bar{\imath}}{\partial s}=\frac{1}{\sigma}\frac{\partial}{\partial\psi}\left(\bar{u}\frac{\partial\bar{\imath}}{\partial\psi}\right)+b\bar{u}\left[\left(\frac{\partial\bar{u}}{\partial\psi}\right)^2+\frac{\omega^2r^2}{{u_1}^2}\left(\frac{\partial\bar{w}}{\partial\psi}\right)^2\right], \quad \ldots \quad (17)$$

where $b={u_1}^2/i_1=(\gamma-1){M_1}^2$, M_1 being the Mach number of the main stream. When $\sigma=1$, (17) is replaced by

$$\frac{\partial\bar{h}}{\partial s}=\frac{\partial}{\partial\psi}\left(\bar{u}\frac{\partial\bar{h}}{\partial\psi}\right). \quad \ldots\ldots\ldots \quad (17\,a)$$

It is now proposed to discuss in the following sections various aspects of these equations that are naturally suggested by the well-established theory of plane flow, and axially symmetric flow round a non-rotating body.

§ 3. The Associated Incompressible 'Plane' Flow

Consider the equations

$$\frac{\partial U}{\partial X}+\frac{\partial V}{\partial Y}=0, \quad \ldots\ldots\ldots \quad (18)$$

$$U\frac{\partial U}{\partial X}+V\frac{\partial U}{\partial Y}-\frac{W^2}{R}\frac{dR}{dX}=U_1\frac{dU_1}{dX}+N_*\frac{\partial^2U}{\partial Y^2}, \quad \ldots \quad (19)$$

$$U\frac{\partial(RW)}{\partial X}+V\frac{\partial(RW)}{\partial Y}=N_*\frac{\partial^2(RW)}{\partial Y^2}, \quad \ldots\ldots \quad (20)$$

$$U\frac{\partial I}{\partial X}+V\frac{\partial I}{\partial Y}+UU_1\frac{dU_1}{dX}=\frac{N_*}{\sigma}\frac{\partial^2I}{\partial Y^2}+N_*\left[\left(\frac{\partial U}{\partial Y}\right)^2+\left(\frac{\partial W}{\partial Y}\right)^2\right]. \quad (21)$$

Although these equations do not appear to have a physical interpretation as they stand, we will nevertheless refer to them as equations of incompressible ' plane ' flow, because when $W=0$, (18), (19) and (21) are the equations of continuity, momentum and energy for the steady two-dimensional boundary-layer flow of an incompressible fluid round a cylinder. X and Y are coordinates measured along and perpendicular to the surface of the cylinder, U and V are the corresponding velocity components, N_* is the (uniform) kinematic viscosity, and the enthalpy I takes the value

$$I_1=H_1-\tfrac{1}{2}U_1^2$$

in the main stream, for which H_1 is the stagnation enthalpy.†

We first transform eqns. (18) to (21) by changing to s, ψ coordinates. We replace (18) by

$$LP_*U=\frac{\partial\psi}{\partial Y}, \qquad LP_*V=-\frac{\partial\psi}{\partial X}, \quad . \ . \ . \ . \ . \quad (22)$$

where P_* is interpreted as the (uniform) density of the incompressible fluid, and L is a representative length.

Then, with

$$s=L^2M_*P_*\int_0^X U_1\,dX, \quad . \ . \ . \ . \ . \ . \ . \quad (23)$$

where M_* is the uniform viscosity of the incompressible fluid, and with the non-dimensional variables

$$\bar{u}=U/U_1, \qquad \bar{w}=W/\Omega R, \qquad \bar{\imath}=I/I_1, \quad . \ . \ . \quad (24)$$

the eqns. (18) to (21) become

$$\frac{1}{U_1}\frac{dU_1}{ds}(\bar{u}^2-1)+\bar{u}\frac{\partial\bar{u}}{\partial s}-\frac{\Omega^2}{U_1^2}R\frac{dR}{ds}\bar{w}^2=\bar{u}\frac{\partial}{\partial\psi}\left(\bar{u}\frac{\partial\bar{u}}{\partial\psi}\right), \quad . \quad (25)$$

$$\frac{\partial(R^2\bar{w})}{\partial s}=\frac{\partial}{\partial\psi}\left[\bar{u}\frac{\partial(R^2\bar{w})}{\partial\psi}\right], \quad . \ . \ . \ . \ . \ . \ . \quad (26)$$

$$\frac{\partial\bar{\imath}}{\partial s}=\frac{1}{\sigma}\frac{\partial}{\partial\psi}\left(\bar{u}\frac{\partial\bar{\imath}}{\partial\psi}\right)+B\bar{u}\left[\left(\frac{\partial\bar{u}}{\partial\psi}\right)^2+\frac{\Omega^2R^2}{U_1^2}\left(\frac{\partial\bar{w}}{\partial\psi}\right)^2\right], \quad . \ . \quad (27)$$

where $B=U_1^2/I_1$.

Now (25), (26) and (27) are formally the same as (15), (16) and (17) except for one difference in the first terms of (15) and (25). The $\bar{\imath}$ in (15) is replaced by 1 in (25).

---

† Starting from the equations of compressible flow, with $W=0$, we obtain the incompressible flow equations mentioned provided that the Mach number M_1 of the main stream is small, the fractional change in absolute temperature between wall and main stream is also small, but comparable with M_1^2, and N_* is any kinematic viscosity representative of the flow, e.g. the value at the stagnation point in the main stream. In short, the incompressible equations are valid under the conditions

$$(I_0-I_1)/I_1=O(M_1^2), \qquad M_1^2\ll 1.$$

In the special case of a uniform main stream, u_1=const. and the first term in (15) is absent. Therefore if we choose

$$\left.\begin{aligned} U_1 &= u_1 \ (=\text{const.}), \\ I_1 &= i_1 \ (=\text{const.}), \\ \Omega &= \omega, \\ \text{and} \qquad R(s) &= r(s), \end{aligned}\right\} \qquad \ldots\ldots \quad (28)$$

it follows that $B=b$ and the two sets of s, ψ-equations are identical. Furthermore, the boundary conditions are, at $\psi=0$,

$$\left.\begin{aligned} &\bar{u}=0, \qquad \bar{w}=1, \qquad \bar{\imath}=\begin{cases} i_0(s)/i_1 & \text{(compressible case)} \\ I_0(s)/I_1 & \text{(incompressible case)} \end{cases} \\ &\text{and, at } \psi=\infty, \\ &\bar{u}=1, \qquad \bar{w}=0, \qquad \bar{\imath}=1, \end{aligned}\right\} \qquad (29)$$

which are the same in both cases if we choose

$$I_0(s)=i_0(s). \qquad \ldots\ldots \quad (30)$$

Of course, the wall enthalpy i_0 need not be uniform.

Hence, with the relations (28) and (30), the solution of the compressible flow may be found by obtaining $\bar{u}$, $\bar{w}$ and $\bar{\imath}$ from eqns. (18) to (21). This correlation is just the analogue of that for a flat plate in a uniform stream in plane flow.

It is hardly necessary to mention that the conditions of low speed and small temperature variation required for the physical interpretation of eqns. (18) to (21) given above are not at all necessary for the correlation we have established. For the purposes of this correlation, and of later ones, (18) to (21) are to be regarded simply as formal equations, as indeed the presence of W suggests.

There are other cases in which the two sets of s, ψ-equations can be made identical, but the discussion of these is postponed to the Appendix. Meanwhile, we shall examine the case of a uniform main stream in more detail.

§ 4. The Rotating Circular Cone in Supersonic Flow

When we recall that the earliest boundary-layer solutions in plane flow concerned a flat plate in a uniform stream, we should expect flow with a uniform main stream to yield one of the more elementary solutions for rotating bodies. Moreover, we have just seen in § 3 that this is one of the cases in which the equations of incompressible 'plane' flow can be utilized to provide the solution also for compressible flow. Now in the important case of a circular cone in a high-speed stream sufficiently supersonic for the shock to be attached to the tip of the cone, the main stream is uniform because conditions are uniform along each ray from the tip.

For a cone of semi-angle θ, $r(x)=x\sin\theta$. Now,

$$\frac{dX}{dx}=\frac{dX/ds}{dx/ds}=\frac{r^2\mu_1\rho_1u_1}{L^2M_*P_*U_1}=\frac{x^2\sin^2\theta}{L^2},$$

when M_*, P_*, U_1 are chosen to have the uniform values μ_1, ρ_1, u_1 respectively. Hence

$$X=\tfrac{1}{3}x^3\sin^2\theta/L^2, \quad . . . . . (31)$$

and

$$R(X)=r(x)=(3L^2\sin\theta\, X)^{1/3}. \quad . . . . . (32)$$

Accordingly, (18), (19) and (20) become, in this case,

$$\frac{\partial U}{\partial X}+\frac{\partial V}{\partial Y}=0, \quad . . . . . (33)$$

$$U\frac{\partial U}{\partial X}+V\frac{\partial U}{\partial Y}-\frac{W^2}{3X}=N_*\frac{\partial^2U}{\partial Y^2}, \quad . . . . (34)$$

and

$$U\frac{\partial W}{\partial X}+V\frac{\partial W}{\partial Y}+\frac{UW}{3X}=N_*\frac{\partial^2W}{\partial Y^2}. \quad . . . . (35)$$

Now, (33) is satisfied if

$$U=\partial\Psi/\partial Y, \qquad V=-\partial\Psi/\partial X.$$

With

$$\Psi=(U_1N_*X)^{1/2}\sum_{n=0}^{\infty}\xi^n f_n(\eta), \quad . . . . . (36)$$

where $\xi=\Omega^2R^2/{U_1}^2$ and $\eta=\frac{1}{2}(U_1/N_*X)^{1/2}Y$,

$$U=\tfrac{1}{2}U_1\sum_{n=0}^{\infty}\xi^n f_n'(\eta), \quad . . . . . (37)$$

and

$$V=-(U_1N_*/X)^{1/2}\sum_{n=0}^{\infty}\xi^n[(\tfrac{2}{3}n+\tfrac{1}{2})f_n(\eta)-\tfrac{1}{2}\eta f_n'(\eta)], \quad . . (38)$$

where dashes denote $d/d\eta$. The boundary conditions on the f_n are

$$\left.\begin{aligned} f_n(0)=f_n'(0)=0\,; \\ f_0'(\infty)=2, \qquad f_n'(\infty)=0 \qquad (n\neq0). \end{aligned}\right\} \quad . . . . (39)$$

Let

$$W=\Omega R\sum_{n=0}^{\infty}\xi^n g_n(\eta), \quad . . . . . (40)$$

with the boundary conditions

$$\left.\begin{aligned} g_0(0)=1, \qquad g_n(0)=0 \qquad (n\neq0)\,; \\ g_n(\infty)=0. \end{aligned}\right\} \quad . . . . (41)$$

Then, (34) is satisfied if

$$f_0'''+f_0f_0''=0, \quad . . . . . (42)$$

$$f_1'''+f_0f_1''-\tfrac{4}{3}f_0'f_1'+\tfrac{7}{3}f_0''f_1=-\tfrac{8}{3}{g_0}^2, \quad . . . . . (43)$$

$$f_2'''+f_0f_2''-\tfrac{8}{3}f_0'f_2'+\tfrac{11}{3}f_0''f_2=-\tfrac{7}{3}f_1f_1''+\tfrac{4}{3}{f_1'}^2-\tfrac{16}{3}g_0g_1, \quad . (44)$$

etc., and (35) is satisfied if

$$g_0''+f_0g_0'-\tfrac{4}{3}f_0'g_0=0, \quad . . . . . (45)$$

etc.

$$g_1''+f_0g_1'-\tfrac{8}{3}f_0'g_1=\tfrac{4}{3}f_1'g_0-\tfrac{7}{3}f_1g_0', \quad . . . . (46)$$

Now, eqn. (42) together with (39) shows that $f_0(\eta)$ is Blasius's function, which has been tabulated by Howarth (1938). Each of the following

equations in the order (45), (43), (46), (44), etc. is linear, involving one dependent variable and coefficients that depend upon the solutions of the previous equations. The only trouble in the numerical solution of each of these equations arises from the two-point boundary conditions. Consider (45) for example. It is necessary to integrate this equation twice, first with $g_0'(0)=0$ and secondly with $g_0'(0)=1$. The two solutions $(g_0)_1$, $(g_0)_2$ are then combined to give

$$g_0=[\lambda(g_0)_1+(g_0)_2]/[\lambda+1], \qquad \text{where} \qquad \lambda=-[g_0(\infty)]_2/[g_0(\infty)]_1.$$

Similarly,

$$f_1=[\lambda(f_1)_1+(f_1)_2]/[\lambda+1], \qquad \text{where} \qquad \lambda=-[f_1'(\infty)]_2/[f_1'(\infty)]_1,$$

in which $(f_1)_1$, $(f_1)_2$ are the solutions of (43) with $f_1''(0)=0$, 1 respectively. Only the equations actually written down above have been solved, but they suffice to give a rough indication of the relative importance of successive terms in the series. The solutions are recorded in the table.

The skin frictional force component along the generators of the cone is

$$\tau_x(x)=\left(\mu\frac{\partial u}{\partial y}\right)_{y=0}=\mu_1\rho_1{u_1}^2\,x\sin\theta\left(\bar{u}\frac{\partial\bar{u}}{\partial\bar{\psi}}\right)_{\psi=0}.$$

In the corresponding flow in the X, Y-plane, the X-component of skin friction is

$$T_X(X)=M_*\left(\frac{\partial U}{\partial Y}\right)_{Y=0}=M_*P_*{U_1}^2L\left(\bar{u}\frac{\partial\bar{u}}{\partial\bar{\psi}}\right)_{\psi=0},$$

so
$$\tau_x(x)=\frac{x\sin\theta}{L}M_*\left(\frac{\partial U}{\partial Y}\right)_{Y=0}=\frac{1}{4}\left(\frac{3\mu_1\rho_1{u_1}^3}{x}\right)^{1/2}\sum_{n=0}^{\infty}\xi^n f_n''(0), \quad . \quad (47)$$

where
$$\xi=\Omega^2R^2/{U_1}^2=\omega^2r^2/{u_1}^2.$$

This may be expressed by means of a drag coefficient f_R in terms of the Reynolds number for a slant length l of the cone, viz.

$$f_R=D/(\rho_1{u_1}^2l^2\sin^2\theta), \qquad \text{where} \qquad D=2\pi\sin\theta\cos\theta\int_0^l\tau_x(x)\,x\,dx.$$

This gives

$$f_R=\cot\theta(Re)^{-1/2}\left[2{\cdot}4092+0{\cdot}6900\frac{\omega^2l^2\sin^2\theta}{{u_1}^2}-0{\cdot}0531\frac{\omega^4l^4\sin^4\theta}{{u_1}^4}+\ldots\right], \quad . \quad . \quad . \quad (48)$$

where $Re=\rho_1u_1l/\mu_1$ is the Reynolds number.†

Similarly, the transverse component of skin friction reducing the spin of the cone is

$$\tau_z(x)=-\left(\mu\frac{\partial w}{\partial y}\right)_{y=0}=-\mu_1\rho_1u_1\omega x^2\sin^2\theta\left(\bar{u}\frac{\partial\bar{w}}{\partial\bar{\psi}}\right)_{\psi=0}$$
$$=-\frac{x\sin\theta}{L}M_*\left(\frac{\partial W}{\partial Y}\right)_{Y=0}=-\tfrac{1}{2}(3\mu_1\rho_1u_1x)^{1/2}\,\omega\sin\theta\sum_{n=0}^{\infty}\xi^n g_n'(0). \quad (49)$$

† It is often convenient to use the velocity of the cone and the density and viscosity of the undisturbed air ahead of the cone as the representative quantities instead of u_1, ρ_1 and μ_1.

η	f_0	f_0'	f_0''	f_1	f_1'	f_1''	f_2	f_2'	f_2''	g_0	g_0'	g_1	g_1'
0	0	0	1·3282	0	0	0·8876	0	0	−0·1074	1	−0·9796	0	−0·1161
0·1	0·00664	0·1328	1·3280	0·00401	0·0763	0·6461	−0·00053	−0·0106	−0·1045	0·9023	−0·9711	−0·0114	−0·1109
0·2	0·02656	0·2655	1·3259	0·01453	0·1308	0·4507	−0·00211	−0·0207	−0·0966	0·8063	−0·9471	−0·0219	−0·0978
0·3	0·05974	0·3979	1·3203	0·02958	0·1677	0·2952	−0·00465	−0·0298	−0·0850	0·7133	−0·9098	−0·0308	−0·0799
0·4	0·10611	0·5294	1·3096	0·04762	0·1909	0·1733	−0·00803	−0·0376	−0·0709	0·6247	−0·8613	−0·0378	−0·0596
0·5	0·16557	0·6596	1·2920	0·06741	0·2033	0·0793	−0·01213	−0·0440	−0·0556	0·5414	−0·8040	−0·0427	−0·0389
0·6	0·23795	0·7876	1·2664	0·08801	0·2075	0·0078	−0·01678	−0·0488	−0·0401	0·4641	−0·7402	−0·0456	−0·0192
0·7	0·32298	0·9125	1·2315	0·10870	0·2055	−0·0457	−0·02183	−0·0520	−0·0251	0·3935	−0·6721	−0·0466	−0·0014
0·8	0·42032	1·0335	1·1867	0·12896	0·1988	−0·0854	−0·02713	−0·0538	−0·0111	0·3298	−0·6018	−0·0460	+0·0138
0·9	0·52952	1·1495	1·1317	0·14836	0·1888	−0·1141	−0·03254	−0·0543	+0·0015	0·2731	−0·5312	−0·0440	+0·0258
1·0	0·65003	1·2595	1·0670	0·16663	0·1763	−0·1343	−0·03795	−0·0536	+0·0126	0·2235	−0·4623	−0·0409	+0·0346
1·1	0·78120	1·3626	0·9934	0·18356	0·1622	−0·1475	−0·04322	−0·0518	+0·0220	0·1806	−0·3966	−0·0372	+0·0403
1·2	0·92230	1·4580	0·9124	0·19903	0·1470	−0·1551	−0·04828	−0·0492	+0·0298	0·1440	−0·3351	−0·0330	+0·0432
1·3	1·07252	1·5449	0·8258	0·21295	0·1313	−0·1578	−0·05304	−0·0459	+0·0358	0·1134	−0·2790	−0·0286	+0·0436
1·4	1·23099	1·6230	0·7360	0·22529	0·1156	−0·1563	−0·05744	−0·0421	+0·0401	0·0880	−0·2287	−0·0243	+0·0421
1·5	1·39682	1·6921	0·6454	0·23607	0·1002	−0·1510	−0·06145	−0·0379	+0·0428	0·0674	−0·1846	−0·0203	+0·0391
1·6	1·56911	1·7522	0·5565	0·24535	0·0855	−0·1426	−0·06503	−0·0336	+0·0438	0·0509	−0·1467	−0·0165	+0·0352
1·7	1·74696	1·8035	0·4715	0·25320	0·0717	−0·1316	−0·06817	−0·0292	+0·0434	0·0379	−0·1147	−0·0132	+0·0307
1·8	1·92954	1·8467	0·3923	0·25974	0·0592	−0·1188	−0·07088	−0·0250	+0·0417	0·0278	−0·0883	−0·0104	+0·0261
1·9	2·11605	1·8822	0·3205	0·26509	0·0480	−0·1048	−0·07317	−0·0209	+0·0389	0·0200	−0·0668	−0·0080	+0·0216
2·0	2·30576	1·9110	0·2569	0·26939	0·0383	−0·0904	−0·07507	−0·0172	+0·0353	0·0143	−0·0497	−0·0061	+0·0175
2·1	2·49806	1·9339	0·2021	0·27279	0·0299	−0·0762	−0·07662	−0·0139	+0·0311	0·0100	−0·0364	−0·0045	+0·0138
2·2	2·69238	1·9517	0·1559	0·27542	0·0230	−0·0628	−0·07786	−0·0110	+0·0268	0·0069	−0·0262	−0·0033	+0·0107
2·3	2·88826	1·9654	0·1179	0·27743	0·0173	−0·0506	−0·07883	−0·0085	+0·0225	0·0047	−0·0185	−0·0023	+0·0080
2·4	3·08534	1·9756	0·0875	0·27893	0·0128	−0·0399	−0·07958	−0·0065	+0·0184	0·0031	−0·0129	−0·0017	+0·0059
2·5	3·28329	1·9831	0·0636	0·28003	0·0093	−0·0307	−0·08014	−0·0048	+0·0147	0·0020	−0·0088	−0·0011	+0·0043
2·6	3·48189	1·9885	0·0454	0·28082	0·0066	−0·0231	−0·08056	−0·0035	+0·0114	0·0013	−0·0059	−0·0008	+0·0030
2·7	3·68094	1·9923	0·0317	0·28138	0·0046	−0·0170	−0·08086	−0·0025	+0·0087	0·0008	−0·0039	−0·0005	+0·0021
2·8	3·88031	1·9950	0·0217	0·28176	0·0032	−0·0123	−0·08107	−0·0018	+0·0065	0·0005	−0·0025	−0·0003	+0·0014
2·9	4·07990	1·9968	0·0146	0·28203	0·0021	−0·0086	−0·08122	−0·0012	+0·0047	0·0003	−0·0016	−0·0002	+0·0009
3·0	4·27964	1·9980	0·0096	0·28220	0·0014	−0·0060	−0·08132	−0·0008	+0·0033	0·0002	−0·0010	−0·0002	+0·0006
3·1	4·47948	1·9987	0·0062	0·28232	0·0009	−0·0039	−0·08139	−0·0005	+0·0023	0·0001	−0·0006	−0·0001	+0·0004
3·2	4·67938	1·9992	0·0039	0·28240	0·0006	−0·0027	−0·08143	−0·0004	+0·0016	0·0001	−0·0004	−0·0001	+0·0002
3·3	4·87931	1·9995	0·0024	0·28245	0·0004	−0·0016	−0·08146	−0·0002	+0·0010	0·0000	−0·0002	−0·0001	+0·0001
3·4	5·07928	1·9997	0·0015	0·28248	0·0003	−0·0011	−0·08148	−0·0001	+0·0006				
3·5	5·27296	1·9998	0·0009	0·28251	0·0002	−0·0006	−0·08149	−0·0001	+0·0004				
3·6	5·47925	1·9999	0·0005	0·28253	0·0002	−0·0003	−0·08150	−0·0001	+0·0002				
3·7	5·67924	2·0000	0·0003	0·28254	0·0001	−0·0001							
3·8	5·87924	2·0000	0·0002										
3·9	6·07923	2·0000	0·0001										

The non-dimensional coefficient of the spin reducing torque is given by

$$f_I = 2\pi \sin^2\theta \int_0^l \tau_z(x) x^2\, dx/(\rho_1 u_1 \omega l^4 \sin^4\theta)$$

$$= \operatorname{cosec}\theta\, (Re)^{-1/2}\left[1{\cdot}5230 + 0{\cdot}1149\frac{\omega^2 l^2 \sin^2\theta}{u_1^2} + \ldots\right]. \quad . \quad (50)$$

In the formulae (48) and (50) for the two skin friction coefficients, the leading terms will be far more important than the succeeding ones in some ballistic applications. For, at the muzzle of a gun, $\omega l \sin\theta/u_1 = \pi u_\infty/n u_1$, where n is the rifling of the gun, u_x is the translational velocity of the conical projectile and u_1 is of course the velocity along the generators of the cone. Now values of n less than 15 hardly ever occur in practice, and one may take 2 as the maximum value of u_∞/u_1, so $\omega^2 l^2 \sin^2\theta/u_1^2$ initially will not exceed 0·2. This means that the second terms in (48) and (50) are, at most, 6% and 1·5% corrections of the leading terms, respectively. When all but the leading terms are neglected, we notice that $\tau_z/\tau_x = -[2g_0'(0)/f_0''(0)]\omega x \sin\theta/u_1 = 1{\cdot}48\ \omega x \sin\theta/u_1$, so the direction of the skin frictional force at any point on the cone is upstream of the relative velocity vector.

The variation of $\omega l \sin\theta/u_1$ in later stages of the flight of the projectile will depend upon the steepness of the trajectory and the axial moment of inertia of the projectile. There will certainly be cases where $\omega l \sin\theta/u_1$ increases with time (because the translational velocity falls off more rapidly than the angular velocity), as for example when a heavy projectile is fired almost vertically upwards.

It will be observed that there has been no need to consider the enthalpy distribution (and consequently no need to consider eqn. (21)) in determining the skin friction on the cone. If, however, any further information is required, such as the velocity distribution across the boundary-layer, it becomes necessary to stipulate the thermal condition of the cone and then to solve (21) for $\bar{\imath}$, in order to recover the y-coordinate from the equation

$$y = \frac{1}{\rho_1 u_1 x \sin\theta}\int_0^\psi \frac{\bar{\imath}}{\bar{u}}\, d\psi.$$

For example, consider the problem when thermal equilibrium has been attained so that no heat is being transferred between the wall and the gas. This is a problem analogous to that of Pohlhausen's flat plate thermometer (see *Modern Developments in Fluid Dynamics*, Vol. II, p. 627), and the enthalpy may be written

$$I = I_1 + \tfrac{1}{8}U_1^2 \sum_{n=0}^{\infty} \xi^n \theta_n(\eta), \quad . \quad . \quad . \quad . \quad . \quad . \quad (51)$$

where $\theta_n'(0) = 0$, $\theta_n(\infty) = 0$ for all n. This satisfies the appropriate form of (21) provided that

$$\frac{1}{\sigma}\theta_0'' + f_0\theta_0' = -2f_0''^2, \quad . \quad . \quad . \quad . \quad . \quad . \quad . \quad . \quad . \quad (52)$$

$$\frac{1}{\sigma}\theta_1'' + f_0\theta_1' - \tfrac{4}{3}f_0'\theta_1 = -\tfrac{7}{3}f_1\theta_0' - 4f_0''f_1'' - 8g_0'^2, \quad . \quad . \quad . \quad (53)$$

etc.

Equation (52) is precisely the differential equation solved by Pohlhausen, but the remaining equations are new. We may reasonably approximate in the ballistic problem by retaining only the leading term in the series $\sum_{n=0}^{\infty} \xi^n \theta_n(\eta)$. We have already found that this approximation is valid for the velocity distribution functions, and it is confirmed for the enthalpy by the special solution

$$I+\tfrac{1}{2}(U^2+W^2)=\text{const.}=I_1+\tfrac{1}{2}U_1^2=I_0+\tfrac{1}{2}\Omega^2R^2, \quad . \quad . \quad (54)$$

of the energy eqn. (21) when $\sigma=1$. For, from (54),

$$I_0=I_1+\tfrac{1}{2}U_1^2(1-\xi)$$

and if we retain only the leading term in this expression the error involved (in discarding ξ) is not greater than 20%.

It follows that an approximate expression for the equilibrium temperature t_0 on the rotating cone in a stream of temperature t_1 is given by

$$t_0=t_1\left[1+\frac{u_1^2}{8i_1}\theta_0(0)\right]=t_1[1+\tfrac{1}{8}(\gamma-1)M_1^2\alpha_2(\sigma)], \quad . \quad . \quad (55)$$

where $\alpha_2(\sigma)$ is tabulated on p. 630 of *Modern Developments in Fluid Dynamics*.

§ 5. The Case of Slow Rotation

The results obtained in the last section suggest that in some ballistic problems involving sharp nosed projectiles (whether entirely conical or only conical near the tip) it is only necessary to obtain the first terms in the series for the longitudinal and transverse velocity distributions. This is tantamount to neglecting the effects of transverse flow on the longitudinal motion (including the energy equation). In other words, the ballistic problem (at least for sharp nosed projectiles) is essentially one of slow rotation, and for slow rotations the centrifugal force field has a negligible effect on the longitudinal motion. The boundary-layer flow is mainly that round a non-rotating body of revolution and is described by eqns. (1), (2) and (4) without the terms involving w. The rotation will of course be gradually reduced, and to find the transverse component of the skin frictional force (which is responsible for reducing the rotation) it is necessary to solve the remaining eqn. (3) for w after the other three equations have been solved.

Now, eqns. (1), (2) and (4) without terms involving w are the equations of compressible plane boundary-layer flow except for the appearance of the factor r in each term of the continuity equation. For a non-uniform main stream, they are not easy to solve except under the special conditions, that

(i) $\sigma=1$,

(ii) there is no heat transfer at the wall,

and (iii) the viscosity is proportional to the absolute temperature.

We shall adopt these conditions here. When we change to s, ψ as independent variables and introduce non-dimensional dependent variables using

conditions (i) and (iii) (as in § 2) we obtain as the equations for slow rotation

$$\frac{1}{u_1}\frac{du_1}{ds}(\bar{u}^2-\bar{\imath})+\bar{u}\frac{\partial\bar{u}}{ds}=\bar{u}\frac{\partial}{\partial\psi}\left(\bar{u}\frac{\partial\bar{u}}{\partial\psi}\right), \quad \ldots\ldots \quad (56)$$

$$\frac{\partial}{\partial s}(i+\tfrac{1}{2}u^2)=\frac{\partial}{\partial\psi}\left[\bar{u}\frac{\partial}{\partial\psi}(i+\tfrac{1}{2}u^2)\right], \quad \ldots \quad (57)$$

and

$$\frac{\partial(r^2\bar{w})}{\partial s}=\frac{\partial}{\partial\psi}\left[\bar{u}\frac{\partial(r^2\bar{w})}{\partial\psi}\right]. \quad \ldots \quad (58)$$

Now, under condition (ii), the required solution of (57) is

$$i+\tfrac{1}{2}u^2=\text{const.}=h_1 \quad \ldots\ldots \quad (59)$$

which shows that at the wall the enthalpy has the uniform value $i_0=h_1$, when there is no heat transfer. From (59), we obtain $\bar{u}^2-\bar{\imath}=(1+\frac{1}{2}b)(\bar{u}^2-1)$, and so (56) is the same as (25) without the term involving $\bar{w}$ provided that†

$$\frac{u_1(s)}{a_1(s)}=\frac{U_1(s)}{A_*}, \quad \ldots\ldots \quad (60)$$

where a_1, A_* are the speeds of sound at a general point and at the stagnation point in the compressible main stream. Also, (58) is the same as (26) provided that

$$r(s)=R(s). \quad \ldots\ldots \quad (61)$$

Now, the boundary conditions on $\bar{u}$ and $\bar{w}$ are

$\bar{u}=0, \quad \bar{w}=1 \quad$ at $\quad \psi=0, \quad s>0, \quad$ and

$\bar{u}=1, \quad \bar{w}=0 \quad$ at $\quad \psi=\infty, \quad s>0, \quad$ and at $\quad s=0$ for all ψ,

whether we are considering the eqns. (56) and (58), or (25) and (26). Hence, it follows that we can determine the functions $\bar{u}, \bar{w}$ for compressible flow round a slowly rotating body by solving

$$\frac{\partial U}{\partial X}+\frac{\partial V}{\partial Y}=0, \quad \ldots\ldots \quad (62)$$

$$U\frac{\partial U}{\partial X}+V\frac{\partial U}{\partial Y}=U_1\frac{dU_1}{dX}+N_*\frac{\partial^2 U}{\partial Y^2}, \quad \ldots \quad (63)$$

$$U\frac{\partial(RW)}{\partial X}+V\frac{\partial(RW)}{\partial Y}=N_*\frac{\partial^2(RW)}{\partial Y^2}, \quad \ldots \quad (64)$$

from which (25) (without the term in $\bar{w}$) and (26) are derived.

In detail, one would proceed to carry out the solution of the compressible rotating flow as follows. Given a compressible main stream expressed by $b(x)=(\gamma-1)\,M_1^2(x)$ round a body of given radius $r(x)$, one assumes that the density, viscosity, etc., in the associated incompressible flow have the values P_*, M_* etc., corresponding to the stagnation point in the compressible flow. Then, since

$$\frac{dX}{dx}=\frac{r^2\mu_1\rho_1 u_1}{L^2M_*P_*U_1},$$

and $\dfrac{\mu_1\rho_1}{M_*P_*}=\left(\dfrac{a_1}{A_*}\right)^{2\gamma/(\gamma-1)}$ from the adiabatic law, while

$$\left(\frac{A_*}{a_1}\right)^2=1+\tfrac{1}{2}b \qquad \text{from (6)},$$

† See the discussion of a more general case in the Appendix.

it follows that, with the help of (60),

$$X=\int_0^x [r(x)/r_m]^2[1+\tfrac{1}{2}b(x)]^{-[(3\gamma-1)/2(\gamma-1)]}\,dx, \quad . \quad . \quad . \quad (65)$$

where L is chosen to be r_m, a representative radius of the body, say the maximum. Then, according to (60) and (61),

$$U_1(X)=A_*[b(x)/(\gamma-1)]^{1/2}, \quad . \quad . \quad . \quad . \quad . \quad . \quad (66)$$

and

$$R(X)=r(x). \quad . \quad . \quad . \quad . \quad . \quad . \quad . \quad . \quad . \quad (67)$$

Having determined the quantities $U_1(X)$, $R(X)$ from (65), (66) and (67), one is in a position to solve (62), (63) and (64), and so obtain $\bar{u}$ and $\bar{w}$. The eqns. (62) and (63) describing plane incompressible boundary-layer flow are well known, and solutions of them are available for various forms of the function $U_1(X)$. The eqn. (64) is of the same form as the ordinary equation of forced convection, i.e. the energy equation in incompressible plane flow when the impressed temperature variations, though small compared with the absolute temperature, outweigh the effect of kinetic temperature variations. For with $1 \gg (I_0-I_1)/I_1 \gg M_1^2$, (21) (with $W=0$) reduces to

$$U\frac{\partial I}{\partial X}+V\frac{\partial I}{\partial Y}=\frac{N_*}{\sigma}\frac{\partial^2 I}{\partial Y^2},$$

subject to $I=I_0(X)$ at the wall, and $I=H_1=$const. in the main stream. Therefore, $RW=I-H_1$, provided $\sigma=1$ and $I_0(X)=H_1+\Omega R^2$.

One of the chief points of interest in the solution of the flow is the value of the skin frictional force. Since

$$\tau_x(x)=\mu_1\rho_1 u_1^2 r\left(\bar{u}\frac{\partial\bar{u}}{\partial\psi}\right)_{\psi=0},$$

and

$$T_X(X)=M_*P_*U_1^2 r_m\left(\bar{u}\frac{\partial\bar{u}}{\partial\psi}\right)_{\psi=0},$$

$$\tau_x(x)=[1+\tfrac{1}{2}b(x)]^{-[(2\gamma-1)/(\gamma-1)]}[r(x)/r_m]T_X(X), \quad . \quad . \quad . \quad (68)$$

and similarly

$$\tau_z(x)=[1+\tfrac{1}{2}b(x)]^{-[(3\gamma-1)/2(\gamma-1)]}[r(x)/r_m]T_Z(X), \quad . \quad . \quad . \quad (69)$$

provided $\Omega=\omega$,

where $$T_X(X)=M_*\left(\frac{\partial U}{\partial Y}\right)_{Y=0}, \qquad T_Z(X)=-M_*\left(\frac{\partial W}{\partial Y}\right)_{Y=0}.$$

We may also relate the spin-reducing torque to the heat transfer in the problem of forced convection mentioned at the end of the last paragraph. For, if we introduce the Nusselt number

$$Nu(X)=-\frac{\int_0^X (\partial I/\partial Y)_{Y=0}\,dX}{I_0-H_1},$$

in the convection problem, we obtain

$$Nu(X)=-\frac{\int_0^X R(\partial W/\partial Y)_{Y=0}\,dX}{\Omega R^2}=\frac{\int_0^X R(X)T_Z(X)\,dX}{M_*\Omega R^2(X)}.$$

Then, with the coefficient of the torque defined as

$$f_I(x)=\frac{2\pi\int_0^x r^2(x)\tau_z(x)\,dx}{\rho_1 u_1 \omega r^4},$$

it follows that

$$f_I(x)=\frac{2\pi\mu_1(x)[1+\frac{1}{2}b(x)]r_m}{\rho_1(x)u_1(x)r^2(x)}Nu(X),$$

and the problem of determining $Nu(X)$ given the distribution of the difference between wall and stream enthalpy (here ΩR^2) has been discussed by Lighthill (1950).

The simplest application of these formulae arises in the case, already treated in § 4, of the conefield flow past a circular cone in a supersonic stream. For then $r=x\sin\theta$ where θ is the semi-angle of the cone, and $b(x)=$const., so $U_1=$const. and (62) and (63) refer to the well-known flow past a flat plate. In this case,

$$T_X(X)=0{\cdot}332(M_*P_*U_1{}^3/X)^{1/2},$$

and

$$X=\tfrac{1}{3}x[r(x)/r_m]^2(1+\tfrac{1}{2}b)^{-[(3\gamma-1)/2(\gamma-1)]},$$

so

$$\tau_x(x)=3^{1/2}[0{\cdot}332(\mu_1\rho_1u_1{}^3/x)^{1/2}],$$

a result given by Mangler (1948). Similarly, since

$$T_Z(X)=-\tfrac{1}{2}g_0'(0)(M_*P_*U_1/X)^{1/2}\Omega R,$$

where $g_0'(0)$ is given in the table,

$$\tau_z(x)=3^{1/2}[0{\cdot}490(\mu_1\rho_1u_1x)^{1/2}\omega\sin\theta],$$

which is the leading term in (49).

ACKNOWLEDGMENT

I am grateful to Mr. D. F. Ferguson, M.A. for preparing the table.

APPENDIX

THE ASSOCIATED INCOMPRESSIBLE 'PLANE' FLOW FOR NON-UNIFORM MAIN STREAMS

In § 5, the compressible flow for slow rotation with an arbitrary main stream has been correlated to an incompressible 'plane' flow. It is the object of this section to examine the possibility of effecting a similar correlation when the rotation is not slow. We again assume the condition $\sigma=1$, used in § 5, so that (10*a*) may be used as the energy equation, and we further particularize by adopting the special solution

$$h=\text{const.}=h_1$$

of eqn. (10*a*). This means that

$$i+\tfrac{1}{2}(u^2+w^2)=\text{const.}=i_1+\tfrac{1}{2}u_1{}^2=i_0+\tfrac{1}{2}\omega^2r^2. \quad . \quad . \quad . \quad (70)$$

This equation implies that the wall temperature is non-uniform, having the particular distribution of temperature

$$t_0=(h_1-\tfrac{1}{2}\omega^2r^2)/c_p, \quad \ldots\ldots\ldots \quad (71)$$

and that there is heat transfer q per unit area from the wall to the gas given by

$$q=-\left(\mu\frac{\partial i}{\partial y}\right)_{y=0}=\left(\mu w\frac{\partial w}{\partial y}\right)_{y=0}. \quad \ldots\ldots \quad (72)$$

From (70) it follows that

$$\bar{\imath}+\tfrac{1}{2}b\left(\bar{u}^2+\frac{\omega^2r^2}{{u_1}^2}\bar{w}^2\right)=1+\tfrac{1}{2}b,$$

and so

$$\bar{u}^2-\bar{\imath}=(1+\tfrac{1}{2}b)(\bar{u}^2-1)+\tfrac{1}{2}b\frac{\omega^2r^2}{{u_1}^2}\bar{w}^2. \quad \ldots\ldots \quad (73)$$

With the help of (73), (15) becomes

$$(1+\tfrac{1}{2}b)\frac{1}{u_1}\frac{du_1}{ds}(u^2-1)+\bar{u}\frac{\partial\bar{u}}{\partial s}-\frac{\omega^2}{2{u_1}^2i_1}\frac{d}{ds}(i_1r^2)\bar{w}^2=\bar{u}\frac{\partial}{\partial\psi}\left(\bar{u}\frac{\partial\bar{u}}{\partial\psi}\right). \quad (74)$$

This equation is identical with (25) provided that

$$(1+\tfrac{1}{2}b)\frac{1}{u_1}\frac{du_1}{ds}=\frac{1}{U_1}\frac{dU_1}{ds}, \quad \ldots\ldots\ldots \quad (75)$$

and

$$\frac{\omega^2}{{u_1}^2i_1}\frac{d(i_1r^2)}{ds}=\frac{\Omega^2}{{U_1}^2}\frac{d(R^2)}{ds}. \quad \ldots\ldots \quad (76)$$

Moreover, (16) and (26) are identical provided that

$$\frac{1}{r}\frac{dr}{ds}=\frac{1}{R}\frac{dR}{ds}. \quad \ldots\ldots\ldots \quad (77)$$

Since the boundary conditions for the velocities are independent of compressibility (see (29)), under the conditions (75), (76) and (77) the non-dimensional functions $\bar{u}$ and $\bar{w}$ may be found from the incompressible flow eqns. (18), (19) and (20) instead of the more complicated equations of § 2.

However, these conditions place a limitation on the main stream. For the integrals of (75) and (77) are

$$\frac{{u_1}^2}{i_1}=k_1{U_1}^2, \quad \ldots\ldots\ldots \quad (78)$$

and

$$r=k_2R, \quad \ldots\ldots\ldots \quad (79)$$

where k_1 and k_2 are constants of integration. The integral of (76) is

$$\frac{1-(k_1\Omega^2/k_2{}^2\omega^2)i_1}{i_1}=k_3r^2, \quad \ldots\ldots\ldots \quad (80)$$

where k_3 is another constant of integration. Now, (80) shows that the Mach number of the compressible flow must be given by

$$M_1=\left[\frac{2}{\gamma-1}\left\{h_1\left(k_3r^2+\frac{k_1\Omega^2}{k_2{}^2\omega^2}\right)-1\right\}\right]^{1/2}=(\alpha r^2+\beta)^{1/2}, \quad \text{say.} \quad (81)$$

Since there are two arbitrary constants, this formula can be made to agree with the observed Mach number distribution for a given body of radius $r(x)$

at two points. For a projectile, the formula shows the right behaviour in making M_1 become constant as r becomes constant (on the cylindrical part of the projectile).* One might expect that for some sharp-nosed projectiles, the formula would represent the main-stream flow round the projectile reasonably well, with $\beta = M_1^2(0)$, the square of the Mach number at the surface of the tip, and with α chosen to give the appropriate Mach number on the cylindrical part of the projectile.

References

Howarth, L., 1938, *Proc. Roy. Soc.* A, **164,** 547.
Illingworth, C. R., 1949, *Proc. Roy. Soc.* A, **199,** 533.
Lighthill, M. J., 1950, *Proc. Roy. Soc.* A, **202,** 359.
Mangler, W., 1948, *Z.A.M.M.*, **28,** 97.

* This remark is due to Professor M. J. Lighthill.

XLIII. *The Reaction* $^{181}Ta(\gamma, 2n)^{179}Ta$ *at* 17·6 MeV *and Some Remarks on Nuclear Photodisintegration*

By J. H. Carver,* R. D. Edge and D. H. Wilkinson
Cavendish Laboratory, Cambridge†

[Received January 7, 1953]

Abstract

The problem of determining the variation with gamma-ray energy of the total nuclear absorption cross section is discussed with a view to testing the applicability of specific nuclear models such as that of Goldhaber and Teller for the form of the cross section and the validity of the general account of the integrated cross section given by Levinger and Bethe. While for light elements many competing processes must be considered, in the very heavy elements only $(\gamma, 2n)$ is a possible competitor for (γ, n) at not too high energies. The seriousness of this competition is estimated by a measurement of the ratio of the cross sections of $^{181}Ta(\gamma, 2n)^{179}Ta$ at 17·6 MeV to $^{181}Ta(\gamma, n)^{180}Ta$ at 14·6 MeV ; the result is $0{\cdot}29 \pm 0{\cdot}11$. This competition is not enough to destroy the apparent ' resonance ' character of the absorption. It is pointed out that the large value of $\sigma_{\gamma, n}$ at 17·6 MeV is inconsistent with the idea that a conventional compound nucleus is always formed and so the idea of purely statistical competition for the gamma-ray energy should be modified in comparing neutron yields with the predictions of the dipole sum rule. The present measurements are correlated with the neutron yield curve of Halpern, Nathans and Mann.

§1. Introduction

The phenomena associated with the interaction of gamma-rays of high energy and nuclei show a remarkable independence of the particular nucleus studied ; throughout the periodic table certain features of the interaction remain almost unchanged while others show only a regular and monotonic dependence on atomic number. It is impossible to avoid the feeling that we are dealing with some rather general property of nuclear matter which is only slightly modified by the details of the particular nucleus that it happens to be constituting. What this general property is has yet to be elucidated. It is the purpose of this paper to present an observation that, while it is isolated and not of great

* Now at the National University, Canberra, Australia.
† Communicated by the Authors.

accuracy, seems to us to justify to some degree the basis of certain recent attempts to systematize nuclear photodisintegration and so to confirm the overall impression of an essentially simple phenomenon which, though well-understood in certain of its aspects, displays features whose explanation may be of some fundamental interest for a description of nuclear forces.

It may be convenient to summarize the present state of observation and theory in that part of the field that concerns the present measurements so as to show their relevance. Many workers, principally in the U.S.A. and at the University of Saskatchewan (references A), have measured the dependence on gamma-ray energy E of the cross section $\sigma_{\gamma, n}$ for the (γ, n) process using the bremsstrahlung from betatrons or synchrotrons and usually identifying the reaction by a characteristic radioactive end-product. These cross section curves are all of ' resonance '* form, rising to a maximum at a gamma-ray energy E_m above which they decline rather sharply to a small value. E_m is about 20 MeV for light elements and it declines steadily to about 14 MeV for the heaviest elements. The width of the ' resonance ' is even less dependent on atomic number than is E_m and, with few exceptions. lies between 5 and 6 MeV (at half maximum) throughout the periodic table. The (γ, n) cross sections themselves, above about $Z=20$ at any rate, increase smoothly towards the heavy elements and are more-or-less proportional to Z. Now these ' resonances ' may be explained in two ways : they may be genuine sharp maxima in the total cross section for photon absorption, and this was the view taken by Goldhaber and Teller (1948) and elaborated by Steinwedel and Jensen (1950) who saw in them evidence of a particularly simple form of nuclear excitation in which all neutrons move against all protons in the dipole vibration of lowest order ; the dependence of E_m on Z is correctly explained by this hypothesis as is also the dependence of σ on Z ; alternatively the rapid decline in $\sigma_{\gamma, n}$ above its maximum may be due to the onset of competing processes such as (γ, 2n) or (γ, p), the total cross section showing little ' resonance ' or none at all. (γ, p) processes are of great importance for light elements, where the proton binding energy is usually a few MeV less than the neutron binding energy, as pointed out by Heidmann and Bethe (1951) ; for heavy elements ($A>70$), however, with which we shall chiefly be concerned proton emission is almost completely suppressed by the Coulomb barrier and (γ, 2n) is the only effective competitor. On the second view of the ' resonances ' E_m should be correlated, in heavy elements, with the (γ, 2n) threshold ; by and large it is (Eyges 1952). It is essential that

* Throughout this paper we shall write resonance as 'resonance' because we do not consider that the time is yet ripe to decide whether a resonance in the commonly-accepted sense of a well-defined long-lived state of a compound nucleus is involved or not ; it is possible that some aspect of nuclear forces may produce such an effect without the intervention of an excitation which involves the whole nucleus in the first instance.

some measure of the competing processes be available to decide whether the ' resonances ' are indeed an indication of a general property of nuclear matter in bulk, perhaps such as Goldhaber and Teller propose, or are merely a reflection of the nuclear energy surface. If light nuclei are used for this purpose the investigation becomes complicated as effective competing processes include the emission of charged particles as well as of neutrons and a combination of techniques is demanded. No experiments on light elements exist which investigate the energy dependence of all possible competing reactions and are therefore of use in settling the present issue.* Among the heavy elements only $(\gamma, 2n)$ can be an effective competitor to (γ, n) at not-too-high energies since the Coulomb barrier for protons at mass number 180 is about 13 Mev and so in principle the problem is wholly soluble by measuring $\sigma_{\gamma, 2n}$ as a function of E ; in practice, however, this is impossible as the appropriate end-product, if radioactive, has either unknown or very unsuitable properties. We have sought to make a contribution to the resolution of this problem by measuring $\sigma_{\gamma, 2n}$ for ^{181}Ta at $E=17{\cdot}6$ Mev. $\sigma_{\gamma, 2n}$ should be near its maximum value at this gamma-ray energy and so our observation indicates the degree to which the ' resonance ' is blunted by competition ($E_m=14{\cdot}0$ Mev and the width of $\sigma_{\gamma, n}$ at half-maximum is 4·5 Mev). If $\sigma_{\gamma, 2n}$ at 17·6 Mev is comparable with $\sigma_{\gamma, n}$ at E_m the ' resonance ' is abolished and no explanation based on the characteristics of nuclear forces or the behaviour of nuclear matter in bulk is to be sought ; if, however, $\sigma_{\gamma, 2n}$ is small the problem of the ' resonances ' remains.

That $\sigma_{\gamma, 2n}$ is large is made improbable by the considerations of Levinger and Bethe (1950, 1952), with which the present work is also concerned. These authors point out that a fundamental upper limit exists for that part of

$$\int_0^\infty \sigma \, . \, dE$$

* The experiments of Strauch (1951) on ^{64}Zn show the presence of competition from several processes but the shapes of the excitation functions are not determined in detail, there being merely an indication that the more complicated processes are due to gamma-rays of higher energy than those producing (γ, n) as is to be expected.

Sagane (1952) has compared the excitation functions for the processes (γ, n), $(\gamma, 2n)$, (γ, pn) and $(\gamma, 2np)$ on ^{64}Zn up to 40 Mev. The results agree well with the more indirect measurements of Strauch, (γ, n) being by far the most important process. For the present purpose both these experiments suffer the disadvantage that the most potent competitor to (γ, n) in the region of the 'resonance', namely (γ, p) is not investigated ; one must expect (Heidmann and Bethe 1951, Mann and Halpern 1951) that (γ, p) and (γ, n) processes are of roughly equal importance in this region so the omission is a serious one.

Although all competing processes are not measured, Katz and Cameron (1951) have given plausible reasons for supposing that the total absorption cross section for aluminium preserves a well-defined peak.

that is due to electric dipole transitions—the greater part. They extend the familiar dipole sum rule of atomic spectroscopy to nuclear absorption and obtain

$$\int_0^\infty \sigma \, . \, dE = 0{\cdot}060 \frac{NZ}{A} (1 + 0{\cdot}8x) \text{ MeV—barns}$$

where x is the fraction of exchange force in the nucleon–nucleon interaction. As

$$\int \sigma_{\gamma, n} \, dE$$

over the 'resonance' already accounts for almost the whole of the theoretical

$$\int_0^\infty \sigma \, . \, dE$$

it is clear that no great contribution from $\sigma_{\gamma, 2n}$ can be tolerated if the Levinger–Bethe formula is correct. Now the neutron yield under high energy bremsstrahlung (~300 MeV) (Kerst and Price 1950, Terwilliger, Jones and Jarmie 1951) increases rather more rapidly than NZ/A: Levinger and Bethe (1952) seek to explain this as due to the reactions (γ, xn) which set in more readily in the heavy elements owing to the smaller binding energies there encountered. By this means neutron yields which, on the basis of one neutron per gamma-ray absorbed, would have indicated values of

$$\int_0^\infty \sigma \, . \, dE$$

considerably in excess of the theoretical limit were shown to be compatible with this limit if still too large by perhaps 60–70%. Although a discrepancy of this magnitude may perhaps be covered by experimental inaccuracies in the rather difficult measurements involved and by the uncertainty of the calculation, it may yet be increased if the basic assumption made by Levinger and Bethe is incorrect, namely that the gamma-ray energy is spread throughout a conventional compound nucleus of high excitation, and that neutrons simply boil off in accordance with statistical theory. In this connection it must be noted that this is not always so as is shown by the emission of nucleons of order 100 MeV (e.g. Levinthal and Silverman 1951, Walker 1951, Keck 1952) and the anomalous yields of protons from heavy elements (Hirzel and Wäffler 1947, Wäffler and Hirzel 1948—but see Paskin 1952), their angular distribution (e.g. Curtis, Hornbostel, Lee and Salant 1950, Diven and Almy 1950), and the interpretation by Courant (1951) as a direct photo-electric ejection of a single nucleon.* The relative yields of protons and neutrons from light elements accord quantitatively with the idea that a compound nucleus is formed (Heidmann and Bethe 1951—though

* See also Jensen (1948) and Marquez (1951) for qualitative remarks of a similar nature.

Katz and Cameron (1951) would differ with them on this conclusion), though similar phenomena would be expected to some degree if a single nucleon were directly ejected. A clear test of whether a compound nucleus is formed or not is afforded by the energy spectrum of neutrons or protons under monochromatic gamma-ray bombardment ; so far the only investigation reported (Wilkinson and Carver 1951) concerns the reaction $^{40}A(\gamma, p)^{39}Cl$ at 17·6 Mev and shows that the bulk of the effect is to be associated with compound nucleus formation, though it does not exclude a fair amount of direct interaction. Energy spectra under bremsstrahlung bombardment are relatively uncritical of the mechanism of the photodisintegration process and though measurements on both neutrons and protons (e.g. Diven and Almy 1950, Byerly and Stephens 1951) agree with the formation of a compound nucleus a direct photo-process cannot be excluded by them. It must also be noted that although the tail of $\sigma_{\gamma, n}$ above the ' resonances ' is small it is large enough to imply here a value of $\sigma_{\gamma, 2n}$ very much greater than the maximum value of $\sigma_{\gamma, n}$ if a conventional compound nucleus is formed ;* this is wholly inadmissible and shows that, if the $\sigma_{\gamma, n}$ measurements are correct, the bulk of $\sigma_{\gamma, n}$ at an energy of more than 17 Mev or so in heavy elements is probably due to processes other than compound nucleus formation. Although photo-processes involving the emission of as many as 10 neutrons from heavy elements have been observed (Sugarman and Peters 1951) the seriousness of the competition so afforded has not been estimated with any certainty. It is evident that the assumption that a compound nucleus is always or even usually formed has little experimental justification, particularly at high energy. If compound nucleus formation were indeed small the multiplicities used by Levinger and Bethe (1952) would be too high and the neutron yields would disagree even more than at present with the predictions of the dipole sum rule.† It is therefore important to determine whether, above the ' resonance ', $\sigma_{\gamma, 2n}$ is or is not negligible as compared with $\sigma_{\gamma, n}$; this we have done in the present work. If $\sigma_{\gamma, 2n}$ is small compared with $\sigma_{\gamma, n}$ then compound nucleus formation must also be improbable as compared with direct interaction ; if $\sigma_{\gamma, 2n}$ is comparable with or bigger than $\sigma_{\gamma, n}$ then a significant amount of compound nucleus formation, either immediate or subsequent to a direct interaction, is established and the basis of Levinger and Bethe's argument is made somewhat firmer.

Eyges (1952) has used measured curves of $\sigma_{\gamma, n}$, neutron yields from bremsstrahlung of 18 and 22 Mev (Price and Kerst 1950) and from the

* For example $\sigma_{\gamma, n}$ for ^{181}Ta at 17·6 Mev is 0·23 in terms of its value at E_m (Haslam, Smith and Taylor 1951) ; but at 17·6 Mev the neutron multiplicity with compound nucleus formation is 1·95 which implies that $\sigma_{\gamma, 2n}$ at 17·6 Mev should be about four times the maximum value of $\sigma_{\gamma, n}$.

† The production of neutrons in meson-induced stars is not included in the dipole sum but is estimated by Levinger and Bethe (1952) to be a small correction only. Justification of their estimate comes from the work of Jones and Terwilliger (1952).

gamma-rays of the reaction ^{7}Li(p, γ)^{8}Be (McDaniel, Walker and Stearns 1950) to obtain information about $\sigma_{\gamma, 2n}$. Such analysis is difficult and inevitably involves some guesswork, but provides a good indirect indication for a finite value of $\sigma_{\gamma, 2n}$ above E_m.

Since this work was completed Halpern, Nathans and Mann (1952) have published a total neutron yield curve for tantalum as a function of gamma-ray energy. Their work, though not of great accuracy, clearly reveals a considerably greater yield of neutrons above 16 MeV than may be accounted for by the (γ, n) process alone.

Fig. 1

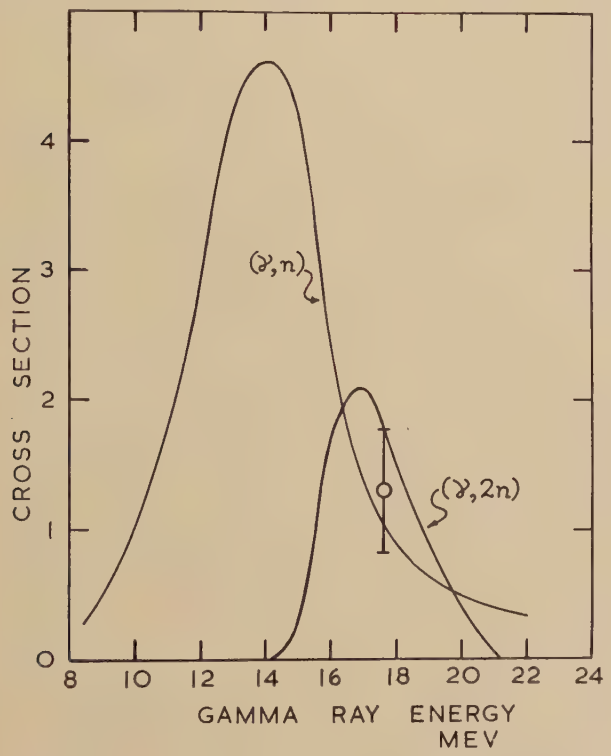

Cross section for ^{181}Ta(γ, n)^{180}Ta as measured by Haslam, Smith and Taylor; $\sigma_{\gamma, 2n}$ predicted by Eyges and our result for $\sigma_{\gamma, 2n}$ at 17·6 MeV (cross section units are arbitrary).

We may now conveniently summarize our own result in its relation to the (γ, n) cross section in fig. 1 which shows $\sigma_{\gamma, n}$ for ^{181}Ta as measured by Haslam, Smith and Taylor (1951)* and $\sigma_{\gamma, 2n}$ as predicted by Eyges

* These workers measure only the *form* of $\sigma_{\gamma, n}$; the absolute ordinate scale (which is of no concern for the present experiment) has been provided by Halpern, Nathans and Mann (1952); Eyges (1952) deduced absolute values 1·5 times as great.

(1952). We have measured the ratio of $\sigma_{\gamma, 2n}$ at 17·6 MeV to $\sigma_{\gamma, n}$ at 14·6 MeV with the result indicated by the point on the figure. A considerable (γ, 2n) cross section is established though perhaps not quite as large as predicted by Eyges. We shall return to this result and its relation to the work of Halpern, Nathans and Mann, with which it is in good agreement, after a discussion of the experiment.

§2. Principles of the Experiment

We have already remarked that a direct determination of $\sigma_{\gamma, 2n}$ by the method of induced activities is not generally available in the heavy elements and the (γ, 2n) process must therefore be detected through its neutron yield. A heavy element must be used in order that (γ, 2n) be the only effective competitor to (γ, n); $\sigma_{\gamma, n}$ (or at least its *form*) must be well known and should preferably fall rapidly above E_m; the element used should preferably possess only one isotope. The only element satisfying these conditions is tantalum.

In principle the same technique may be used as for $\sigma_{\gamma, n}$, a measurement of total neutron output replacing one of induced activity; knowledge of $\sigma_{\gamma, n}$ would then enable one to deduce $\sigma_{\gamma, 2n}$. This experiment is very difficult but, as remarked above, has been performed by Halpern, Nathans and Mann (1952). We have adopted the more modest objective of a measurement of $\sigma_{\gamma, 2n}$ at a single energy of gamma ray.

$\sigma_{\gamma, n}$ in tantalum reaches its maximum value at $E_m = 14{\cdot}0$ MeV; the threshold for the (γ, 2n) reaction is 14·1 MeV according to Eyges (1952) and 14·0 MeV according to Levinger and Bethe (1952). Eyges suggests that $\sigma_{\gamma, 2n}$ reaches its maximum value at about 17 MeV. If, then, we had available monochromatic gamma-rays of about 14 and 17 MeV we might, by comparing their neutron yields per quantum, and knowing the form of $\sigma_{\gamma, n}$ as a function of energy, obtain a value for $\sigma_{\gamma, 2n}$ near its maximum relative to $\sigma_{\gamma, n}$. Such gamma-rays are not available, but we may approximate to the ideal situation in the following way:

When ^{7}Li is bombarded by protons radiative capture may take place to the ground state of ^{8}Be and to the state of width about 2 MeV centred at 3·0 MeV, the respective Q-values being 17·2 and 14·2 MeV (Hornyak, Lauritsen, Morrison and Fowler 1950). With protons of low energy these transitions have energies close to the ideal energies of the preceding paragraph; unfortunately it is not possible to obtain either gamma-ray free of the other and a mixture is given at all proton energies so far investigated.* At the well-known resonance at a proton energy of 440 kev the ground state transition is the stronger by a factor two, at a proton energy of 1·15 MeV (thin target) the lower energy line is the stronger by about the same factor (Stearns and McDaniel 1951). Thus

* Transitions doubtless occur to other states of ^{8}Be though not very readily: Nabholtz, Stoll and Wäffler (1951) have reported weak radiation of 12·5 MeV accompanying the strong lines; it is not of sufficient intensity to be of interest to the present investigation.

though we may not employ monochromatic radiation we may vary the relative abundance of the two lines quite considerably and so sort out their individual effects to some degree.

Stearns and McDaniel have used a pair spectrometer to determine the relative abundances; in the range of angles of emission of the gamma-rays relative to the proton beam covered in their investigations the biggest change in abundance ratio is obtained at 75°. At a proton energy of 500 kev (thick target) they find an intensity ratio of $1{\cdot}70\pm0{\cdot}20$ in favour of the high energy radiation; at 1·15 MeV (target thickness 250 kev) this ratio is $0{\cdot}45\pm0{\cdot}06$. We have irradiated tantalum under these conditions and determined the total neutron yield per incident quantum. The details of the results will be discussed later.

§3. Experimental Methods

The experimental problem is two-fold: the relative numbers of high energy quanta must be determined at the two proton energies and also the relative photo-neutron yields; in the latter case an energy-insensitive detector must be used, in the former it is to be desired.

It might at first sight appear that an ordinary Geiger counter of known relative efficiency for the two gamma-ray energies of interest is an adequate solution to the first problem. This is not so because at a proton energy of about 550 kev excitation of the first (478 kev) excited state of ^{7}Li becomes possible by inelastic scattering and at 1·15 MeV there is a large cross section for this process. We have adopted the simplest solution and used an NaI(Tl) crystal biased at about 7·5 MeV to exclude this low energy radiation and any other that might arise in the radiative capture itself or in a second-order reaction such as that which we shall discuss shortly. The relative efficiency of the crystal for the two gamma-ray mixtures was evaluated by comparing the shapes of the complete pulse distributions obtained at the two proton energies and by calculating the intrinsic efficiencies of detection of the two gamma-ray mixtures in the crystal; these two effects together provided a correction of 5·2% to the raw yield of neutrons per quantum. The overall sensitivity of the crystal, multiplier and amplifier over the several weeks of the experiment was checked from day to day with a gamma-ray source (^{137}Cs).

The second problem is a more difficult one. The neutron detector must be both energy-insensitive and very efficient as the yield is very low. We have used the Szilard–Chalmers reaction in the manganese of a solution of sodium permanganate. The tank containing the solution had a cross-section of $11{\cdot}5\times12{\cdot}5$ cm and a length of 16·0 cm. At one end metallic tantalum* of the same cross section as the tank and of thickness 20 g/cm^2 was placed, and the whole assembly was pointed towards the target of evaporated lithium metal which was 12 cm from the

* The purity of the tantalum was greater than 99·6%.

face of the solution.* Such a device is quite energy-insensitive (see, for example, the ' long counter ' of Hanson and McKibben 1947), and, to within the accuracy of our experiment, it is safe to assume that the various photo-neutron spectra, which in any case differ but little, are detected with equal efficiency. Several strengths of permanganate solution have been used ; the bulk of the work was done with a solution containing 54 g of sodium permanganate per litre. The solution was filtered with the addition of 1·0 g of MnO_2, the precipitate (on a filter paper of diameter 5·5 cm) was wrapped around a thin-walled aluminium Geiger counter and the activity measured. The counting rate was always high enough† for the principal uncertainty in the interpretation of the experiment to reside elsewhere. The reproducibility of the procedure using a standard neutron source was about $\pm 5\%$ on a single extraction.

Throughout the irradiations of one hour each the gamma-ray output was monitored continuously by the NaI(Tl) crystal placed symmetrically with respect to the Szilard–Chalmers tank at 75° to the proton beam on the other side of the target tube. Fluctuations in the gamma-ray output were allowed for assuming the half-life of ^{56}Mn to be 2·59 hr.

§4. Experimental Results

Severe difficulties were encountered in the shape of a large background activity obtained in irradiations without the tantalum. This was estimated by performing irradiations in which the tantalum was replaced by a thin shell of cadmium of identical overall dimensions whose thickness was such that the absorption for slow neutrons was the same as that of the tantalum. At the lower proton energy the background estimated in this way was roughly half the total effect with the tantalum in place ; at the higher proton energy it was sometimes as high as nine-tenths. This background is very grave and its origins must be carefully considered.

The background has two sources : the gamma-rays themselves produce photoneutrons from the detecting solution and the room, the latter effect giving a general neutron atmosphere ; alpha-particles from the reaction ^{7}Li(pα)^{4}He act on the target to give neutrons principally through the reaction ^{7}Li(αn)^{10}B. In the conditions of our experiment the latter source of background appears to be the more important. That the production of photoneutrons in the sodium permanganate is of little importance was established by calculation and by performing irradiations with different strengths of solution when no inconsistencies appeared such as would have arisen had such photo-neutron production

* The rather large angle ($\pm 34°$) subtended by the tantalum at the gamma-ray source is not of great importance as the radiations are isotropic at the lower proton energy and do not vary by more than 12% from 75° to 35° at 1·15 Mev. Allowance was made for this small variation.

† At the beginning of the counting periods about 40 counts/min due to the tantalum at the lower proton energy and 35 counts/min at the high.

been a sensible fraction of that in the tantalum ; calculation also showed that the water of the solution and the glass of the tank are negligible in this respect (using the results of McDaniel, Walker and Stearns 1950). That photo-neutrons in general are less important than neutron generation by the (α, n) mechanism is shown by the great change in background ratio between the two proton energies. Had photo-neutrons been the principal source of background the background ratio would have changed little between the two proton energies—if anything in the opposite sense to that observed since the room is made principally of light elements which are ' resonant ' nearer 17·6 MeV than 15·2 MeV, whereas with the tantalum the reverse is true. On the other hand, the ratio of alpha-particle to gamma-ray yield increases by a large factor from the low to high proton energies as did the background. Furthermore, the background ratio at the higher proton energy decreased with the thickness of the target in the way expected, the gamma-ray yield being proportional to the target thickness, the neutron yield to its square. As thin a target as was consistent with the production of an adequate supply of gamma-rays was used.

Two questions must now be answered : what fraction of the background neutrons comes directly from the target and of this fraction how much is scattered away by the insertion of the tantalum ? The first question was answered by performing an inverse-square law experiment moving the detecting tank relative to the target. This gave the result (assuming the effective face of the detecting solution to be 3 cm behind its geometrical face) that, in the working position, 0·55 of the background came directly from the target, the rest constituting an atmosphere of partially-moderated neutrons constant in density in the immediate vicinity of the target. The second question is a more difficult one to answer satisfactorily. It divides into two parts : what is the primary background neutron spectrum from the target and how much of the neutron scattering by the tantalum is potential scattering ? The first part of the question determines the total interaction between the background neutrons and the tantalum,* and the second the angular distribution, assuming that potential scattering follows the usual Bessel function formula (Bethe and Placzek 1937) and compound-nucleus scattering is isotropic.† The neutron spectrum has been guessed at knowing the various Q-values involved and the various excited states of ^{10}B, it being assumed that the available states are fed proportionally to the neutron energy ; the total cross section of tantalum does not vary rapidly with neutron energy and the results are not very sensitive to the neutron spectrum. The proportion of potential and compound-nucleus scattering has been taken from the continuum theory (Blatt and Weisskopf

* The total cross section of tantalum for scattering fast neutrons is known in the energy region of interest here (see, for example, Miller, Adair, Bockelman and Darden (1952)).

† The energy distribution of the compound-nucleus-scattered neutrons is not important as the detector is energy-insensitive.

1952). The result of these computations is that that part of the background proceeding directly from the target is diminished by 9% by the insertion of the tantalum; this is then coupled with the observation that 0·55 of the whole background came directly from the target to give the result than we should add to the apparent neutron yield with the tantalum in place 0·050 times the background measured with the cadmium shell. A direct measure of the correction was also obtained: the bombardment of the thin metallic lithium target caused it to become thinner and hence to give an improving background ratio on successive irradiations and it was therefore possible empirically to determine the fraction of the background that had to be added to the apparent neutron yield of the tantalum in order to obtain consistent results; the fraction so determined was $0{\cdot}06 \pm 0{\cdot}02$ in good accord with the calculated 0·050.

Some dozens of irradiations were performed, particularly at the higher proton energy where the background is more serious. The simple results were corrected for background as described above using the experimentally-determined probable error on the correction factor in order to estimate the extra error introduced in making this correction; the gamma-ray fluxes were corrected for the different response of the crystal to the various mixtures of gamma-rays as described earlier and our final answer is that the neutron production per quantum incident on the tantalum at the lower proton energy divided by that at the higher is $0{\cdot}92 \pm 0{\cdot}08$.

Before analysing this result we must remark that the gamma-ray spectrum effective in producing photo-neutrons is not quite that incident upon the tantalum and specified above, but is modified by the energy-dependent absorption in the tantalum. Although the absorption is considerable it is almost the same for the two gamma-ray energies; the effective abundance of the lower energy gamma-ray relative to the higher is increased by 3·6%.* Furthermore the difference in absorption for the two gamma-rays implies that the initial spatial distribution within the tantalum is different for the photo-neutrons which they produce; this implies a different detection efficiency on account of the difference in the solid angle subtended by the detector and in the scattering on the way to the detector; this correction is negligible.

Finally we must enquire if the angular distribution of the photo-neutrons may be sufficiently strong to falsify the results. It is very improbable that this effect is serious as the bulk of the neutrons in the (γ, n) process at the lower gamma-ray energy probably comes via a compound nucleus and so has a rather feeble angular distribution and only a small fraction of relatively high energy neutrons with a possibly strong angular distribution comes from the direct interaction mechanism while the second neutron of a $(\gamma, 2n)$ reaction is almost certainly from a compound nucleus with but little memory of the initial photon

* The absorption itself does not have to be corrected for and introduces no error as we do not attempt an absolute measurement; only the difference in the absorptions is of interest here.

direction. The most serious effect might arise in the (γ, n) process at the higher gamma-ray energy which, as will be seen below, is probably due to direct interaction and so may possess a stronger angular distribution (Courant 1951). However, for so heavy an element as tantalum, neutron shells of rather high angular momentum must be involved, with a corresponding tendency to return towards spherical symmetry for the photo-neutrons. Even if all the (γ, n) neutrons at the higher gamma-ray energy possess a pure $\sin^2\theta$ distribution (and Price (1951) has surprisingly obtained a distribution as strong as $1+5\sin^2\theta$ for neutrons of greater than 3 MeV from Pb, Bi, W and Ni under bremsstrahlung of 22 MeV) the geometry of the detecting tank is so poor that it would still accept well over 60% of the neutrons it would have accepted had the emission been spherically symmetrical. This would increase our value of $\sigma_{\gamma, 2n}$ by only about a third of its probable error. (For isotropy of the bulk of the neutrons see, for example, Price and Kerst (1950); for anisotropy of high energy neutrons see, for example, Poss (1950) and Price (1951).)

§5. Analysis of the Results

As the threshold for the (γ, 2n) reaction is below the lower gamma-ray energy it may appear that our single observation is not enough to determine $\sigma_{\gamma, 2n}$ at any energy. Near the lower gamma-ray energy, however, $\sigma_{\gamma, 2n}$ is expected to be rather small; we have, in the first place, used Eyges' prediction of its value there in analysing our results. At the lower proton energy the gamma-ray energies are 14·6 and 17·6 MeV and at the higher 15·2 and 18·2 MeV (allowing for the target thickness). It is therefore necessary to assume some relation between $\sigma_{\gamma, 2n}$ at 18·2 MeV and at 17·6 MeV; we have again, in the first place, taken the *ratio* of these cross sections to be that predicted by Eyges, though we have made no assumptions as to their absolute values. We have also taken into account the width of the 3·0 MeV level in ^{8}Be in determining the expected yields at the lower gamma-ray energy. In this way a rough value for $\sigma_{\gamma, 2n}$ was obtained and so a first attempt at the form of the total cross section; the (γ, 2n) curve of Eyges was changed in scale to suit our value of $\sigma_{\gamma, 2n}$ at 17·6 MeV. This rough total cross section curve was then used to predict the form of $\sigma_{\gamma, 2n}$ by assuming that the bulk of the total cross section involves compound nucleus formation; $\sigma_{\gamma, 2n}$ was derived from the total cross section by the usual statistical theory of (γ, n) versus (γ, 2n) competition as presented by Blatt and Weisskopf (1952). The scale of $\sigma_{\gamma, 2n}$ was then altered to fit our measured point and our value of $\sigma_{\gamma, 2n}$ at 17·6 MeV computed again with this new data on $\sigma_{\gamma, 2n}$ at the lower energies and the relation between $\sigma_{\gamma, 2n}$ at 17·6 and 18·2 MeV. The whole procedure was repeated until stability was reached (always permitting the final change of scale of $\sigma_{\gamma, 2n}$ to fit the measured point). This procedure is fundamentally inconsistent because of the large experimental value of $\sigma_{\gamma, n}$ above 18 MeV where the neutron multiplicity for compound nucleus formation is almost two

which means that direct interaction must be here of considerable importance (see below). Our method effectively assumes that, at high energy, the *form* of $\sigma_{\gamma, 2n}$ follows that of $\sigma_{\gamma, n}$ which would be very reasonable if, in this region, immediate compound nucleus formation were small compared with direct interaction (whether this ultimately resulted in a compound nucleus or not); it is reasonable to suppose a more-or-less constant probability for direct interaction to lead to compound nucleus formation (i.e. to a (γ, 2n) process).* Our method for the form of $\sigma_{\gamma, 2n}$ is good enough near the threshold for (γ, 2n) as the bulk of the total cross section in this region (near E_m) is probably due to compound nucleus formation and the final change of scale brings a correction consistent with the estimated direct effect near the 'resonance'. Our hypothesis concerning the predominance of direct interaction at high energies leads us to suppose a more slowly-falling $\sigma_{\gamma, 2n}$ than predicted by Eyges (see fig. 1). It seems to us very unreasonable that $\sigma_{\gamma, 2n}$ should indeed fall to a very low value at 22 Mev as compared with $\sigma_{\gamma, n}$ as this would imply a negligibly-small probability that the nucleon partaking of the direct interaction suffer collision and form a compound nucleus. This is unreasonable enough for neutrons; for protons (which, together, will take part in the direct interaction more frequently by a factor N/Z than neutrons) it is even less likely.

Our final version of $\sigma_{\gamma, 2n}$ and hence of the total cross section† is shown, with our measured point, in fig. 2. We find that $\sigma_{\gamma, 2n}$ at 17·6 Mev divided by $\sigma_{\gamma, n}$ at 14·6 Mev‡ is $0{\cdot}29 \pm 0{\cdot}11$; § the error takes account of

* Some justification for this assumption that the fall of $\sigma_{\gamma, 2n}$ follows in *form* that of $\sigma_{\gamma, n}$ derives from the work of Sagane (1952) who finds that in ^{64}Zn $\sigma_{\gamma, 2n}$, $\sigma_{\gamma, pn}$ and $\sigma_{\gamma, 2np}$ all fall like $\sigma_{\gamma, n}$.

† We have already noted that charged-particle emission is most improbable; the cross sections for (γ, γ) and (γ,γ') are small both theoretically and experimentally (Stearns 1952) and the threshold for (γ, 3n) is 22·2 Mev (Levinger and Bethe 1952).

‡ By this we mean the value for monochromatic gamma-rays of 14·6 Mev, not for the broad line used in this experiment.

§ A totally independent and largely abortive experiment was performed in which the fast neutron output (>0·5 Mev) from a large mass of tantalum was measured by a pulse ionization chamber filled with hydrogen at 40 atmospheres while the (γ, n) reaction was monitored by the activity induced in a Geiger counter made almost entirely of tantalum. This experiment, like the other, was beset by background troubles which were even more difficult to allow for accurately than those of the experiment already described, though not so large in proportion, and gave the result that $\sigma_{\gamma, 2n}$ at 17·6 Mev is close to zero, though with so large a probable error that the result is consistent with the present one. From the irradiations at low proton energy alone, where the gamma ray flux was measured by a standardized Geiger counter (Barnes, Carver, Stafford and Wilkinson 1952) we can quote a figure for 0·37 ($\sigma_{\gamma, n}+2\sigma_{\gamma, 2n}$) at '14·6 Mev' (broad line)+0·63 ($\sigma_{\gamma, n}+2\sigma_{\gamma, 2n}$) at 17·6 Mev of (400 ± 60) mb. This is to be compared with the 320 mb from the results presented in fig. 2 and the cross section scale established by Halpern, Nathans and Mann or with the 470 mb using the cross section scale of Eyges, suggesting that the correct scale may be roughly mid-way between the two.

the uncertainty in the composition of the gamma-rays as estimated by Stearns and McDaniel (1951). Note that we suppose $\sigma_{\gamma, 2n}$ to be rather greater than $\sigma_{\gamma, n}$ throughout the region (above 18 MeV) where the neutron multiplicity for compound nucleus formation is virtually two. This should be so if we are correct in assuming that $\sigma_{\gamma, n}$ is almost wholly due to direct interaction; if we assume that every direct interaction involving a proton leads to a compound nucleus, the relation of fig. 2 between $\sigma_{\gamma, 2n}$ and $\sigma_{\gamma, n}$ suggests that the probability that the

Fig. 2

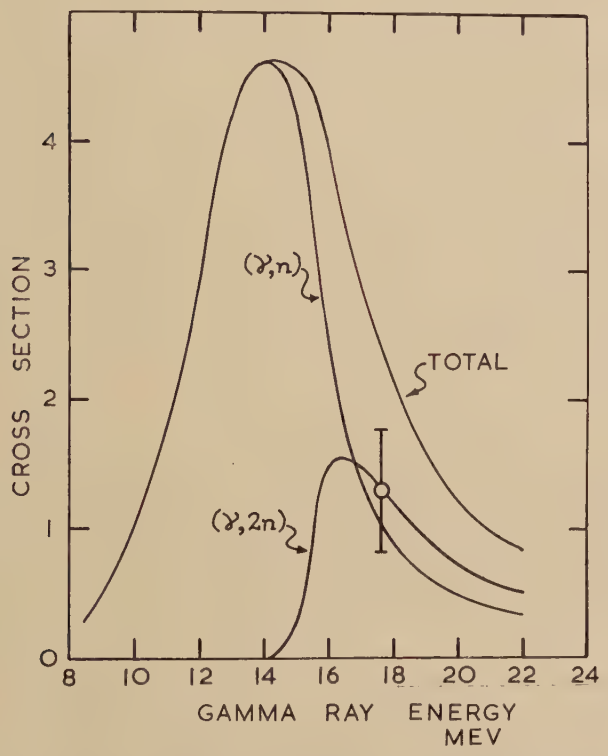

Cross section for ^{181}Ta(γ, n)^{180}Ta, our experimental value of $\sigma_{\gamma, 2n}$ at 17·6 MeV, the full $\sigma_{\gamma, 2n}$ constructed with its aid and the corresponding total cross section (cross section units are arbitrary).

neutron of a direct interaction should collide seriously enough to form a compound nucleus* is less than 0·2. This appears to be rather small but not, perhaps, impossible (the nucleon energy within the nucleus is about 50 MeV).

* It is also possible for a direct process to lead to a (γ, 2n) reaction without the intervention of a collision; if the direct ejection takes place from a sufficiently low-lying neutron shell sufficient excitation may remain in the nucleus for the emission of a second neutron.

§6. Discussion of the Result

We must first of all note that our measurement agrees with the prediction of Eyges to within our probable error though the experimental result may be somewhat the lower.

We have already remarked that, in tantalum at an excitation of 17·6 Mev, the neutron multiplicity, if a compound nucleus is formed, is 1·95 so our value of $\sigma_{\gamma,2n}$ is virtually the cross section for compound nucleus formation, while the bulk of $\sigma_{\gamma,n}$ probably belongs to some mechanism of direct excitation of the neutron.* Thus while our result supports the hypothesis of Levinger and Bethe (1952) that neutron emission processes of higher multiplicity are of considerable importance and so their explanation of nuclear photo-disintegration of the heavy elements in terms of the electric dipole sum rule, it shows that it may not be proper to neglect, as they do, the contribution of processes not involving compound nucleus formation. Off-hand one should expect the relative cross section for direct processes to increase with gamma-ray energy and so the ratio σ(direct)/σ(compound nucleus)=0·81 at 17·6 Mev is disturbingly large ; it may indicate that Levinger and Bethe's estimate of neutron multiplicity may be seriously high ; if corrected it would lead to an even larger value of

$$\int_0^\infty \sigma \, . \, dE$$

than they deduced, which value seemed already considerably higher than the prediction of the dipole sum rule. We must enquire into the possibility of error in $\sigma_{\gamma,n}$ at the higher energies : the results of Haslam, Smith and Taylor (1951) are based on careful and accurate work and appear to rule out a very small value of $\sigma_{\gamma,n}$ at 17·6 Mev, particularly as they

---

* A considerably lower value of the neutron multiplicity would result from Schiff's (1948) modification of the statistical theory in which the initial state is assumed to be of an especially-simple type (an extreme example of which would be that envisaged by Goldhaber and Teller) ; this simple state then tends to combine with other simple states whose density does not increase as rapidly with nuclear excitation as that of all states put together and in consequence the maximum of the photo-nucleon spectrum is shifted to higher energy. This theory might then be able to reconcile the high value of $\sigma_{\gamma,n}$ relative to $\sigma_{\gamma,2n}$ with compound nucleus formation and avoid the present rather-embarrassing assumption of a very considerable amount of direct interaction, and the perhaps even more embarrassing consequence of a probability of immediate escape of 80% or more for the neutron concerned. There is, however, little evidence for Schiff's hypothesis, though the possibility of an unexpectedly large $\sigma_{\gamma,n}$ following an excitation of the Goldhaber–Teller or other simple type must be borne in mind.

extend a further 4 MEV in gamma-ray energy.* If, in fact, $\sigma_{\gamma, n}$ were very small at 17·6 MEV the value of $\sigma_{\gamma, 2n}$ at 17·6 MEV derived from our experiment would increase to 0·42 in terms of $\sigma_{\gamma, n}$ at 14·6 MEV which is not far outside our experimental error. It is not, therefore, of great importance to the present work to determine the results of $\sigma_{\gamma, n}$ at the higher energy, though their relevance to the problem of neutron multiplicity at high energy may be considerable.†

We now turn to the other problem of interest stated in the introduction, namely the sharpness of the ' resonance ' and its possible implications for an explanation in terms of some general property of nuclear matter. We now know the ratio of the total cross section $(\sigma_{\gamma, n}+\sigma_{\gamma, 2n})$ at 17·6 MEV to that at its peak ; if we accept the measured $\sigma_{\gamma, n}$ this ratio is 0·51 and if we adopt the extreme view that $\sigma_{\gamma, n}$ is zero at 17·6 MEV the ratio is little different, namely 0·41. In either event it is clear that much of the ' resonance ' remains even in the total cross section, the width increasing from about 4·5 MEV for $\sigma_{\gamma, n}$ to a probable value of about 6 MEV for the total cross section as may be seen from fig. 2. This result then shows that there is indeed a need for a general account of the ' resonances ' in photonuclear processes, perhaps in terms of some aspect of the nucleon–nucleon interaction, perhaps in terms of the excitation of nuclear alpha-particles (Levinger and Bethe 1950), or perhaps in terms of a specific nuclear model such as that of Goldhaber and Teller.‡

---

* Some rather tenuous evidence for the reality of a large direct interaction (γ, n) cross section at 17·6 MEV may be obtained in the following way : Courant's (1951) theory of the direct interaction effect for the emission of protons from heavy elements predicts systematically too low a cross section ; if we accept that the emission of protons from heavy elements is due principally to direct interaction it is perhaps sensible to apply Courant's theory to direct neutron emission, multiplying its prediction by the factor by which it falls short for proton emission. For tantalum this gives $\sigma_{\gamma, n}$ about 70 mb as against the 85 mb of Haslam, Smith and Taylor with the cross section scale supplied by Halpern, Nathans and Mann (1952).

Very long 'tails' extending to over 40 MEV have been reported (Sagane 1951) in $\sigma_{\gamma, n}$ for $^{12}C(\gamma, n)^{11}C$ and $^{16}O(\gamma, n)^{15}O$ as also in $^{64}Zn(\gamma, n)^{63}Zn$ and $^{54}Fe(\gamma, n)^{53}Fe$ (Sagane 1952) ; these can only be due to a direct photo-effect, and suggest that this (γ, n) 'tail' in tantalum is probably real.

† It should also be noted that if the large (γ, n) cross section at high energies is indeed real and due to direct interaction we must anticipate that $\sigma_{\gamma, p}$ will not be negligible as the Coulomb barrier of about 13 MEV would be already overcome by protons from gamma-rays of energy 20 MEV (proton binding energy is 5·8 MEV according to Heidmann and Bethe (1951)). This would again raise

$$\int_0^\infty \sigma \, . \, dE.$$

The (γ, p) process would not, of course, have been detected by Haslam, Smith and Taylor as ^{180}Hf is stable.

‡ It is not suggested, of course, that this theory in its simple form is complete. The possible presence of the large cross section for direct interaction even in the neighbourhood of the 'resonance' shows that other processes may be of comparable importance. The magnitude of the (γ, γ') cross section (Stearns 1952) also argues against a pure Goldhaber–Teller theory.

If we accept all available experimental results at their face value the $(\gamma, 2n)$ process is seen almost wholly as a by-product of direct interaction and so should not be added to $\sigma_{\gamma, n}$ in discussing the significance of the 'resonances' if one believes these to be due to immediate compound nuclear formation of some sort. It also appears that the amount of immediate compound nucleus formation (as opposed to that via the reabsorption within the nucleus of a nucleon from a direct interaction) must be very small at 17·6 Mev. This may suggest that, when the direct effect is subtracted, the 'resonances' are even sharper than has been supposed and may even fall from their maxima more rapidly than they rise to them. The slower rise may be due to the relative importance, near the threshold, of dipole transitions which excite a compound nucleus but which are not part of the 'resonance', and of electric quadrupole and magnetic dipole transitions, again not part of the 'resonance'. This is to be expected. Indeed cross section curves exist that exhibit a sharp rise from the threshold followed by a plateau (e.g. Horsley, Haslam and Johns for $^{19}F(\gamma n)^{18}F$; Krohn and Shrader (1952) for $^{63}Cu(\gamma n)^{62}Cu$) or even a dip (e.g. Johns, Horsley, Haslam and Quinton (1951) for $^{14}N(\gamma n)^{13}N$) before the rise to the principal 'resonance'. In light nuclei such behaviour may, of course, merely reflect local fluctuations in level density or even excitation of individual nuclear levels (as observed, for example, by Goward and Wilkins (1952) in $^{16}O(\gamma, 4\alpha)$ and $^{12}C(\gamma, 3\alpha)$). If it is proper to suppose such a subtraction at the beginning, due to alternative modes of compound nuclear absorption and at the end, due to the direct effect, the present considerations suggest that, rather than being thought wider than at one time supposed, the 'resonances' should be regarded as narrower than they appear in $\sigma_{\gamma, n}$ alone.

§7. Comparison with the Total Neutron Yield Curve

We may compare our ideas of the forms of $\sigma_{\gamma, n}$ and $\sigma_{\gamma, 2n}$ with the total neutron yield curve obtained by Halpern, Nathans and Mann (1952) using betatron bremsstrahlung. This we do in fig. 3; the full curve is derived from the (γ, n) and $(\gamma, 2n)$ curves of fig. 2, and the circles are the experimental results of the above workers.* It is seen that agreement is as good as could be wished considering the rather inaccurate nature of both experiments.† Halpern, Nathans and Mann have interpreted their results in terms of a $\sigma_{\gamma, 2n}$ that rises rather slowly from the threshold‡ and reaches a maximum at about 20·5 Mev; this maximum is large enough to persist as a second maximum in the total cross section itself.

* A short comparison of these results has already been presented by Carver, Edge and Wilkinson (1953).

† It may be seen from fig. 1 that the predicted $\sigma_{\gamma, n}$ of Eyges would be in rather poor agreement with the neutron yield measurements; it would pass far above them around 17 Mev and fall badly below at the highest energies.

‡ This is very difficult to believe in view of the rapid rise in neutron multiplicity above the threshold.

This, if true, would be very startling. It might be that this second maximum is due to resonance dipole absorption in alpha-particle-like sub-units of the nucleus ; such a resonance may be expected at about 20–30 MEV. Again, one of the two maxima may be of the Goldhaber–Teller type and the other be due to some specific aspect of nuclear forces. The only theory at present available that predicts such a double

Fig. 3

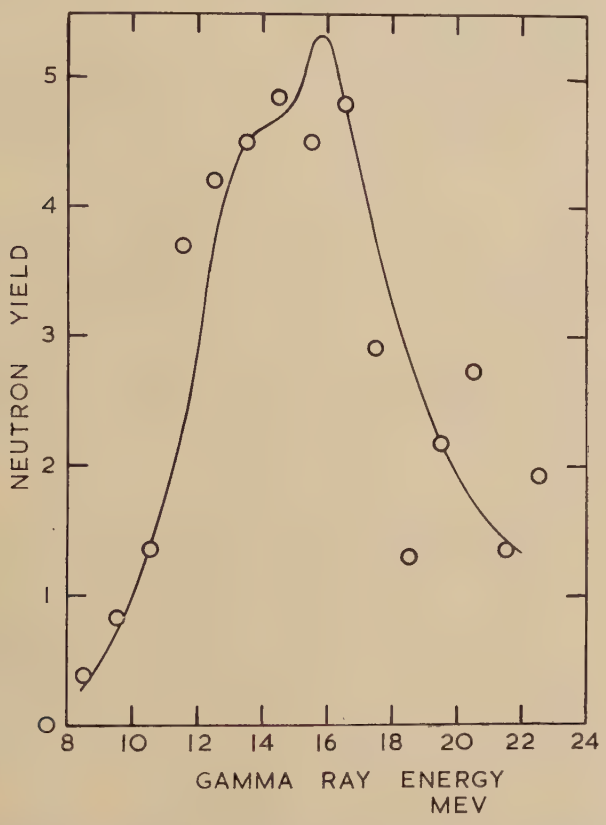

Total expected neutron yield (full line) as a function of gamma-ray energy derived from $\sigma_{\gamma,n}$ and $\sigma_{\gamma,2n}$ (taken from fig. 2) compared with the experimental neutron yield of Halpern, Nathans and Mann (circles). (Units of neutron yield are arbitrary.)

resonance is that of Danos and Steinwedel (1951) and Danos (1952) ; it extends the Goldhaber–Teller theory to resonance absorption of higher order. According to it the lowest mode of electric quadrupole absorption should take place at an energy 1·6 times higher than that of the fundamental dipole mode and would, of course, manifest itself chiefly as a (γ, 2n) resonance, since such absorption forms a compound nucleus with neutron multiplicity almost two. This would predict the second

maximum at 22·8 MeV instead of the observed 20·5 MeV.* It also appears from the work of Danos and Steinwedel using direct calculation and of Levinger and Bethe (1950) using a quadrupole sum rule that the observed cross section is of order two times greater relative to the dipole cross section at its resonance than should be expected for quadrupole absorption. If the second maximum becomes firmly established it will be a matter of the greatest importance, but it seems to us that the evidence is so far not completely convincing in view of the theoretical considerations and the good agreement between the neutron yield data and our own simpler suggestions.

It must be pointed out that convincing evidence for higher multipole absorption can only come from the establishment of subsidiary maxima in the total nuclear absorption cross section for gamma-rays. For example, Danos and Steinwedel (1951) and Danos (1952) have seen in Strauch's (1951) observation that the effective energy of gamma-ray for the production of the reaction $^{64}Zn(\gamma, pn)^{62}Cu$ is 30 MeV evidence for a quadrupole resonance. The more detailed work of Sagane (1952) however, shows that no pronounced corresponding maximum exists in the total cross section and that the energy at which this particular process enjoys a maximum is probably merely the result of competition (though it may be significant that $\sigma_{\gamma, 2n}$ shows a maximum at the same energy). In this example no final decision could be arrived at in any case on the basis of present evidence because $\sigma_{\gamma, p}$ is not known.

§8. Conclusions

1. The ratio of $\sigma_{\gamma, 2n}$ in tantalum at 17·6 MeV to $\sigma_{\gamma, n}$ at 14·6 MeV is $0{\cdot}29 \pm 0{\cdot}11$.

2. The total cross section for gamma-ray absorption still displays a resonance form such as predicted by the theory of Goldhaber and Teller.

3. The considerable value of $\sigma_{\gamma, 2n}$ found supports the idea that higher order processes are important in estimating the integrated cross section from the neutron yield in heavy elements.

4. The large value of $\sigma_{\gamma, n}$ above 18 MeV suggests that even at such a comparatively modest energy direct effects are of importance and that it is dangerous to base an analysis of high-energy photodisintegration on the idea that a compound nucleus is always involved.

5. There is some suggestion that the ' resonances ' may be regarded as even sharper than is indicated by $\sigma_{\gamma, n}$.

6. The possibility of higher multipole disintegration must be considered; this would be detected as a second ' resonance ' in the total absorption cross section.

---

* The relative positions of the two resonances may be changed by the strong damping suffered by each initial mode, but this effect cannot be estimated at the present time. Again the relative positions of the resonances may change if one relaxes the restriction imposed by Danos and Steinwedel that the surface neutrons and protons do not move relative to one another.

7. It seems to us that two measurements are of great importance in the attempt to elucidate more fully the mechanism of these processes: one is that of $\sigma_{\gamma, n}$ which should be done with the greatest attention to the region near the threshold and to the region above about 17 MEV; the other is of the total neutron yield, particularly above the ' resonance ' where $\sigma_{\gamma, 2n}$ becomes appreciable. It is not necessary that these measurements be made absolutely, but considerable accuracy is needed in the comparison of the forms of the cross sections and so it is highly desirable that both measurements be made by the same group; certain systematic errors in the form of both cross sections would then be of little importance where they would vitiate a comparison of the results of two groups each performing one measurement only.

ACKNOWLEDGMENTS

One of us (J. H. Carver) would like to thank the Australian National University for the award of a Scholarship, and one (R. D. Edge) would like to thank the Department of Scientific and Industrial Research for the award of a Research Grant.

We would like to express our thanks to Messrs. Murex Limited for the loan of the tantalum metal with which this work was performed.

REFERENCES A (AN HISTORICAL SELECTION)

BALDWIN, G. C. and KLAIBER, G. S., 1948, *Phys. Rev.*, **73,** 1156.
BYERLY, P. R. and STEPHENS, W. E., 1951, *Phys. Rev.*, **83,** 54.
MCELHINNEY, J., HANSON, A. O., BECKER, R. A., DUFFIELD, R. B. and DIVEN, B. C., 1949, *Phys. Rev.*, **75,** 542.
JOHNS, H. E., KATZ, L., DOUGLAS, R. A. and HASLAM, R. N. H., 1950, *Phys. Rev.*, **80,** 1062.
KATZ, L. and PENFOLD, A. S., 1951, *Phys. Rev.*, **81,** 815.
KATZ, L., JOHNS, H. E., BAKER, R. G., HASLAM, R. N. H. and DOUGLAS, R. A., 1951, *Phys. Rev.*, **82,** 271.

REFERENCES

BARNES, C. A., CARVER, J. H., STAFFORD, G. H. and WILKINSON, D. H., 1952, *Phys. Rev.*, **86,** 359.
BETHE, H. A. and PLACZEK, G., 1937, *Phys. Rev.*, **51,** 450.
BLATT, J. M. and WEISSKOPF, V. F., 1952, *Theoretical Nuclear Physics* (Wiley).
BYERLY, P. R. and STEPHENS, W. E., 1951, *Phys. Rev.*, **81,** 473.
CARVER, J. H., EDGE, R. D. and WILKINSON, D. H., 1953, *Phys. Rev.* (in press).
COURANT, E. D., 1951, *Phys. Rev.*, **82,** 703.
CURTIS, N. W., HORNBOSTEL, J., LEE, D. W. and SALANT, E. O., 1950, *Phys. Rev.*, **77,** 290.
DANOS, M., 1952, *Ann. d. Phys.*, **10,** 265.
DANOS, M. and STEINWEDEL, H., 1951, *Z. f. Naturforsch.*, **6A,** 217.
DIVEN, B. C. and ALMY, G. M., 1950, *Phys. Rev.*, **80,** 407.
EYGES, L., 1952, *Phys. Rev.*, **86,** 325.
GOLDHABER, M. and TELLER, E., 1948, *Phys. Rev.*, **74,** 1046.
GOWARD, F. K. and WILKINS, J. J., 1952, *Proc. Phys. Soc.* A, **65,** 671.

HALPERN, J., NATHANS, R. and MANN, A. K., 1952, *Phys. Rev.*, **88,** 679.
HANSON, A. O. and MCKIBBEN, J. L., 1947, *Phys. Rev.*, **72,** 673.
HASLAM, R. N. H., SMITH, L. A. and TAYLOR, J. G. V., 1951, *Phys. Rev.*, **84,** 840.
HEIDMANN, J. and BETHE, H. A., 1951, *Phys. Rev.*, **84,** 274.
HIRZEL, O. and WÄFFLER, H., 1947, *Helv. Phys. Acta*, **20,** 373.
HORNYAK, W. F., LAURITSEN, T., MORRISON, P. and FOWLER, W. A., 1950, *Rev. Mod. Phys.*, **22,** 291.
HORSLEY, R. J., HASLAM, R. N. H. and JOHNS, H. E., 1952, *Phys. Rev.*, **87,** 756.
JENSEN, P., 1948, *Naturwiss.*, **35,** 190.
JOHNS, H. E., HORSLEY, R. J., HASLAM, R. N. H. and QUINTON, A., 1951, *Phys. Rev.*, **84,** 856.
JONES, L. W. and TERWILLIGER, K. M., 1952, *Phys. Rev.*, **85,** 689.
KATZ, L. and CAMERON, A. G. W., 1951, *Phys. Rev.*, **84,** 1115.
KECK, J. C., 1952, *Phys. Rev.*, **85,** 410.
KERST, D. W. and PRICE, G. A., 1950, *Phys. Rev.*, **79,** 725.
KROHN, V. E. and SHRADER, E. F., 1952, *Phys. Rev.*, **87,** 685.
LEVINGER, J. S. and BETHE, H. A., 1950, *Phys. Rev.*, **78,** 115 ; 1952, *Ibid.*, **85,** 577.
LEVINTHAL, C. and SILVERMAN, A., 1951, *Phys. Rev.*, **82,** 822.
MCDANIEL, B. D., WALKER, R. L. and STEARNS, M. B., 1950, *Phys. Rev.*, **80,** 807.
MANN, A. K. and HALPERN, J., 1951, *Phys. Rev.*, **82,** 733.
MARQUEZ, L., 1951, *Phys. Rev.*, **81,** 897.
MILLER, D. W., ADAIR, R. K., BOCKELMAN, C. K. and DARDEN, S. E., 1952, *Phys. Rev.*, **88,** 83.
NABHOLTZ, H., STOLL, P. and WÄFFLER, H., 1951, *Phys. Rev.*, **82,** 963.
PASKIN, A., 1952, *Phys. Rev.*, **87,** 197.
POSS, H. L., 1950, *Phys. Rev.*, **79,** 539.
PRICE, G. A., 1951, see KERST, D. W., *Proceedings of Nuclear Physics Conference*, Chicago, 1951, p. 197.
PRICE, G. A. and KERST, D. W., 1950, *Phys. Rev.*, **77,** 806.
SAGANE, R., 1951, *Phys. Rev.*, **84,** 587 ; 1952, *Ibid.*, **85,** 926.
SCHIFF, L. I., 1948, *Phys. Rev.*, **73,** 1311.
STEARNS, M. B., 1952, *Phys. Rev.*, **87,** 706.
STEARNS, M. B. and MCDANIEL, B. D., 1951, *Phys. Rev.*, **82,** 450.
STEINWEDEL, H. and JENSEN, J. H. D., 1950, *Z. f. Naturforsch.*, **5A,** 413.
STRAUCH, K., 1951, *Phys. Rev.*, **81,** 973.
SUGARMAN, N. and PETERS, R., 1951, *Phys. Rev.*, **81,** 951.
TERWILLIGER, K. M., JONES, L. W. and JARMIE, W. N., 1951, *Phys. Rev.*, **82,** 820.
WÄFFLER, H. and HIRZEL, O., 1948, *Helv. Phys. Acta*, **21,** 200.
WALKER, D., 1951, *Phys. Rev.*, **81,** 634.
WILKINSON, D. H. and CARVER, J. H., 1951, *Phys. Rev.*, **83,** 466.

XLIV. *Neutrons Produced by High Energy Protons*

By T. C. Randle, J. M. Cassels, T. G. Pickavance and A. E. Taylor
Atomic Energy Research Establishment, Harwell*

[Received December 31, 1952]

Abstract

The energy spectra and yields of neutrons produced by the bombardment of beryllium, carbon, aluminium and uranium with protons of energy 160 Mev have been measured at an angle near the forward proton direction.

§ 1. Introduction

The neutrons obtained from internal targets in the 110″ Harwell synchrocyclotron have already been used for many experiments, and the purpose of this paper is to describe some measurements of the neutron flux and energy distribution. The preliminary results already briefly reported (Cassels, Randle, Pickavance and Taylor 1951) have been improved by calibrating the neutron detector experimentally instead of relying on calculated correction factors.

§ 2. Principle

The target, made either of beryllium, carbon, aluminium or uranium, intercepted the circulating proton beam of the cyclotron at a radius where the maximum proton energy was 171 Mev. A hole 5 cm in diameter in the concrete shielding walls enabled neutrons produced at 2·5° from the forward direction to pass through to the neutron detector. The position of the cyclotron and the shielding walls made it inconvenient to use a smaller angle to the forward direction. The neutrons emerged from the cyclotron vacuum chamber through an aluminium window 3 mm thick. The relative positions of the cyclotron target, shielding walls and neutron detector were as shown in fig. 1 of a paper on another subject (Taylor, Pickavance, Cassels and Randle 1951). The same neutron monitor was used.

The neutron detector, which measured the number of neutrons within a predetermined energy band, consisted of a counter telescope and a polythene radiator. The radiator was placed in the neutron beam and protons recoiling at an angle of 10° to the forward direction of the neutrons passed successively through 53 cm of air, two proportional counters, a carbon absorber and an ionization chamber. In general the ionization chamber responded to protons near the end of their range, so that only

* Communicated by the Authors.

those protons which emerged from the radiator in a defined energy band could cause a triple coincidence between the two counters and the ionization chamber. The mean energy of the protons detected was set by the thickness of the carbon absorber. Since there was a one to one correlation between neutron and proton energies only for recoils from the hydrogen nuclei in the polythene, it was necessary to subtract a background taken with a carbon radiator. The polythene and carbon radiators contained the same number of carbon atoms.

§ 3. The Ionization Chamber

The ionization chamber (fig. 1) contained a grid to ensure that the height of the output pulses depended only on the amount of ionization produced. The sensitive volume between the grid and the high voltage

Fig. 1

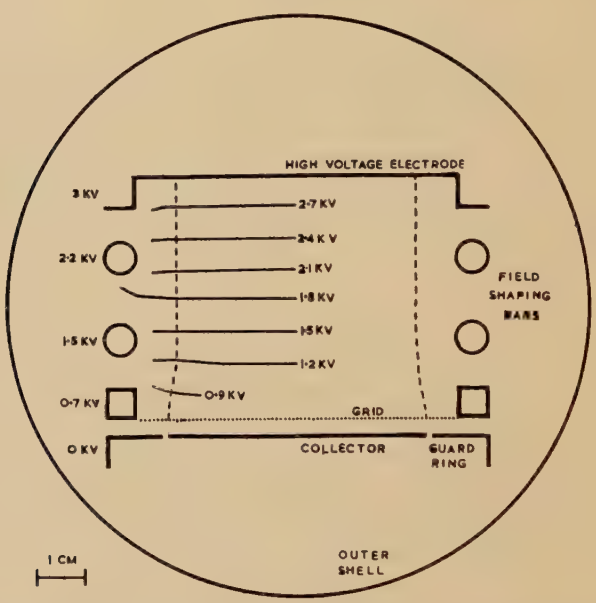

A section of the ionization chamber showing the equipotential surfaces of the electrostatic field. The sensitive volume is between the dashed lines.

electrode was 34 cm long and had a breadth and height both equal to 5 cm. The chamber was aligned so that the protons, after entering through a copper window 46 mg-cm^{-2} thick, travelled along its length. It was filled to a pressure of 70 cm Hg with argon (90%) and carbon dioxide (10%).

The electrostatic potentials applied to four field shaping bars, which ran the whole length of the chamber, were adjusted to give a sufficiently uniform field in the sensitive volume. The correct potentials for the bars were found by experimenting with a model in an electrolytic tank.

The equipotential surfaces so found are also shown in fig. 1, and the boundaries of the sensitive volume are indicated by dashed lines.

The grid conformed to the design data given by Bunemann, Cranshaw and Harvey (1946); it consisted of a number of parallel strands of 36 S.W.G. copper wire separated by gaps of 0·81 mm and was supported on a brass frame 3·2 mm away from the collector.

A thin polonium alpha particle source was mounted on a flap in the centre of the high voltage electrode in such a way that it could be exposed to the sensitive volume when required. A differential bias curve of the polonium alpha particles, plotted with the aid of a 30 channel pulse amplitude analyser, is shown in fig. 2. The tail on this curve was caused by those particles which did not have their whole range within the sensitive volume. The full width at half height of the main peak was 4·3% of the mean pulse height, and it was concluded that the ionization chamber and its grid were working satisfactorily.

Fig. 2

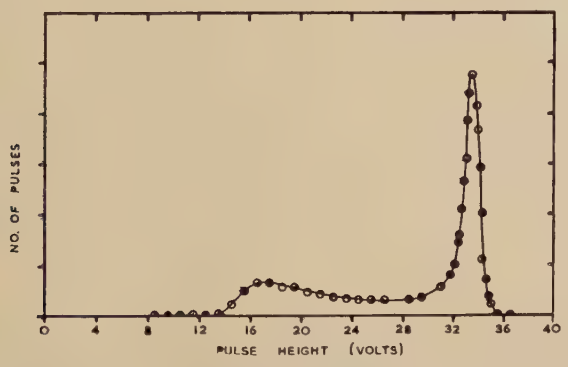

The pulse height distribution obtained from the ionization chamber on exposure to the source of 5·3 MeV alpha particles.

§ 4. The Counter Telescope

The proportional counters in the telescope were cylindrical, 5 cm in diameter and 5 cm in length, with copper end windows 46 mg-cm^{-2} thick. A 0·02 cm tungsten wire, stretched across a diameter, acted as the collecting electrode. The counters were filled to a pressure of 52 cm Hg with a mixture of argon (96%) and carbon dioxide (4%).

The voltage pulses from the counters and ionization chamber were amplified and fed into a triple coincidence unit after amplitude discrimination. Pulses from the two proportional counters were mixed first (resolving time 0·5 μs) and the resulting double coincidence pulses were then mixed with pulses from the ionization chamber (resolving time 1 μs). The resolving times, the channel delay times and the voltages applied to the proportional counters, were adjusted in the standard way to bring each on to a ' plateau ' of the triple coincidence counting rate.

The amplitude discrimination on the pulses from the chamber was set so that a proton dissipating 0·67 MeV within the sensitive volume was on the threshold of detection. The setting was made by using the internal polonium source of 5·3 MeV alpha particles. The amplifier noise pulses rarely appeared above half this setting.

A calculation involving the length of the ionization chamber and the stopping power of the filling gas showed that a proton entering the sensitive volume with an energy greater than 29·5 MeV was not normally counted because its specific ionization was too small. Thus the chamber was sensitive to protons entering it with an energy between 0·67 MeV and 29·5 MeV. A neutron could therefore be detected if it was able to produce a proton recoil which, after being slowed down in its passage through the telescope, reached the chamber with an energy between these limits.

It was, however, possible for neutrons of higher energy to be detected by a different mechanism. They could produce proton recoils which made a nuclear collision in the absorber, or elsewhere, and the reaction products could pass through the chamber and cause enough ionization for a count to be recorded. The magnitude of this effect, which was small, was determined in the calibration experiment.

The random triple coincidences were recorded during each run by feeding the double coincidences from the proportional counters and delayed pulses from the ionization chamber into a separate mixer unit. A delay time of 2·5 microseconds was used. The number of genuine coincidences was found by subtracting the random coincidences. The random rate was usually about 1% of the genuine rate.

The polythene and carbon radiators were cylindrical in shape and their diameter (5 cm) was less than the diameter of the neutron beam in which they were placed. Their masses were 38·17 and 32·55 g respectively. An extra absorber was put into the telescope when using the carbon radiator in order to compensate for the difference in stopping powers of the carbon and polythene radiators.

§ 5. The Range–Energy Relation

The range–energy relation for protons in carbon was computed for a value of the mean ionization potential (I) equal to 74 ev. In the earlier report of this work (Cassels *et al.* 1951) a value of I equal to 50·3 ev (Taylor 1950) was used, but the experimental evidence is now in favour of the higher value. The new value, which is in agreement with the work of Mather and Segrè (1951) and of Bakker and Segrè (1951), was obtained by comparing the range of the cyclotron external proton beam in carbon and aluminium. The aluminium range–energy relation published by Smith (1947) was assumed to be correct, as Bloembergen and van Heerden (1951) and Mather and Segrè (1951) have shown that the ranges predicted are accurate to 2% or better.

§ 6. Calibration

The thickness of absorber in the counter telescope was varied during the spectrum measurements and this resulted in a variation of some of the characteristics of the neutron detector. For example, the width of the main detection band was not constant owing to the properties of the range–energy relation for protons in matter, and there was also a variable loss of protons by multiple coulomb scattering and nuclear absorption, which occurred mainly in the absorber. Therefore a calibration experiment was necessary. It was also possible from this experiment to find the mean detection energy and the small response to energies higher than the main detection band.

The response to various proton energies was measured by placing the telescope, without a radiator, in the external proton beam of the cyclotron. The incident energy was changed by slowing down the protons in varying amounts of carbon absorber (the primary absorber) 3 metres in front of the telescope. The number of triple coincidences was measured for each incident proton energy, the double coincidences between the two proportional counters being used as a monitor. In this way the proton efficiency curves were plotted. Each was converted to a neutron efficiency curve by multiplying the ordinates by the neutron–proton cross-section at 10°, and the incident proton energies were changed to the equivalent neutron energies by considering the kinematics of the neutron–proton scattering, allowance being made for ionization losses in the radiator.

The values of the neutron–proton differential cross-section were taken from the expression

$$\sigma\,(10°) = 3{\cdot}64 + 259\,(E)^{-1/2} + 1180\,(E)^{-1}$$

where $\sigma\,(10°)$ is in the laboratory system of co-ordinates and is expressed in units of 10^{-27} cm^2-steradian^{-1} and E is the neutron energy in Mev. The equation was determined empirically so that it agreed with the experimental results (Hadley, Kelly, Leith, Segrè, Wiegand and York 1949 ; Randle, Taylor and Wood 1952).

The external proton beam of the cyclotron was not monoenergetic and an energy spread was also introduced by straggling in the primary absorber. This tended to mask the details in the shape of the efficiency curves. The standard deviation of the energy of the incident protons, varied between 1·8 and 4·5 Mev, depending on the primary absorber thickness.

The neutron efficiency curves determined in this calibration were not the same as the efficiency curves which applied during the spectrum experiments, because the additional energy spreads introduced by the radiator and the finite angular resolution of the telescope were not included. Although these spreads spoil the energy resolution of the detector they do not change the ratio of the areas under the curves and therefore it was permissible to use the curves as at present determined to evaluate the results.

The calibration was done for four thicknesses of the telescope absorber and the results (fig. 3) clearly display the differential nature of the detector. The small response to high energy particles caused by the effect mentioned previously can be seen in the figure. A division was made between this high energy tail and the main part of the efficiency curve at the dashed lines. The lines were chosen so that the corresponding protons were entering the ionization chamber with an energy of 50 MEV. The contribution of the tail to the number of triple coincidences was subtracted during the evaluation of the neutron spectra.

The area under the main part of the efficiency curves was used as a divisor when evaluating the neutron spectra from the triple coincidence counting rates, and the effective neutron energy of the detector was taken to be the abscissa of the centroid of this area. A graph of each of these two quantities against telescope absorber thickness was constructed by using the four experimental points.

Fig. 3

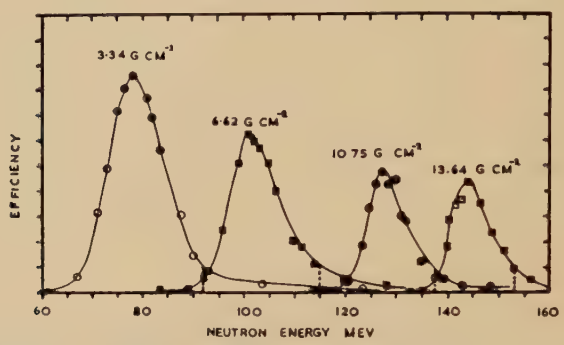

The efficiency of the counter telescope as a function of neutron energy for four thicknesses of telescope absorber. The circles and squares plotted here are about equal to the standard deviation of the counting statistics.

§ 7. The Energy Resolution of the Neutron Detector

The finite radiator thickness contributed in two ways to the width of the efficiency curve. First, the position of the neutron–proton collision within the radiator was uncertain. This caused an uncertainty in the neutron energy of 10 MEV at the highest detection energy and 22 MEV at the lowest. Secondly, the multiple coulomb scattering of the protons in the radiator caused an uncertainty in the scattering angle. The largest consequent uncertainty in neutron energy was about 2% and this occurred at the lowest detection energies. The angular resolution of the telescope (4°) also caused an uncertainty of scattering angle and in this case the spread in neutron energies was 2·4%.

The efficiency curves determined in the calibration experiment contained the spread arising from the straggling in the telescope absorber.

As has been mentioned previously, they also contained an unwanted spread arising from the energy spread introduced into the incident proton beam before reaching the telescope. It was estimated that the total effect of all the spreads which occurred in the spectrum experiments gave a neutron efficiency curve whose full width at half height was about 11 MEV at a mean detection energy of 150 MEV and about 25 MEV at 60 MEV.

§ 8. The Proton Spectrum

The protons which bombarded the internal cyclotron targets were not monoenergetic. The inhomogeneity was caused by radial oscillations of the particles in the cyclotron and by target thickness effects, which were aggravated by multiple traversals (Cassels, Dickson and Howlett 1951). Dickson (1952) has examined the radial oscillations in the Harwell cyclotron, and his results, taken together with the multiple traversal theory, have been used to compute the primary proton spectrum shown by dashed lines in figs. 5, 6, 7 and 8.

Fig. 4

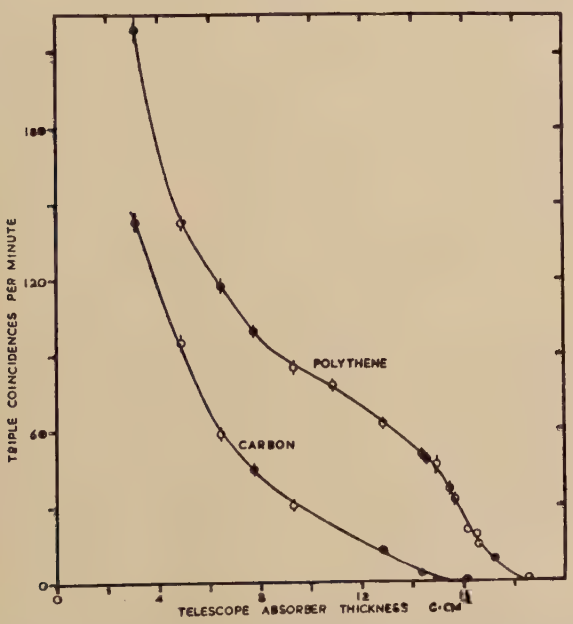

The genuine triple coincidence rate as a function of the telescope absorber thickness obtained with the beryllium target for the polythene and carbon radiators.

§ 9. Evaluation of the Neutron Spectra

Figure 4 shows the genuine triple coincidence counting rates obtained with the beryllium target. The other targets gave similar curves. The number of genuine triple coincidences per monitor count obtained with the polythene and carbon radiators was noted for each absorber thickness.

The difference was divided by the area of the main part of the efficiency curve corresponding to that absorber thickness. This quantity was now proportional to the neutron flux per MeV and a preliminary graph against the effective neutron energy was plotted.

The shape of the neutron energy spectrum was next corrected for the high energy tail on the efficiency curve. The spectrum as determined so far was used to calculate the contribution to the triple coincidences arising from the tail. This contribution, which varied from zero to 20%, was subtracted and a new neutron spectrum calculated. The process could have been repeated but this was not found to be necessary.

§ 10. Absolute Cross Sections

The neutron spectra were placed on an absolute scale by determining the cross-section for the production of neutrons of energy greater than 58 MeV. For this experiment the same detector was used except that the ionization chamber was replaced by a third proportional counter. As usual, polythene and carbon radiators were used and differences taken. The carbon absorber thickness was such that neutrons with an energy above 58 MeV were detected. As the neutron–proton scattering cross-section varied with neutron energy it was necessary to use an effective value when calculating the neutron flux. The scattering cross-section was weighted with the neutron spectrum in order to find this effective value.

Immediately after the neutron flux from the carbon target had been measured, this target was removed from the cyclotron and its ^{11}C activity measured with a calibrated Geiger counter. The cross-section for the reaction $^{12}C(p, pn)^{11}C$ has been determined (Aamodt, Peterson and Phillips 1952) and so the neutron production cross-section could be found. To obtain a similar result for beryllium, two thick pieces of beryllium were sandwiched between three thin pieces of carbon so as to form a composite target. Allowance was made for the small number of neutrons which came from the carbon. The target was dismantled after bombardment and the carbon layers examined with the calibrated counter as before. The neutrons detected in these two experiments left the target at an angle of 5° to the forward direction. The cross-sections were corrected back to 2·5° by using the angular distribution measured by Snowden (1952). The correction amounted to 1% for beryllium and the carbon correction was assumed to be the same.

In another experiment, the neutron production cross-sections in four elements were compared at the usual angle of 2·5° to the forward direction. Beryllium, carbon, aluminium and platinum targets were mounted on a rotating holder. A remote control device enabled any one of the targets to be brought into the proton beam. The thicknesses of the four targets, expressed in radiation lengths, were chosen to be nearly equal so that about the same number of traversals of the beam occurred

with each target. The multiple traversal theory was used to make the small residual corrections. A platinum target was used instead of uranium because of the difficulty of obtaining a thin piece of uranium.

The results of the ratio experiment and the absolute experiment were used to give a combined result (see the table). The uranium production cross-section was calculated to be 1805×10^{-27} cm^2-steradian^{-1} by assuming that the cross-section varied as the 2/3 power of the number of neutrons in the nucleus (Knox 1951).

Cross Sections for the Production of Neutrons near the Forward Direction with an Energy above 58 MeV

Element	Be	C	Al	Pl
Ratio Expt.	1 $\pm$0·036	0·993 $\pm$0·049	2·37 $\pm$0·12	19·2 $\pm$1·1
Absolute Expt. $10^{27}\sigma$ (cm^2 ster.$^{-1}$)	95 $\pm$ 18	67 $\pm$ 14	—	—
Combined Results $10^{27}\sigma$ (cm^2 ster.$^{-1}$)	81 $\pm$ 15	81 $\pm$ 15	192 $\pm$ 35	1560 $\pm$ 280
Theoretical Results of Mandl and Skyrme $10^{27}\sigma$ (cm^2 ster.$^{-1}$)	66	68	105	—

§ 11. Final Results

Figures 5, 6, 7 and 8 show the spectra obtained with the beryllium, carbon, aluminium and uranium targets. The errors shown are the standard deviations due to the counting statistics of the spectrum shape experiment. The cross-section scales have an uncertainty of 18% which arises from the total neutron production experiments, although for relative values between the four curves the uncertainty is only 5%.

§ 12. Discussion

The most striking feature of these results is that all the neutron energy spectra show prominent peaks close to the upper limits set by the energy available. In carbon the limit is unusually low because the Q of the (p, n) reaction in ^{12}C (isotopic abundance 99%) is $-18{\cdot}5$ MeV. Similar peaks have been observed in the energy spectra of the neutrons produced by 245 MeV protons (Nelson, Guernsey and Mott 1952). Experiments with 112 MeV protons (Bodansky and Ramsey 1951, Strauch and Hofmann 1952) have shown that the peaks begin to appear when the emergent neutrons can have energies greater than about 85 MeV.

Many experiments have shown that the mean free path of high energy nucleons in nuclear matter is of the same order as nuclear radii. Because of this ' transparency ' high energy neutron production in the forward direction is mainly the result of direct knock-on collisions between the ingoing proton and individual neutrons in the target nucleus. This process obviously leads to a peak in the neutron spectrum near the

Figs. 5 and 6

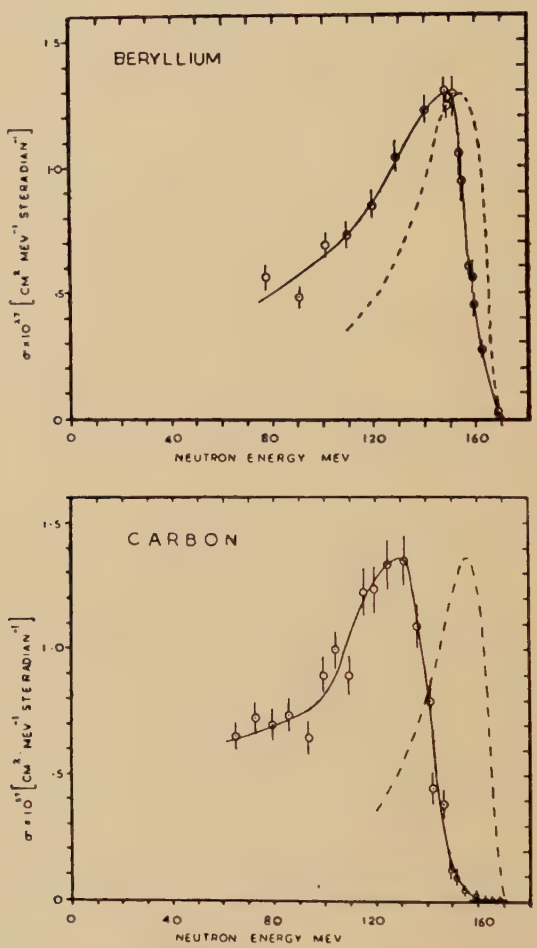

The neutron energy spectra obtained from beryllium and carbon by bombardment with protons. The energy spectra of the primary protons are indicated by the dashed lines.

maximum energy. The peak is broadened by the internal momentum distribution of the struck neutrons, and lower energy neutrons can also be emitted in the forward direction when two or more fast collisions take place inside the target nucleus.

These processes have been examined theoretically by Mandl and Skyrme (1952) whose results are in reasonable agreement with experiment. A very close comparison of experiment with the theory is prevented by the large, and rather uncertain, spread in energy of the primary protons. This spread is now known to be larger than was

Figs. 7 and 8

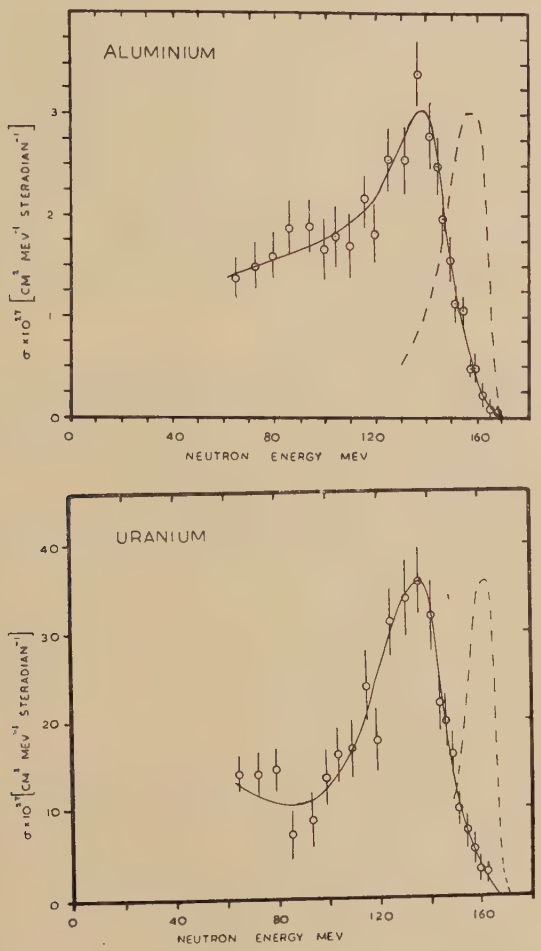

The neutron energy spectra obtained from aluminium and uranium by bombardment with protons. The energy spectra of the primary protons are indicated by the dashed lines.

realized at the time of the earlier communications from Harwell on high energy neutron spectra. In particular, it is not clear whether or not there are more low energy neutrons than would be predicted.

Acknowledgments

The authors wish to thank the cyclotron operating crew for their co-operation during these experiments. This paper is published with the permission of the Director of the Atomic Energy Research Establishment.

References

Aamodt, R. L., Peterson, V., and Phillips, R., 1952, *Phys. Rev.*, **88,** 739.
Bakker, C. J., and Segrè, E., 1951, *Phys. Rev.*, **81,** 489.
Bloembergen, N., and van Heerden, P. J., 1951, *Phys. Rev.*, **83,** 561.
Bodansky, D., and Ramsey, N. F., 1951, *Phys. Rev.*, **82,** 831.
Bunemann, O., Cranshaw, T. E., and Harvey, J. C., 1946, Canadian Report C.R.P. 247. P.D. 285.
Cassels, J. M., Dickson, J. M., and Howlett, J., 1951, *Proc. Phys. Soc.* B, **64,** 590.
Cassels, J. M., Randle, T. C., Pickavance, T. G., and Taylor, A. E., 1951, *Phil. Mag.*, **42,** 215.
Dickson, J. M., 1952, to be submitted for publication.
Hadley, J., Kelly, E., Leith, C., Segrè, E., Wiegand, C., and York, H., 1949, *Phys. Rev.*, **75,** 351.
Knox, W. J., 1951, *Phys. Rev.*, **81,** 687.
Mandl, F., and Skyrme, T. H. R., 1952, *Proc. Phys. Soc.* A, **65,** 101.
Mather, R., and Segrè, E., 1951, *Phys. Rev.*, **84,** 191.
Nelson, B. K., Guernsey, G., and Mott, G., 1952, *Phys. Rev.*, **88,** 1.
Randle, T. C., Taylor, A. E., and Wood, E., 1952, *Proc. Roy. Soc.* A, **213,** 392.
Smith, J. H., 1947, *Phys. Rev.*, **71,** 32.
Snowden, M., 1952, *Phil. Mag.*, **43,** 285.
Strauch, K., and Hofmann, J. A., 1952, *Phys. Rev.*, **86,** 563.
Taylor, A., E. 1950, *Phil. Mag.*, **41,** 966.
Taylor, A. E., Pickavance, T. G., Cassels, J. M., and Randle, T. C., 1951, *Phil. Mag.*, **42,** 20.

XLV. *The Role of Preferred Orientation in Elasticity Investigations*

By G. Bradfield and H. Pursey
National Physical Laboratory, Teddington*

[Received January 13, 1953]

Abstract

The purpose of the paper is firstly to investigate the role of preferred orientation in the elastic properties of polycrystalline metals, and secondly to apply these considerations to some experimental results. The analysis is confined to metals in the cubic crystalline system constituted so that the preferred orientation has circular symmetry about the axis of a bar, expressions being derived for the apparent elastic constants of the bar in terms of the single crystal constants and an anisotropy index. The experimental results used for illustration relate to alloys of copper with members of the first long period and cover variations in the annealing processes used.

It is not widely known that most polycrystalline metals prepared by ordinary laboratory and industrial methods are markedly anisotropic on account of preferred orientation, and that this preferred orientation changes its character on annealing. Unless a correction for anisotropy is applied, the normal effect of annealing in raising the elastic moduli will be completely masked. This paper describes a method of estimating the degree of anisotropy, and of correcting for it. Using this method of correction some results are given on a series of alloys of copper with elements of the first long period, showing the way in which annealing influences their elastic properties, especially for very dilute alloys.

The extent of these effects is shown in the table below by tests on two bars of copper and two of silver, which are typical of certain methods of manufacture. The bars were tested dynamically in longitudinal vibration, which yields an apparent Young's Modulus E', and in torsional vibration, which yields an apparent Modulus of Rigidity G', using methods discussed briefly by Bradfield (1951) and in *Nature* (1952). An apparent Poisson's Ratio σ_{MF} (equal to $\frac{1}{2}E/G-1$) has been derived from these results, together with a lateral inertia Poisson's Ratio σ_{LI} which was deduced from the theory of dispersion of longitudinal waves in round bars evolved by Pochhammer (1876) whose mathematical treatment was simplified by Bancroft (1941). It is assumed in this theory that the elastic moduli are invariant with frequency, and other experiments on these materials had shown this to be the case (over the frequency range in the table).

The table shows that annealing may result in an increase of as much as 35% in E' together with a decrease of 13% in G'. Consequently, unless

---

* Communication from the National Physical Laboratory.

Specimen	Heat Treatment	Frequency Range	Apparent Young's Modulus $E'(\times 10^{-11}$ dynes/cm$^2)$	Apparent Modulus of Rigidity $G'(\times 10^{-11}$ dynes/cm$^2)$	Apparent Poisson's Ratio σ_{LI}	σ_{MF}
N.P.L. Pure Copper	As received	20–100 kc/s	12·69	$4{\cdot}72_9$	0·340	0·342
N.P.L. Pure Copper	1½ hours at 550°c	20–150 kc/s	13·00	$4{\cdot}79_7$	0·344	0·357
N.P.L. Pure Copper	3 hours at 550°c	20–150 kc/s	13·01	$4{\cdot}79_7$	0·344	0·356
No. 2M Pure Copper	As received	20–100 kc/s	12·07	$4{\cdot}75_0$	0·345	0·271
No. 2M Pure Copper	1½ hours at 550°c	20–100 kc/s	14·99	$4{\cdot}20_7$	0·345	0·781
No. 2M Pure Copper	3 hours at 550°c	20–100 kc/s	14·93	$4{\cdot}20_4$	0·300	0·776
No. 2M Pure Silver	As received	20–100 kc/s	7·13	3·00	0·380	0·185
No. 2M Pure Silver	1½ hours at 550°c	20–120 kc/s	9·60	2·66	0·378	0·802
Isotropic Pure Copper	Thoroughly annealed		12·96	4·83	0·342	0·342
Isotropic Pure Silver	Thoroughly annealed		8·28	$3{\cdot}02_5$	0·368	0·368

Referred to 20°c

a correction is made for anisotropy the results are meaningless. It is only fair to add that several of the above specimens were so anisotropic as to be beyond the scope of the present first-order correction theory, and in such cases the value of the system of testing lies in its ability to indicate that such specimens should be rejected.

More detailed accounts of the methods of test and the derivation of the anisotropy corrections will be published separately by the present authors, but because of its outstanding importance in elasticity research the method of deriving the corrections and hence obtaining the true elastic constants for the material tested will now be indicated.

If we assume that the specimen has circular symmetry about its principal axis then it can be shown that its elastic constants may be expressed in terms of the three single-crystal constants of the material (supposing this to have cubic symmetry) and a constant K, equal to the average value of $l^2m^2+m^2n^2+n^2l^2$ over all grains, where l, m and n are the direction cosines of the specimen axis relative to the crystallographic axes of an individual grain.

The ' anisotropy index ' α is defined by

$$\alpha=\frac{\sigma_{MF}-\sigma_{LI}}{\sigma_{LI}}. \quad . \quad . \quad . \quad . \quad . \quad . \quad . \quad . \quad (1)$$

Then it may be shown that

$$\alpha=\frac{-125c\,(K-1/5)}{2(c_{11}-c_{12}+3c_{44})(c_{11}+4c_{12}-2c_{44})}, \quad . \quad . \quad . \quad . \quad (2)$$

where c_{11}, c_{12} and c_{44} are the elastic moduli of a single crystal of the material and $c=(c_{11}-c_{12}-2c_{44})$. For an isotropic (randomly oriented) polycrystalline material the value of K is 1/5 and α is zero.

Hence the elastic constants of the specimen may be expressed in terms of the three single-crystal constants and the anisotropy index.

We find that

$$E'=\frac{(c_{11}+2c_{12})(c_{11}-c_{12}-3Kc)}{c_{11}+c_{12}-Kc}. \quad . \quad . \quad . \quad . \quad . \quad (3)$$

For small values of α,

$$E'=E+\alpha\left(\frac{\partial E'}{\partial \alpha}\right)_{\alpha=0} \quad . \quad . \quad . \quad . \quad . \quad (4)$$

$$=E+\alpha\left(\frac{\partial E'}{\partial K}\right)_{K=1/5}\left(\frac{\partial K}{\partial \alpha}\right) \quad . \quad . \quad . \quad . \quad . \quad (5)$$

where E is the isotropic modulus (i.e. the value of E' when $K=1/5$) and from eqns. (2) and (3)

$$\left(\frac{\partial E'}{\partial K}\right)_{K=1/5}\left(\frac{\partial K}{\partial \alpha}\right)=\left(\frac{E}{5}\right)\left(\frac{c_{11}+4c_{12}-2c_{44}}{2c_{11}+3c_{12}+c_{44}}\right). \quad . \quad . \quad . \quad (6)$$

Substituting (6) in eqn. (5) gives

$$E=E'\left\{1-\frac{c_{11}+4c_{12}-2c_{44}}{2c_{11}+3c_{12}+c_{44}}\cdot\frac{\alpha}{5}\right\} \quad . \quad . \quad . \quad . \quad . \quad (7)$$

and similarly

$$G=G'\left\{1+\frac{c_{11}+4c_{12}-2c_{44}}{c_{11}+2c_{12}}\cdot\frac{2\alpha}{25}\right\}. \quad . \quad . \quad . \quad . \quad (8)$$

Calculations on a number of materials show that the coefficients of α in these expressions are of order $\pm 0{\cdot}1$, and provided α is reasonably small (experience shows that it should not exceed $0{\cdot}1$) the coefficients need only be known to an accuracy of about $\pm 5\%$. A similar analysis can cover the effect of circularly symmetric preferred orientation on the stress–strain elastic constants, e.g. effective c_{11}, c_{44} etc. of such a specimen. It should be pointed out that if the analysis is carried out by averaging the single-crystal moduli of compliance s_{11}, s_{12} and s_{44} then the analogous

Fig. 1

Values referred to 20°C

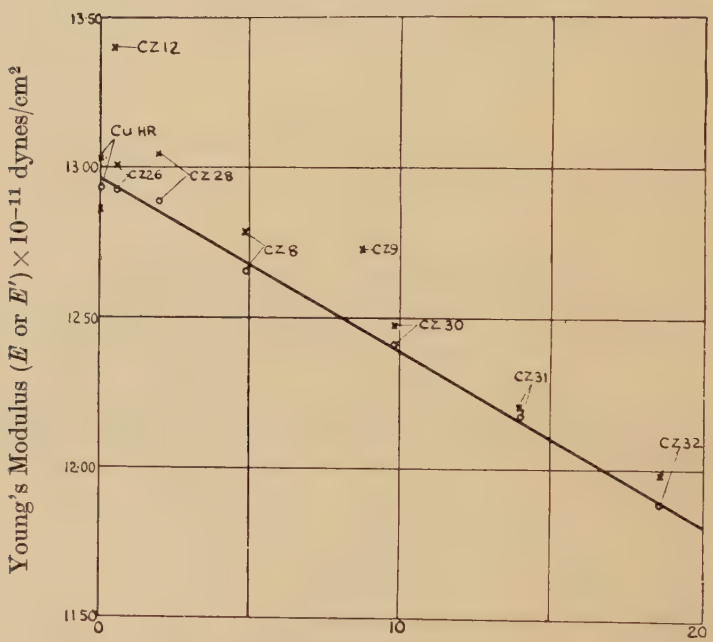

Variation of Young's Modulus with Zinc Content in Copper–Zinc Alloys, showing effect of corrections for anisotropy and of correct annealing.

○ Corrected for anisotropy.

× Uncorrected for anisotropy and inadequately annealed.

expressions corresponding to eqns. (7) and (8) yield coefficients for α which are identical in value with those obtained above.

In conclusion, the value of these methods will be illustrated in connection with an investigation on the elasticity of copper–zinc alloys. In figs. 1 and 2, Young's Modulus and Modulus of Rigidity are plotted

against atomic percentage of the alloying element. The final results when the specimens were thoroughly annealed (650°C for $1\frac{1}{2}$ hours) and corrected for anisotropy are shown in comparison with the original results in which the specimens had not been completely annealed and were uncorrected for anisotropy. The former values show a linear relationship to the proportion of alloying element with a standard deviation of about 0·2% while the values for inadequately annealed and uncorrected specimens are almost useless.

Fig. 2

Values referred to 20°C

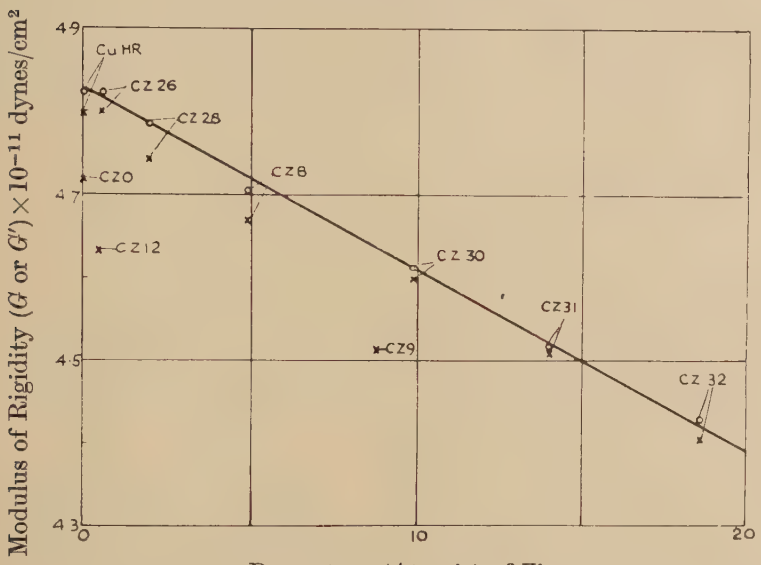

Variation of Modulus of Rigidity with Zinc Content in Copper–Zinc Alloys, showing effect of corrections for anisotropy and of correct annealing.

○ Corrected for anisotropy.
× Uncorrected for anisotropy and inadequately annealed.

An interesting phenomenon is revealed by figs. 3 and 4 which show the results obtained on inadequately annealed specimens (including both copper–zinc alloys and alloys of copper with other elements of the first long period), after correcting for anisotropy. The moduli of pure copper and very dilute alloys are lower than those obtained after more thorough annealing, but the more concentrated alloys are relatively unchanged. This has been taken to indicate that the initial depression is due to very mobile dislocations which are anchored by the stranger atoms when these are sufficiently numerous. The whole subject of annealing is very complicated, for we have found that after stabilizing the elasticity at, say, 550°C, it is possible to stabilize at a higher value by repeated annealing at 650°C. In this way much can be learned of the behaviour of dislocations under thermal agitation, and the investigation is being continued.

Fig. 3

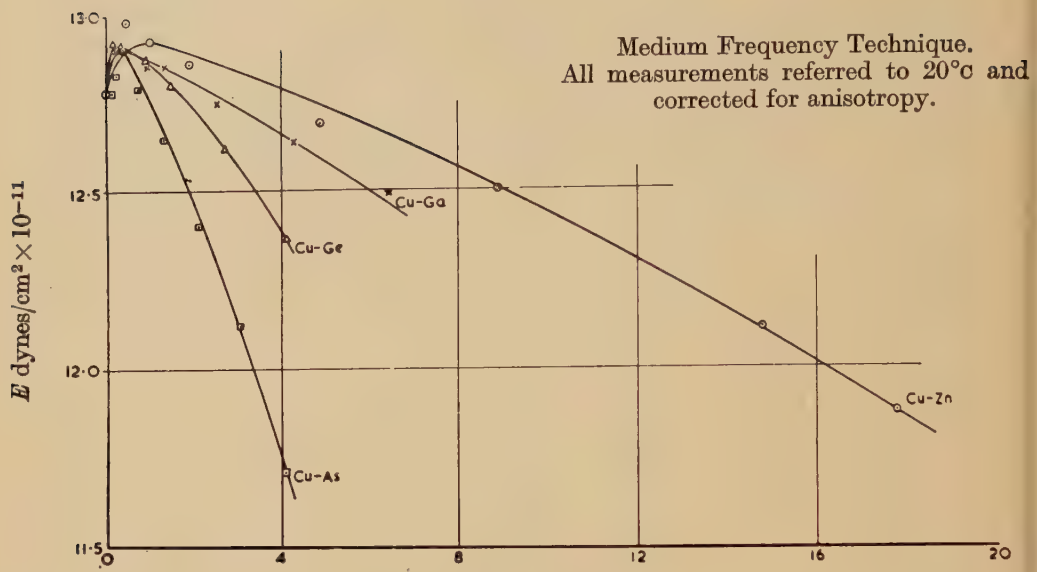

Young's Modulus/Atomic per cent Curves for substitutional Copper Alloys, showing anomaly at extreme dilution when inadequately annealed.

Fig. 4

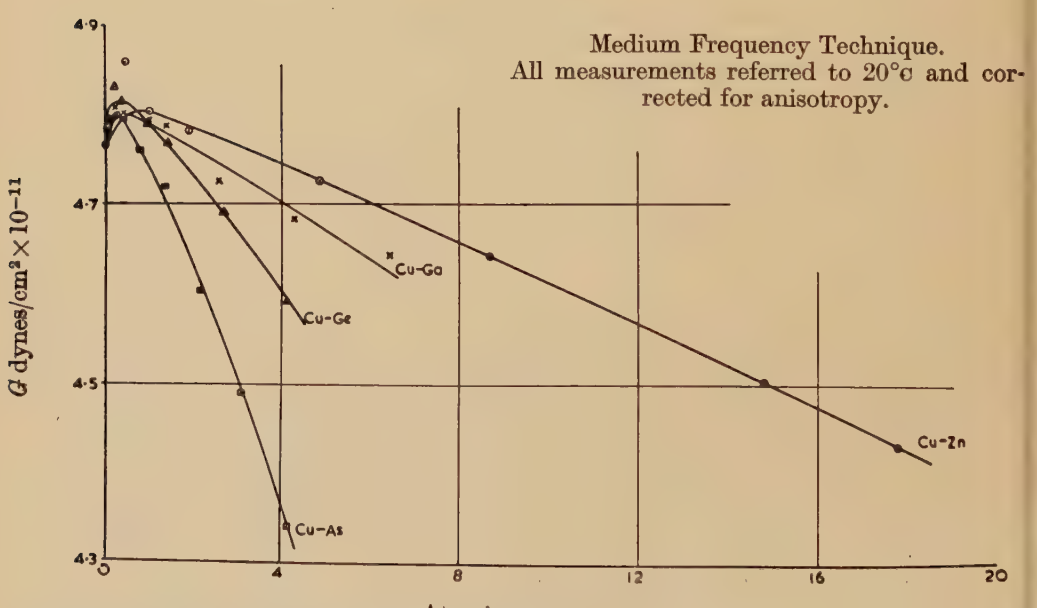

Modulus of Rigidity/Atomic per cent Curves for substitutional Copper Alloys, showing anomaly at extreme dilution when inadequately annealed.

The work described above has been carried out as part of the research programme of the National Physical Laboratory, and this paper is published by permission of the Director of the Laboratory. Acknowledgement is made of the assistance provided to the authors by the Metallurgy Division in preparing and processing specimens, and by Miss M. A. Trott who carried out many of the elasticity measurements.

References

Bancroft, D., 1941, *Phys. Rev.*, **59**, 935.

Bradfield, G., 1951, Second Interim Memorandum concerning Elastic Constants of Dilute Copper Alloys. *Nat. Phys. Lab. Memo.*

Nature, Lond., 1952, **170**, 527. Measurement and Importance of Elastic Properties of Metals.

Pochhammer, L., 1876, *Crelles J. Mathem.*, **81**, 324.

XLVI. *Anomaly in the Rigidity Modulus of Copper Alloys for Small Concentrations*

By J. Friedel
Centre de Recherches Métallurgiques de l'Ecole des Mines de Paris*

[Received February 2, 1953]

Summary

In his recent theory of work hardening, Mott assumes that face-centred cubic crystals usually contain, prior to deformation, a network of dislocations, as suggested first by Frank ; and he computes the decrease in the modulus of rigidity due to the existence of such a network. His computation may be extended to solid solutions, if one assumes the dislocations to be ' pinned down ' by the solute atoms. Thus the addition of solute atoms will always at first *increase* the shear modulus, though larger concentrations may lead to a decrease. An anomaly of the type predicted has actually been observed by Bradfield and Pursey (1953) for small concentrations in copper alloys. One deduces from Bradfield's recent measurements an average length of about 10^{-5} cm for the dislocations of the network ; and the small value of the anomaly for pure copper perhaps indicates that a large fraction of the dislocations are sessile. The anomaly has also been observed for silver alloys. It disappears after long annealing at 650°c, probably by formation of loose Cottrell clouds.

§ 1. Review of Mott's Theory of the Anomaly for Pure Metals

In a recent paper on work-hardening (1952 a), Mott assumes that face-centred cubic crystals usually contain, before deformation, a network of dislocations. That they contain dislocations seems necessary to explain their low critical shear stresses σ_c. This is of order $10^{-4}G$ (G is the rigidity modulus), while, as shown by Frank, the stress necessary to induce plastic flow in a perfect crystal is at least $10^{-1}G$, even at high temperature. It seems also reasonable energetically that these dislocations should form a network, and this allows the operation of Frank–Read sources (1950) to create the large number of dislocations necessary for plastic flow.

The presence of such a network decreases the rigidity modulus G of the metal. For, under a *small* shear stress σ in its glide plane, a dislocation line AB locked at A and B (fig. 1) will assume a curvature $1/\rho$, which disappears elastically with σ. Balancing σ by the line tension W of the dislocation, one has :

$$\sigma \mathbf{b} = W/\rho \,, \qquad \ldots\ldots\ldots \quad (1)$$

with

$$W \simeq \frac{G\mathbf{b}^2}{4\pi k} \ln\left(\frac{l}{\mathbf{b}}\right),$$

* Communicated by the Author.

where l is the size of the network and $\mathbf{b}$ the Burgers vector of AB ; k is unity for a screw and $1-\nu$ for an edge dislocation (ν is the Poisson ratio).

Following Mott, the area swept out by AB is

$$A=\tfrac{1}{2}\rho^2(\theta-\sin\theta)\simeq\rho^2\theta^3/12\simeq l^3/12\rho, \quad \text{for} \quad \theta\simeq l/\rho.$$

If there are N dislocation lines such as AB per unit volume, the additional shear is

$$\Delta\epsilon\simeq NA\mathbf{b}\simeq Nl^3\sigma/6G\alpha,$$

where $\alpha(l)=(2k\pi)^{-1}\ln(l/\mathbf{b})$ is a slowly varying function of l, near to unity for $l\simeq 10^{-5}$. The decrease in G is thus*

$$\Delta G/G\simeq -Nl^3/6\alpha. \quad . \quad . \quad . \quad . \quad . \quad . \quad . \quad . \quad (2)$$

Fig. 1

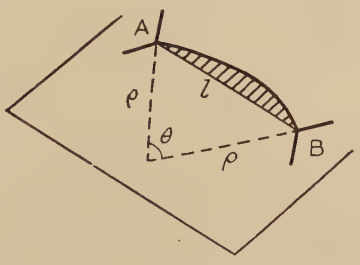

Elastic displacement of a Frank–Read source.

Nl^3 is near to unity if the crystal is filled by a three dimensional network and all the dislocations are mobile. But if a proportion $1-x$ of them are *sessile*, we have $Nl^3\simeq x$. Thus, for a *pure* metal,

$$(\Delta G/G)_0\simeq -x/6\alpha. \quad . \quad . \quad . \quad . \quad . \quad . \quad . \quad . \quad (3)$$

A direct check of this formula is difficult, for the network of dislocations can only be locked by introducing impurity atoms which alter G themselves. It is therefore of interest to extend the theory to solid solutions.

§ 2. Extension of the Theory to Solid Solutions

For a large enough concentration c of the solute elements, a dislocation line AB meets solute atoms on the average at distances say l_0 which decrease when the concentration c of impurity increases (fig. 2). If σ is *small*, as is usual in ultrasonic experiments, we may assume that the dislocation line is ' pinned down ' at the solute atoms, and can only bend between them.

Formula (2) must therefore be replaced by

$$\Delta G/G\simeq -Nl_0^3/6\alpha,$$

where one easily sees that $N\simeq x/l_0l^2$. Hence :

$$\Delta G/G\simeq(\Delta G/G)_0(l_0/l)^2. \quad . \quad . \quad . \quad . \quad . \quad . \quad . \quad (4)$$

---

* For $\alpha=1$, Mott's paper gives 24 instead of 6, owing to a numerical error.

At small concentrations, the rigidity modulus should thus deviate from its quasi linear variation with c and present a negative anomaly ΔG. $|\Delta G|$ should be almost constant for very small concentrations ($l_0 \gg l$), but should decrease as l_0^2 for larger concentrations ($l_0 \ll l$) and become rapidly

Fig. 2

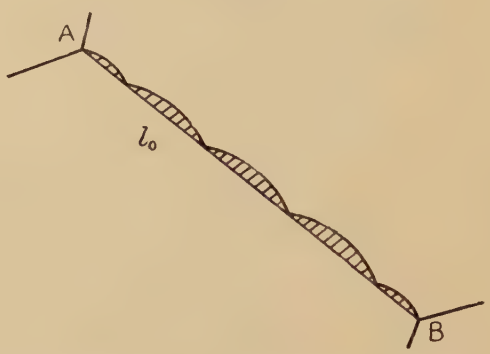

Elastic displacement of a dislocation in a solid solution.

negligible (fig. 3 gives the anomaly $-\Delta E$ of Young's modulus, where the same theory applies and the experimental points are somewhat less scattered).

Fig. 3

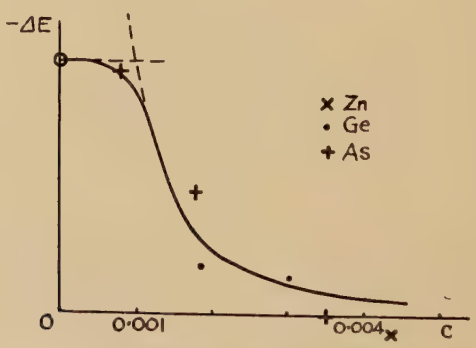

$\Delta E(c)$ for copper alloys. Experimental points after Bradfield.

If the dislocation line AB was perfectly straight, one would have $l_0 \simeq \mathbf{b}/c$. One should however expect the dislocation line to deviate slightly from this path so as to pass through neighbouring solute atoms (Mott 1952 b). This will reduce l_0 somewhat.

Mott shows that

$$l_0 = \mathbf{b}\beta/c,$$

where

$$\beta \simeq (4T\mathbf{b}c/V)^{1/3},$$

varies slowly with concentration. T is the energy of the dislocation line per unit length and V the energy of interaction of a solute atom with the dislocation line. One has

$$T \simeq 2\pi G\mathbf{b}^2,$$

$$V = \gamma G\mathbf{b}^3\epsilon,$$

where ϵ is the ' misfit ' of the solute atom, deduced from the variation of the lattice parameter with composition : $\epsilon = (1/\mathbf{b})(d\mathbf{b}/dc)$. Thus

$$\beta \simeq (8\pi c/\gamma\epsilon)^{1/3}.$$

For carbon in iron, $V \simeq 0{\cdot}5$ to 1 ev (Mott 1952 b) and $\epsilon \simeq 0{\cdot}4$, so that $\gamma \simeq 2$. In the case considered in this paper, $0{\cdot}01 < c < 0{\cdot}001$ and $0{\cdot}05 < \epsilon < 0{\cdot}15$ (Owen 1947). Thus V is of the order of 0·1 ev and β has a value between 0·3 and 1 : the dislocation line does not deviate much from a straight line.

In conclusion, when the concentration c is increased, $|\Delta G|$ should be almost constant and then decrease as c^{-2}. The transition between the two types of curve occurs for $l \simeq l_0$, or $c = c_0 \simeq \mathbf{b}\beta/l$.

§ 3. Comparison with Experiment

A deviation of the type pictured (fig. 3), is well known in copper alloys (Köster and Rauscher 1948). Recent ultrasonic measurements by Bradfield and Pursey (1953) show in CuZn, CuGa, CuGe and CuAs and for large concentrations a quasi-linear variation of G and E. These straight lines converge by extrapolation to pure copper on a value G_1 somewhat larger than the actual value G_0 :

$$(\Delta G/G)_0 = (G_0 - G_1)/G_0 = -0{\cdot}015.$$

The anomalies ΔG and ΔE seem only function of the atomic concentration of impurities, not of their nature. The experimental points fit reasonably well with the theoretical curve (fig. 3), with $c_0 \simeq 0{\cdot}001$ hence $l \simeq 10^{-5}$ cm.

This value of l is somewhat smaller than those deduced by Mott (1952) from the critical shear stress σ_c . σ_c corresponds to $\rho = l/2$ in eqn. (1), thus $\sigma_c \simeq G\mathbf{b}\alpha/l$. Measurements on silver (Andrade and Henderson 1951) and aluminium (Rosi and Mathewson 1950) monocrystals give $l \simeq 10^{-3}$ to 10^{-4} cm. On the other hand crystals with one dimension smaller than l probably have no such network, and should exhibit high critical shear stresses, of the order of $G/10$. Possible examples are Herring and Galt's ' whiskers ' of Sn, Al . . . (1952) with a diameter of about 10^{-4} cm ; also thin plates of silver (Beams, Walker and Morton 1952) with thickness smaller than 5×10^{-5} cm. Finally $l \simeq 10^{-4}$ to 10^{-5} cm corresponds to the usual size of the ' mosaic bloc ' as deduced from x-rays diffraction.

Some other points may be noted. The value of $(\Delta G/G)_0$ gives here $x \simeq 0{\cdot}1$. This seems to indicate that the network is made in major part of sessile dislocations, in agreement with Mott's interpretation of the barriers for the piled up groups (1952 a).

For silver alloys, Smith's measurements (1952) give a similar anomaly with $(\Delta G/G)_0 \simeq (\Delta E/E)_0 \simeq -0{\cdot}025$ and $c_0 < 0{\cdot}01$.

§ 4. Disappearance of the Anomaly by Long Annealing

Finally it is interesting to note that the anomaly disappears completely even for ' pure ' copper (e.g. 99·99%) after long annealing at 650°C (Bradfield and Pursey *loc. cit.*).

This we interpret as due to the crowding by diffusion of impurity atoms on the dislocations. The concentration of solute atoms along the dislocation lines after annealing at temperature T will be (Cottrell 1948) :

$$c' \simeq c \exp (V/kT).$$

For ' pure ' copper, i.e. with probably about $c = 10^{-4}$ iron atoms, $\epsilon \simeq 0{\cdot}2$ (Köster 1948), hence $V \simeq 0{\cdot}4$ ev. At 650°C, this gives $c' \simeq 0{\cdot}015 \gg c_0$. The concentration of iron atoms along the dislocation line is thus large enough to suppress the anomaly completely. For the alloys, the locking is also mainly by iron atoms, but perhaps partly by arsenic atoms in Cu As.

As c' is much smaller than 1, the dislocation lines are far from saturated and no yield point is to be expected. This seems to agree with experiment (Ardley and Cottrell 1953).

The author wishes to thank Professor N. F. Mott and Mr. G. Bradfield for very helpful discussion.

References

Andrade, E. N. da C., and Henderson, C., 1951, *Trans. Roy. Soc.*, **244,** 177.
Ardley, G. W., and Cottrell, A. H., to be published.
Beams, J. W., Walker, W. E., and Morton, H. S., 1952, *Phys. Rev.*, **87,** 524.
Bradfield, G., and Pursey, H., 1953, *Phil. Mag.*, **44,** 437.
Cottrell, A. H., 1948, *Report on the Strength of Solids* (London : Physical Society), p. 30.
Frank, F. C., and Read, W. T., 1950, *Phys. Rev.*, **79,** 722.
Herring, C., and Galt, J. K., 1952, *Phys. Rev.*, **85,** 1060.
Köster, W., and Rauscher, W., 1948, *Zeitschrift f. Metallkunde*, **39,** 145.
Mott, N. F., 1952 a, *Phil. Mag.*, **43,** 1151 ; 1952 b, *Imperfections in Nearly Perfect Crystals* (New York), p. 180.
Mott, N. F., and Nabarro, F. R. N., 1948, *Strength of Solids* (Bristol), p. 1.
Owen, E. A., 1947, *J. Inst. Met.*, **73,** 471.
Rosi, F. D., and Mathewson, C. H., 1950, *J. Met.*, **188,** 1159.
Smith, A. D. W., 1952, *J. Inst. Met.*, May, 477.

XLVII. CORRESPONDENCE

Bombardment of Ordered Cu_3Au *by* 1 MeV *Electrons* *

By C. E. Dixon, C. J. Meechan and J. A. Brinkman
North American Aviation, Inc., Atomic Energy Research Department, Downey, California †

[Received December 23, 1952]

We found the recent letter of Adam, Green and Dugdale (1952) concerning the effect of electron irradiation on Cu_3Au very interesting, as we had just completed similar experiments.

Our first irradiation, made at approximately 60° C, consisted of about 10^{18} electrons/cm^2 of energy 1 MeV. The original resistivity of the specimen was 4·6 micro-ohm-cm at 0° C and a 3% decrease was observed after several hours at 100° C, in agreement with Adam, Green and Dugdale. A second irradiation was made at temperatures below −185° C to determine whether disordering could be produced by 1 MeV electrons. Before irradiation the specimen was held at 375° C for 40 hours, cooled slowly over a period of 400 hours to 200° C, and held at this temperature for 300 hours. The resistivity was found to be 4·10 micro-ohm-cm at 20° C and 1·52 micro-ohm-cm at −195° C. It was subjected to a total flux of $3{\cdot}4\times10^{19}$ electrons/cm^2. Resistance measurements at −195° C after this bombardment showed no change in excess of the experimental error which was approximately 1%. The specimen was then allowed to anneal at room temperature for 350 hours. Intermittent measurements at −195° C showed a decrease of 2·7% in 50 hours. Between 50 hours and 350 hours the resistance showed both increases and decreases which exceeded the errors of the measurements. We have observed similar fluctuations during room temperature anneals of Cu_3Au which had been previously cold worked at −195° C, but have been unable to explain such behaviour. After 350 hours at room temperature, a further anneal of 1 hour at 100° C showed no measurable resistance change.

Calculations indicate that the fraction of atoms which should have been displaced by this irradiation is about 7×10^{-4}. According to Dexter (1952) such a density of interstitial-vacancy pairs should produce about a 5% change in the resistivity at −195° C. Because no such resistance change was observed, considerable recombination of the interstitial-vacancy pairs must have occurred at the temperature of irradiation. As a result of the low average energy of the displaced atoms, the average vacancy-interstitial separation distance may be so small that most of the pairs are unstable and can recombine without thermal activation. There appears to be a fundamental difference in the nature of the damage

* This report is based on studies conducted for the Atomic Energy Commission under contract AT-11-1-GEN-8.

† Communicated by the Authors.

produced in metals by neutrons and by electrons since electrons do not produce disordering. We plan to measure the effect of electron irradiation on mechanical properties of metals and compare with the effects of neutron irradiation.

REFERENCES

ADAM, J., GREEN, A., and DUGDALE, R. A., 1952, *Phil. Mag.*, **43**, 1216.
DEXTER, D. L., 1952, *Phys. Rev.*, **87**, 768.

Radiative Widths of Dipole Transitions in Light Elements

By D. H. WILKINSON
Cavendish Laboratory, Cambridge

[Received February 27, 1953]

THE most recently-proposed formulae for the lifetimes of nuclear states are those put forward by Weisskopf (1951); their value in effecting a classification of nuclear isomers (low gamma-ray energy and large spin change) has been demonstrated in the considerable paper of Goldhaber and Sunyar (1951). So far no attempt has been made to systematize the properties of the other important class of gamma-rays namely those of high energy and small spin change that manifest themselves by virtue of their very short lifetimes. These are to be found principally among the light elements where it is sometimes of great importance to be able to predict the radiative width that might reasonably be expected of a given transition and to have some idea of the reliability of the prediction. The data on which such a systematization must be based are as yet very meagre, but twenty-two dipole transitions are sufficiently well established and measured to enable a start to be made.

Weisskopf's estimates of the connection between the radiative width Γ_γ (in ev) and the energy of the transition E_γ (in MEV) are :

$$\text{Electric dipole } \Gamma_\gamma = 0{\cdot}11 E_\gamma^{\,3} A^{2/3},$$

$$\text{Magnetic dipole } \Gamma_\gamma = 0{\cdot}021 E_\gamma^{\,3}.$$

The available data are presented in the following tables : J is the angular momentum of the emitting nucleus ; $|M|^2$ is the ratio of experimental to theoretical radiative widths. We follow Goldhaber and Sunyar in quoting $(2J+1)|M|^2$ because it has for us the convenience of usually not demanding knowledge of J which we frequently have not got, although we may be certain of the character of the transition. Only those transitions have been used for which it is very probable that Γ_γ is much smaller than the width for re-emission of the incident particle. Status A means that the stated character of the transition is almost certainly correct ; B means that it is very probable. Those transitions bearing a star under Status have $(2J+1)\Gamma_\gamma$ values correct to a few tens of per cent ; the error on the unmarked transitions may be rather greater, perhaps as much as a factor of 2 or 3.

Electric Dipole

Reaction	E_γ	$(2J+1)\Gamma_\gamma$	$(2J+1)\lvert M\rvert^2$	Status	References
$^{9}Be(p\gamma)^{10}B$	7·5	88	0·42	A*	(a), (b), (c), (d)
$^{7}Li(\alpha\gamma)^{11}B$	2·5	1·3	0·16	B*	(f), (g)
$^{7}Li(\alpha\gamma)^{11}B$	4·8	16	0·26	B*	(f), (g)
$^{12}C(p\gamma)^{13}N$	2·4	1·3	0·17	A*	(d), (h), (i)
$^{13}C(p\gamma)^{14}N$	4·1	3·6	0·08	A*	(b), (j), (k), (l), (dd)
$^{13}C(p\gamma)^{14}N$	4·8	7·7	0·11	A*	(j), (k), (l), (dd)
$^{13}C(p\gamma)^{14}N$	8·1	31	0·09	A*	(b), (j), (k)
$^{13}C(p\gamma)^{14}N$	8·7	44	0·11	A*	(j), (k)
$^{14}N(p\gamma)^{15}O$	9·8	280	0·45	A*	(m)
$^{15}N(p\gamma)^{16}O$	13·1	450	0·29	B	(n)
$^{16}O(p\gamma)^{17}F$	3·9	5	0·12	A	(o), (p), (q)

Magnetic Dipole

Reaction	E_γ	$(2J+1)\Gamma_\gamma$	$(2J+1)\lvert M\rvert^2$	Status	References
$^{7}Li^*$	0·48	0·006	5·5	A*	(r), (dd)
$^{7}Li(p\gamma)^{8}Be$	14·6	25	0·38	A*	(b), (d), (dd)
$^{7}Li(p\gamma)^{8}Be$	17·6	50	0·44	A*	(b), (d), (dd)
$^{6}Li(\alpha\gamma)^{10}B$	4·0	0·5	0·35	B*	(s)
$^{9}Be(p\gamma)^{10}B$	7·0	5·6	0·78	A*	(a), (c), (d), (e)
$^{7}Li(\alpha\gamma)^{11}B$	9·3	1·9	0·12	B*	(f), (g)
$^{10}B(p\gamma)^{11}C$	9·5	9	0·51	B	(t), (u)
$^{11}B(p\gamma)^{12}C$	11·7	600	18	A	(v), (w), (x)
$^{11}B(p\gamma)^{12}C$	12·2	80	2·1	B	(w), (x), (y)
$^{12}C(p\gamma)^{13}N$	3·5	2·8	3·1	B*	(i), (dd)
$^{19}F(p\gamma)^{20}Ne$	11·9	300	10	A*	(z), (aa), (bb), (cc)

(a) Cohen, E. R., 1949, *Phys. Rev.*, **75,** 1463.
(b) Devons, S., and Hine, M. G. N., 1949, *Proc. Roy. Soc.* A, **199,** 56, 73.
(c) Thomas, R. G., Rubin, S., Fowler, W. A., and Lauritsen, C. C., 1949, *Phys. Rev.*, **75,** 1612.
(d) Fowler, W. A., and Lauritsen, C. C., 1949, *Phys. Rev.*, **76,** 314.
(e) Richards, H. T., 1952, Pittsburgh Conference.
(f) Bennett, W. E., Roys, P. A., and Toppell, B. J., 1951, *Phys. Rev.*, **82,** 20.
(g) Jones, G. A., and Wilkinson, D. H., 1952, *Phys. Rev.*, **88,** 423.
(h) Jackson, H. L., and Golansky, A. I., 1951, *Phys. Rev.*, **84,** 401.
(i) Thomas, R. G., 1952, *Phys. Rev.*, **88,** 1109.
(j) Seagrave, J. D., 1952, *Phys. Rev.*, **85,** 197.
(k) Woodbury, H. H., Day, R. B., and Tollestrup, A. V., 1952, *Phys. Rev.*, **85,** 760 (and private communication).
(l) Benenson, R. E., 1952, *Phys. Rev.*, **87,** 207.
(m) Duncan, D. B., and Perry, J. E., 1951, *Phys. Rev.*, **82,** 809.
(n) Schardt, A., Fowler, W. A., and Lauritsen, C. C., 1952, *Phys. Rev.*, **86,** 527.
(o) Laubenstein, R. A., Laubenstein, M. J. W., Koester, L. and J., Mobley, R. C., 1951, *Phys. Rev.*, **84,** 12.
(p) Laubenstein, R. A., and Laubenstein, M. J. W., 1951, *Phys. Rev.*, **84,** 18.
(q) Du Bridge, L. A., Barnes, S. W., Buck, J. H., and Strain, C. V., 1938, *Phys. Rev.*, **53,** 447.
(r) Bell, R. E., and Elliott, L. G., 1949, *Phys. Rev.*, **76,** 168.
(s) Jones, G. A., and Wilkinson, D. H., unpublished.
(t) Walker, R. L., 1950, *Phys. Rev.*, **79,** 172.
(u) Brown, A. B., Snyder, C. W., Fowler, W. A., and Lauritsen, C. C., 1951, *Phys. Rev.*, **82,** 159.

(v) Thomson, D. M., Cohen, A. V., French, A. P., and Hutchinson, G. W., 1952, *Proc. Phys. Soc.* A, **65**, 745.
(w) Huus, T., and Day, R. B., 1952, *Phys. Rev.*, **85**, 761.
(x) Huus, T., private communication.
(y) Dissanaike, G. A., and French, A. P., private communication.
(z) Devons, S., and Hereward, H. G., 1948, *Nature, Lond.*, **162**, 331.
(aa) Jones, G. A., and Wilkinson, D. H., 1952, *Proc. Phys. Soc.* A, **65**, 1055.
(bb) Seed, J., and French, A. P., 1952, *Phys. Rev.*, **88**, 1007.
(cc) Clegg, A. B., Jones, G. A., and Wilkinson, D. H., unpublished.
(dd) See also Ajzenberg, F., and Lauritsen, T., 1952.

The electric dipole matrix elements show a remarkable and most unexpected constancy ; $(2J+1)\,|\,M\,|^2$ varies by less than a factor of 2·5 either side of the value 0·2 as $(2J+1)\Gamma_\gamma$ varies by a factor of more than 300. There is no systematic dependence of $(2J+1)\,|\,M\,|^2$ on any feature of the nucleus or the energy of the transition.

The magnetic dipole matrix elements show a rather larger straggle ; $(2J+1)\,|\,M\,|^2$ varies by a factor of about 12 either side of the value 1·5 as $(2J+1)\Gamma_\gamma$ varies by a factor of 10^5. There is again no systematic dependence of $(2J+1)\,|\,M\,|^2$ on any feature of the nucleus or energy of the transition.

Two points emerge from this survey : one is that electric dipole matrix elements are not small at any rate in light nuclei of fairly high excitation ; the other is that, while we may not safely base a distinction between E1 and M1 transitions on the radiative width we may, within limits, predict what the width will be if we know the character of the transition. An important exception to the predictability of E1 (but not M1) lifetimes in self-conjugate nuclei is provided by the isotopic spin selection rule (Radicati 1952) which forbids such transitions between states of the same T ; this may reduce the radiative width by a factor of as much as 10^4 (Radicati 1953, Wilkinson and Jones 1953). All transitions of $\Delta T \geqslant 2$ are also forbidden but are not likely to be met.

The only other transitions to have been identified in light nuclei are a few electric quadrupoles ; these few suggest that the radiative width may be somewhat larger than Weisskopf's estimate but this may be due to the experimenter's seeing only the unusually strong E2 transitions (this selective effect is not to be expected and does not occur in the E1 and M1 transitions analysed above).

I would like to acknowledge my indebtedness to the compilation of Ajzenberg and Lauritsen (1952) which lessened immeasurably the burden of making this survey.

References

Ajzenberg, F., and Lauritsen, T., 1952, *Rev. Mod. Phys.*, **24**, 321.
Goldhaber, M., and Sunyar, A. W., 1951, *Phys. Rev.*, **83**, 906.
Radicati, L. A., 1952, *Phys. Rev.*, **87**, 521; 1953, *Proc. Phys. Soc.* A, **66**, 139.
Weisskopf, V. F., 1951, *Phys. Rev.*, **83**, 1073.
Wilkinson, D. H., and Jones, G. A., 1953, *Phil. Mag.*, in press.

[The Editors do not hold themselves responsible for the views expressed by their correspondents.]